



Friction stir based welding and processing technologies - processes, parameters, microstructures and applications: A review

G.K. Padhy, C.S. Wu*, S. Gao

MOE Key Lab for Liquid-Solid Structure Evolution and Materials Processing, Institute of Materials Joining, Shandong University, Jinan, 250061, China



ARTICLE INFO

Article history:

Received 8 March 2017

Received in revised form 6 June 2017

Accepted 19 June 2017

Available online 15 November 2017

Keywords:

Friction stir welding

Friction stir processing

Friction stir scribe

Friction stir riveting

Friction stir channeling

Friction stir forming

Friction stir surfacing

Friction stir additive manufacturing

Friction stir cladding

ABSTRACT

Friction stir welding (FSW) has achieved remarkable success in the joining and processing of aluminium alloys and other softer structural alloys. Conventional FSW, however, has not been entirely successful in the joining, processing and manufacturing of different desired materials essential to meet the sophisticated green globe requirements. Through the efforts of improving the process and transferring the existing friction stir knowledge base to other advanced applications, several friction stir based daughter technologies have emerged over the timeline. A few among these technologies are well developed while others are under the process of emergence. Beginning with a broad classification of the scattered friction stir based technologies into two categories, welding and processing, it appears now time to know, compile and review these to enable their rapid access for reference and academia. In this review article, the friction stir based technologies classified under the category of welding are those applied for joining of materials while the remnant are labeled as friction stir processing (FSP) technologies. This review article presents an overview of four general aspects of both the developed and the developing friction stir based technologies, their associated process parameters, metallurgical features of their products and their feasibility and application to various materials. The lesser known and emerging technologies have been emphasized.

© 2017 Published by Elsevier Ltd on behalf of The editorial office of Journal of Materials Science & Technology.

1. Introduction

Solid state joining and processing technologies are emerging to be commonplace in industries to join softer metal alloys which are difficult to join using conventional fusion welding techniques. Friction stir welding (FSW), invented in 1991 at The Welding Institute, UK [1], is arguably the most successful solid state joining technology. FSW does not use filler material, leading to considerable weight reduction. Within 26 years of invention, FSW has been proven to be at the forefront of joining high strength aluminium alloys, meant for application in automobile and aerospace sectors, while also savoring partial success in the joining of other metallic alloys [2–10]. Considering the remarkable success of FSW, the friction stir concept has been further modified, improved and refurbished to develop various novel material joining and processing technologies which is gradually enabling transfer of technological feasibility to other high strength structural materials and sophisticated applications [11–21].

This review aims at presenting an overview of all the documented processes and technologies based on the friction stir concept. On the basis of their application, friction stir based operations can be classified into two major categories, welding and processing. The various processes classified under the welding and processing categories are shown in Fig. 1. The operation technologies under the welding category are essentially employed for material coalescence while processing technologies are adopted for applications aimed at improving the quality of the material in terms of its physical, chemical and mechanical properties [18–21].

It is worth mentioning that the friction stir processes involve the rotational motion of a tool in contact with a workpiece. This generates the necessary heat for the operation by friction between the tool and the workpiece. A common notion is that the tool is always non-consumable in the friction stir operations, as in friction stir welding. However, this notion is not necessarily true for some friction stir processes such as friction surfacing where the tool is consumable. The friction stir based technologies operate on the principle of 'third body region' [21,22]. Schematic diagrams of the third body regions in the friction stir operations using non-consumable and consumable electrodes are shown in Fig. 2(a) and (b), respectively.

* Corresponding author.

E-mail address: wucs@sdu.edu.cn (C.S. Wu).

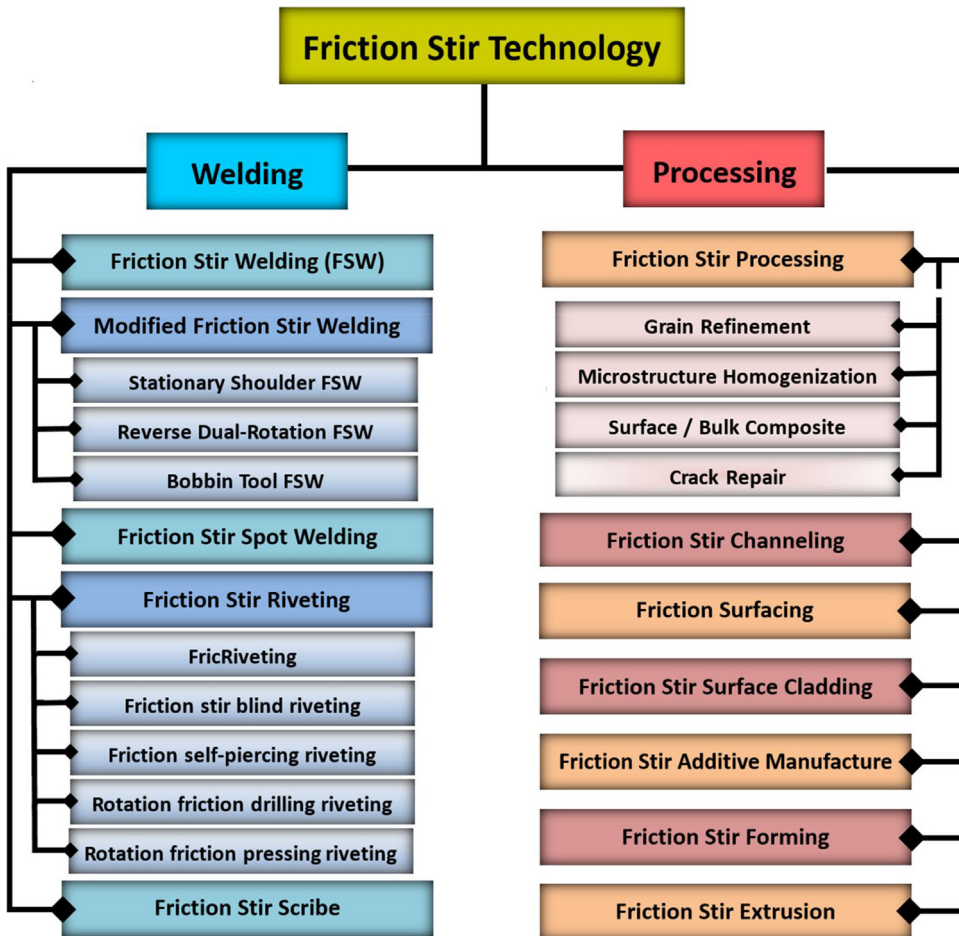


Fig. 1. Classification of friction stir based technologies.

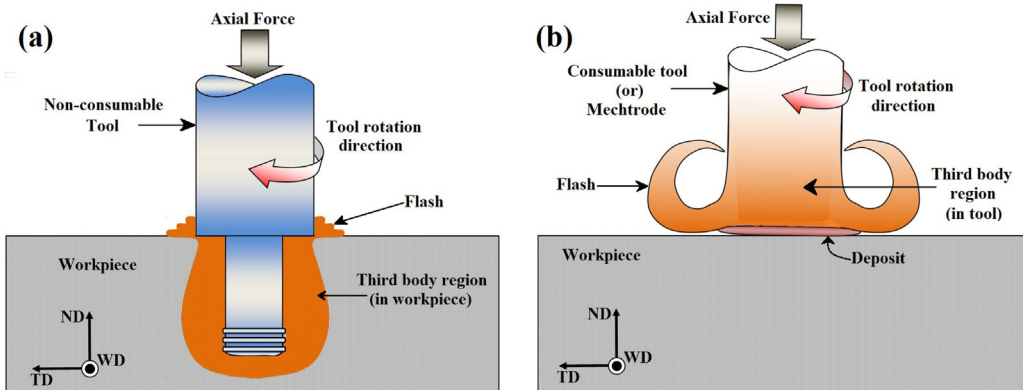


Fig. 2. Third body region in friction stir operations with (a) Non-consumable tool, as in friction stir welding, (b) Consumable tool, as in friction surfacing.

As the term persuades, 'third body region' is a zone physically distinct from both the tool and the workpiece. It is generated either on the workpiece (when the tool is non-consumable) or on the tool (when the tool is consumable) during the friction stir operation. Although still a solid, the third body region exhibits three dimensional fluidity and allows the material in the region to flow and mix with the other material at the interface. Formation of the third body region is driven by frictional heat generation at the working interfaces. This region appears at temperatures between the recrystallization temperature and melting point of material and is characterized by relatively high viscosity and low flow stress.

The material in this region closely corresponds to the plasticized or deformed material in the friction stir based operations.

In general, the third body region is typical to all the friction stir based operations while it is nonexistent in fusion technologies because there is no frictional heat generation at the melting point of material. The third body region allows interatomic diffusion and material intermixing at relatively higher temperatures. Thus, the material in the region can produce strong bonding with similar region of another similar/dissimilar material. At lower temperatures or higher pressures, however, interatomic bonding is also a dominating mechanism of joining or processing [21]. Therefore,

the main objective of the friction stir based technologies is to generate sufficient frictional heat which can produce a third body region of the material in order to join or process the material.

In general, the friction stir equipment in most of the friction stir based operation technologies listed in Fig. 1 constitutes a tool with a shoulder and with or without a pin. The tool is the heart of the friction stir equipment because it generates the necessary frictional heat which is spent in the creation of the third body region. Also, the tool helps enclose the third body region when it is non-consumable. Tool geometry and tool material are extremely important for the success of the friction stir based technologies. Also, the design, material selection, performance and durability of tool are four major criteria that determine the sustainability of a given friction stir technology [23–34]. A process is sustainable if it is efficient, effective and economic. However, detailed study of FSW tool material, design and performance etc. are beyond the scope of this review. Some of the technologies mentioned in Fig. 1 also employ a consumable tool.

This review article presents an overview of four general aspects: the working principles of the processes, the main parameters defining the processes, metallurgical features of their products and the feasibility and application of the processes to different materials. Each of the aforesaid developed as well as the emerging friction stir based technologies are discussed in terms of the above four aspects.

2. Friction stir based welding/joining technologies

2.1. Friction stir welding

Although friction stir welding is not the first invention based on the friction stir concept, it brought about a revolution in the efficient joining of softer and low melting point metal alloys. FSW process generally uses two types of machines, displacement controlled and pressure controlled. Fig. 3(a) shows the schematic of a typical FSW process. A non-consumable FSW tool is the key component of the FSW process. The tool constitutes a shoulder and a pin. The choice of tool material and geometry depends upon the material to be welded, material dimensions, joint configuration and other required specifications. The various types of FSW tools, their designs, material selection, strength, failure mechanisms, prevention of the failures etc. have been documented by several researchers [23–34].

2.1.1. Process features and experimental setup

Fig. 3(b) shows the different stages involved in the FSW process. These stages include,

- **Plunging stage:** The tool, rotating at a constant speed, is plunged through the starting point of the joint line of the workpieces under the action of a vertically downward axial force until the shoulder touches the workpiece surface. This stage initiates the deformation process.
- **Dwelling stage:** The rotating tool, under the action of the axial force and with its shoulder contacting the workpiece surface, is dwelled for 5–10 s depending upon the material and thickness. This dwelling action generates sufficient friction heat at tool-workpiece interface and causes plasticization of the workpiece, generating more heat from plastic deformation. The plastic material ahead of the tool ensures a smooth traverse of tool during the subsequent welding stage.
- **Welding stage:** The rotating tool, under the action of axial load and with its shoulder enclosing the plasticized volume, is traversed at a constant speed along the desired joint line under the action of a traverse force. The tool rotation continues generating heat by friction and deformation. Another important function of the

tool rotation is material stirring or material flow. The rotation and traverse motions of the tool causes the plastic material in the vicinity of tool pin to flow from the advancing side to the back of the pin. The shoulder applies a forging force on the material behind the pin, effectively filling the cavity formed by the forward motion of pin. This causes material intermixing in the form of atomic diffusion or bonding depending upon the conditions of temperature and pressure, resulting in a joint behind the tool.

- **Retracting/cooling stage:** Upon arrival at the weld end, the tool is retracted from the workpiece, leaving behind an exit hole, as shown in Fig. 3(b). Several procedures are adopted to avoid the exit hole in the intended weld. These include refilling of the exit hole or using a longer weld length than the intended length etc.

The major functions of the tool are to: a) generate frictional or deformational heat; b) control the material flow; and c) contain the plastic material under the shoulder. In the welding of thin sheets, majority of the heat generation is caused by the shoulder while in thick workpieces, the pin produces the bulk of the heat. The heat generation and material flow can be aided further by incorporating special features on the surfaces of tool shoulder and the pin [24]. The details of the heat generation principles in friction stir welding can be found elsewhere [37,38].

2.1.2. FSW process parameters

The main process parameters in the FSW process are rotation speed, traverse speed, shoulder plunge depth, and tool tilt angle. Apart from these, the tool geometry is also an important aspect to produce sound welds. The rotation speed and the traverse speed govern the amount of frictional heat generated and subsequent plastic deformation and deformation heat. These two parameters, along with plunge depth, affect the axial force imparted on workpiece which significantly influences the weld quality [4]. The tool is slightly tilted at a known angle and the tool shoulder is provided with a known plunge depth during the welding, both aiding in the consolidation of material on the back of the pin. In general, a higher rotation speed produces higher heat input while a higher traverse speed reduces the heat input by lowering the time duration of tool-workpiece interaction at a given point of action. Moderate amounts of heat inputs are good for the plastic deformation, stirring and material flow in FSW which determine the formation and strength of the welded joints.

2.1.3. Microstructure of FSW joint

The joint formation in FSW is a complex process involving variable thermomechanical action of the FSW tool. Consequently, the FSW joint exhibits microstructure inhomogeneity. On the basis of tool action and material transport, the welded area can be also divided into three zones: (a) shoulder affected zone (SAZ), (b) pin affected zone (PAZ) and (c) weld bottom zone (WBZ), as shown in Fig. 4 [39].

Fig. 5 shows the weld macrograph and the microstructures of various weld zones on the basis of thermomechanical actions experienced by different sections of the weld. As shown in Fig. 5(a), the FSW joint constitutes four distinct zones: (a) unaffected zone or base metal (BM), (b) heat affected zone (HAZ), where material is affected only by heat and no plastic deformation takes place, (c) thermo-mechanically affected zone (TMAZ), where material is affected by heat and plastic deformation, and (d) weld-nugget/stir zone (SZ). The microstructures of these zones are shown in Fig. 5(b) through e.

The SZ comprises of prominent onion ring features, which appear due to the successive shearing of semi-cylindrical plastic material layers from the front of the tool and their deposition at the back of the tool [40]. Hence, grain structure evolution in the SZ is a very complex process and is driven mainly by continuous

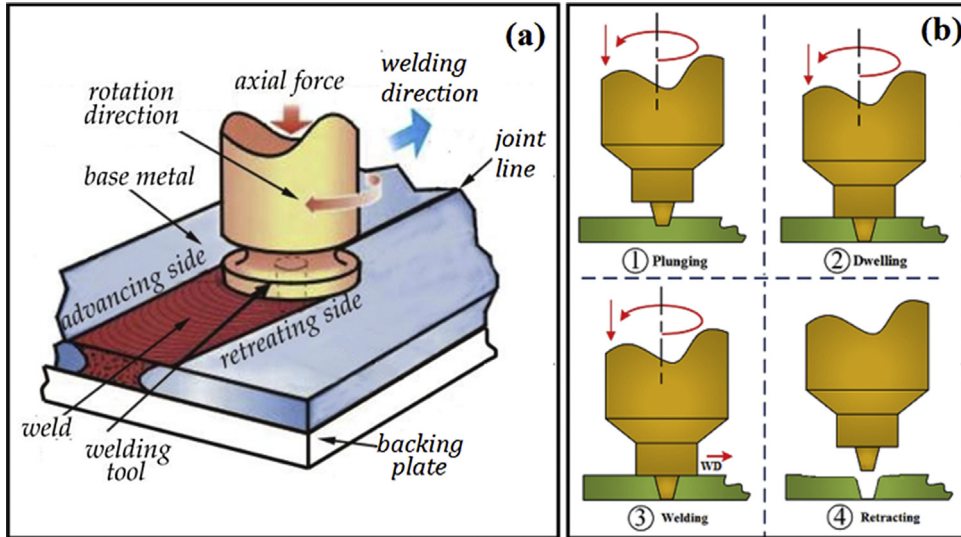


Fig. 3. FSW process (a) schematic [35], and (b) various stages [36].

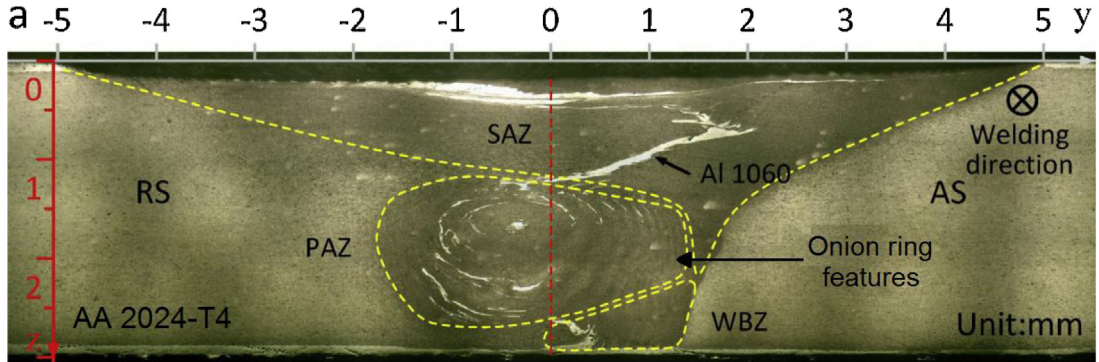


Fig. 4. Macro-section of friction stir welded joint depicting SAZ, PAZ, WBZ and onion ring features [39].

dynamic recrystallization (CDRX) and geometric dynamic recrystallization (GDRX); while particle simulated nucleation (PSN) also plays minor role in particular cases [41–48].

CDRX occurs when the strain and strain rate of the weld zone is high. CDRX is characterized by refined and equiaxed grains and higher fraction of high-angle boundary area. The refined and equiaxed grains are due to strain induced progressive rotation of subgrains by absorption of dislocations at the boundaries, followed by increase in the misorientation and their gradual transformation into grain boundaries [42,49]. However, the occurrence of CDRX in FSW welded zone is debated. GDRX is another continuous recrystallization process observed in locations with high strains. In GDRX, flattened and serrated grains, formed due to dynamic recovery induced by deformation, intimate and annihilate to form equiaxed grains [49]. Discontinuous dynamic recrystallization (DDRX) is generally not common in Al-alloys because of high levels of recovery due to high stacking fault energy [42,50], though it may occur just beyond the SZ at excessive heat inputs [51]. As a result of the above mechanisms, the microstructure in SZ is fine and equiaxed [52–54].

Microstructure development in the TMAZ is mainly due to dynamic recovery because the levels of temperature and strain experienced are insufficient for recrystallization. In the TMAZ, the grains are elongated, narrow and relatively coarse than those in the SZ. The HAZ is often accompanied by grain coarsening due to the effect of heat. Moreover, there is a through thickness variation in the microstructure down the weld nugget center because it has the SAZ and PAZ while the pin diameter may vary from the top to

the bottom of the weld. These differences alter the distribution of temperature and effective strain in the SZ [52–55].

The weld microstructure influences the mechanical properties of the welded joints. For example, the strength of the aluminium alloy welded joints depends upon the grain size and precipitate. These strengthening factors can be controlled and the mechanical properties can be improved by adopting various methods such as careful selection of tool profile [56], use of composite backing plates [57,58], forced cooling during welding [59], post weld heat treatment [60], Application of ultrasonic vibrations [61], friction stir alloying [62] etc. There exists a large amount of documented research in the open literature on the subject of structure-property relationship. However, the scope of the paper is kept limited to the knowledge on the process, its main parameters, microstructure and applications.

2.1.4. Feasibility and application of FSW

FSW, being a relatively cold technology, eliminates the unattractive prospects of fusion welding, mainly the weld defects formed during the solidification of the molten metal in fusion welding. FSW has already been implemented at industrial scale for producing welded joints of Al-alloys for commercial means. From the reported studies, FSW appears very much feasible for the commercial joining of Mg alloys. Moreover, with suitable tool material, geometry and choice of process parameters, FSW is technologically feasible to other high strength and high melting point alloys such as Fe-, Ti-, Ni- and Cu- based alloys and may be implemented

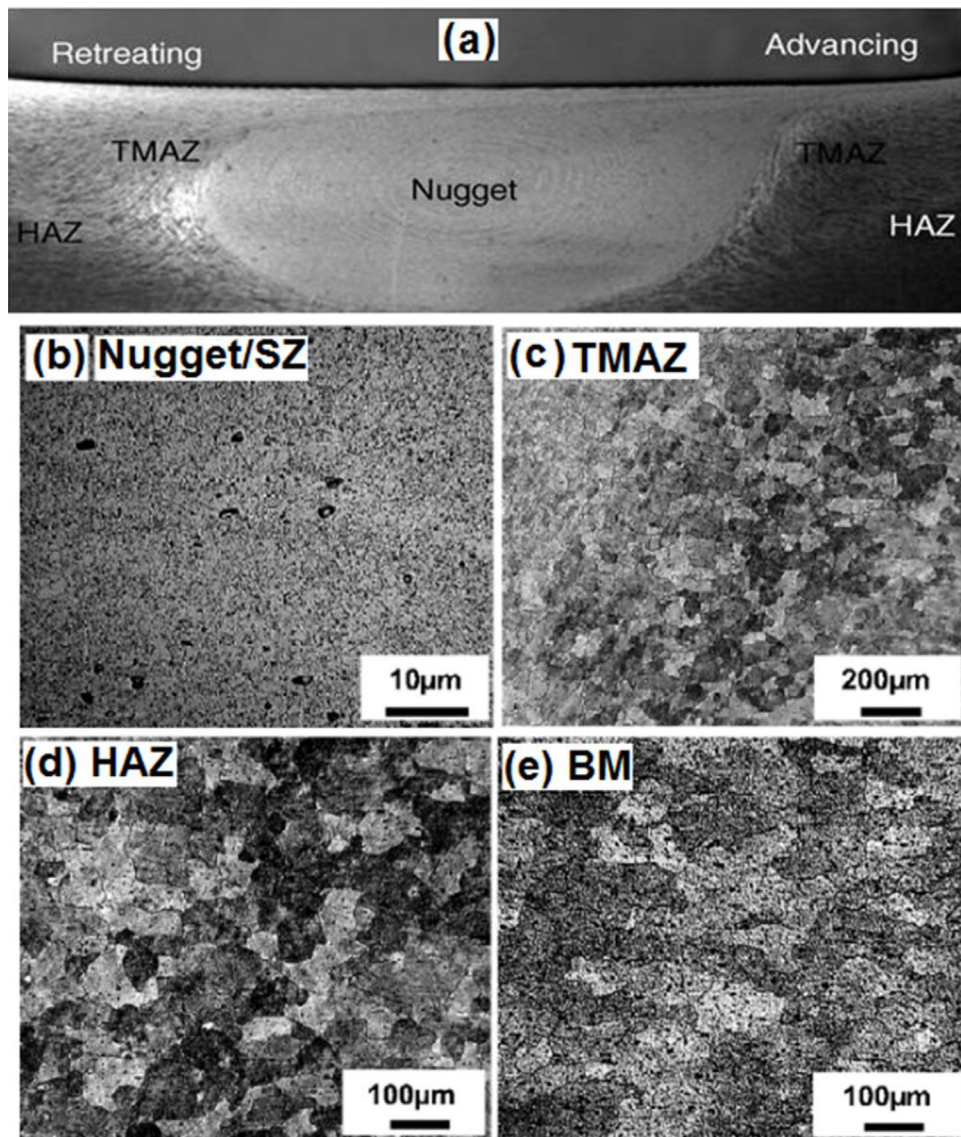


Fig. 5. (a) Typical weld macrograph of 2024 Al alloy in FSW [63], microstructures of 6061-T6 Al alloy friction stir weld (b) Stir zone, (c) TMAZ, (d) HAZ, and (e) BM [64].

by industries in the future. Developments towards its application to these alloys are also under rapid progress and gradually evolving out of the laboratory towards practice. Additionally, FSW is also explored for the effective joining of dissimilar materials, metal matrix composites, ceramics, polymers, and, most recently, wood-plastics [3–12,65,66]. Detailed description and review on the application of FSW to various materials is beyond the scope of this paper.

2.2. Modified friction stir welding processes

The energy efficient, green and solid state nature of FSW process, the attractive physical, mechanical and microstructural properties of friction stir welds and the commitment of FSW community to expand the technological feasibility of the FSW process to a wide range of materials have led to the development of a rich extent of tool designs, technology, and materials [3–12]. Also, there are certain process related issues in FSW such as low traverse speed, high welding load, high torque on workpiece, large machinery, tool wear, application of FSW to high-strength materials etc. To solve these problems, FSW has been continuously redeveloped, improved, redesigned and revisited with respect to the machine,

the tool and the process. This section is aimed at discussing some of the FSW processes based on specially designed tools such as the stationary shoulder FSW (SSFSW) [67–74], reverse dual rotation FSW (RDRFSW) [76–84], bobbin tool FSW (BTFSW) [85–96] and twin tool FSW (TTFSW) [93]. Also, this section extends a quick mention to the FSW processes assisted by secondary energy sources [17].

2.2.1. Stationary shoulder friction stir welding (SSFSW)

SSFSW has been developed at TWI to solve the through-thickness temperature gradient issues in the FSW of titanium-based alloys leading to poor weldability [67]. A schematic of SSFSW is shown in Fig. 6. In SSFSW, a rotating pin located in a non-rotating or stationary shoulder slides over the surface of the material during welding. Thus, the shoulder contributes little to the deformation and heat generated at the top surface during welding, while the rotating pin generates frictional heat focused around the pin, and softens and stirs the material. This reduces the width of the SAZ and improves the process stability, leading to improvement of temperature distribution, hardness distribution and microstructural homogeneity through the weld thickness [67–74].

The main process parameters affecting the SSFWS process and its welded joints are the pin rotation speed, traverse speed, plunge

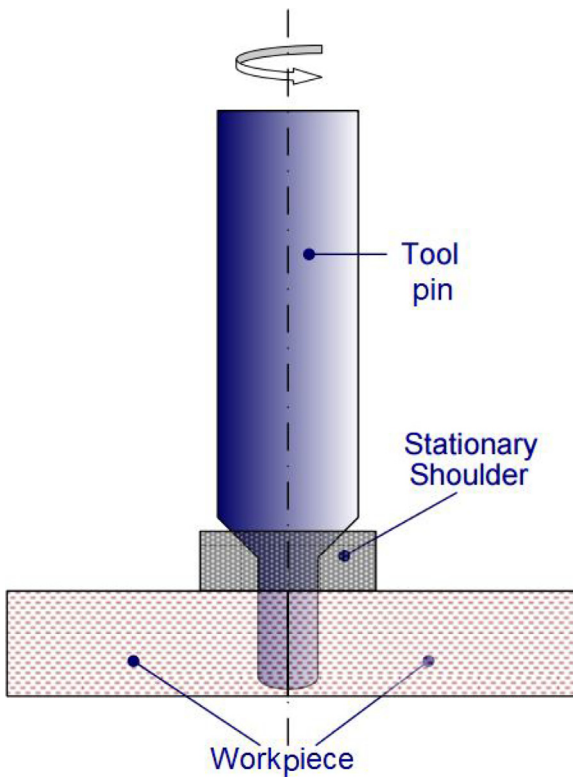


Fig. 6. Schematic diagram of SSFSW [75].

depth and the tool geometry. Lower traverse speeds produce good surface finish while moderate traverse speeds yield good joint strength [70,74]. Low to moderate rotation speeds are ideal to achieve sound physical, mechanical and microstructural property of welded joint, while too high rotation speeds may contribute to their deterioration [68,69]. Improved weld mechanical properties and microstructural homogeneity have been the highlights of SSFSW.

The optical macrograph of Al 7075-T6 weld prepared by SSFSW is shown in Fig. 7(a) [71]. The joint can be divided into SZ, TMAZ, HAZ and BM. The SZ of the weld presents a bowl-shape or drum-shape with the maximum width at mid-thickness. Fig. 7(b) through e shows the microstructures of the BM, HAZ, TMAZ and SZ. The TMAZ is narrow and symmetrical around the SZ on both AS and RS. Grains of the BM are elongated due to the rolling process. The grain structure in the HAZ is similar to that in the BM and is not apparently affected during the welding. The microstructure in the TMAZ presents severe plastic deformation and the grains present the material flow pattern. Besides, partial recrystallization is evident at the TMAZ. The SZ is refined, recrystallized and exhibits homogeneous and equiaxed through thickness grain size [67,72]. The SSFSW process has shown great potential in the welding of Al alloys and solved the overheating issue in the welding of Ti-alloys [73]. At present, however, SSFSW seems far from practical reality in the welding of Fe and Ni alloys [71].

2.2.2. Reverse dual rotation friction stir welding (RDRFSW)

Possible overheating of workpiece is a serious issue in the FSW of thick sections which also degrades the microstructures and mechanical properties of the FSW joint. This issue arises due to the large tangential speed gradient between the center of tool pin and the maximum diameter of the shoulder [76]. It can be resolved by making the shoulder and the tool pin to rotate independently, thus, allowing the pin to rotate at a high speed without increasing the rotation speed of the shoulder periphery. RDRFSW is one such

method where the assisted shoulder and the tool pin are rotated independently at different rotation speeds and in opposite directions [76–82]. Also, the mutually opposite rotations of the shoulder and pin negate a part of the overall torque exerted on the workpiece, thereby reduce clamping requirements for the workpiece [79]. Fig. 8(a) shows the schematic of RDRFSW process [77].

The main process parameters of RDRFSW influencing the welded joint properties are the rotation speed of the assisted shoulder, rotation speed of the pin and the traverse speed [79]. These factors affect the heat generation, temperature and the size of deformation zone and may have an obvious effect on the properties of welded joint. Another important drawback of welds produced by FSW is the difference in microstructure and mechanical properties on the advancing and retreating sides. Reversed rotations of the shoulder and the pin alleviate the symmetry of temperature distribution across the AS and RS, thus reducing the above difference. Thus, RDRFSW increase the weld integrity [80,81]. The properties of RDRFSW joints increase by increasing one of the two rotation speeds simultaneously with the traverse speed while keeping the other rotation speed constant or by increasing the rotation speed of pin and decreasing that of shoulder while keeping the traverse speed constant [82].

Fig. 8(b) and (c) shows the macrograph and typical microstructure of the welded joint in RDRFSW [76]. Owing to the complex thermomechanical action of the tool, the welded joint can be divided into five different regions, shoulder affected zone (SAZ), SZ and TMAZ, HAZ and BM. Grain structures of the SZ and SAZ are recrystallized and equiaxed. However, the grain size in the SAZ is larger than that in the SZ. The grains of the TMAZ are elongated in the direction of shear stress [76] while those in the HAZ are coarser with their average size approaching the grain size in the BM. One of the useful outcomes of the reverse rotation is the higher grain refinement in both SZ and SAZ. The TMAZ and HAZ constitute metastable coarse precipitates while the SZ comprises of smaller and stable precipitates [78].

Based on the available studies, RDRFSW seems to be a useful variant of FSW. However, this process has been applied only to aluminium alloys. More research is necessary to validate its effectiveness to other materials. Another similar process as RDRFSW is the dual rotation speed FSW (DRFSW) [83]. In this method, the shoulder and the pin are rotated independently at different rotation speeds but in the same direction. The main welding parameters of this process are similar as the RDRFSW process. The pin rotation speed has a major contribution to the formation of the SZ and onion ring. The opposite rotations of the shoulder and the pin lead to improvement in the weld properties. This is due to the decrease in microstructure asymmetry about the weld centerline by the oppositely rotating parts of the tool. In addition, the higher rotation speed of the stir pin improves the welding efficiency while the lower rotation speed of the shoulder improves weld formation [84].

2.2.3. Bobbin tool friction stir welding (BTFSW)

The BTFSW process uses a bobbin tool which constitutes two shoulders, one above and one below the workpiece [85–92]. A pin connects the two shoulders and penetrates entirely through the workpiece thickness during the welding. There are two types of bobbins, or self-reacting techniques, one that adopts a fixed gap between the shoulders and the other that is adaptive and allows a gap between the shoulders which can be adjusted during the welding [85–87]. The self-reacting principle of the bobbin technique means that the requirement of downward axial force is lowered or eliminated.

Fig. 9(a) and (b) shows the bobbin tools while Fig. 9(c) and (d) shows the BTFSW process. BTFSW process starts either by driving the tool onto the edge of the plates or from a pre-drilled hole

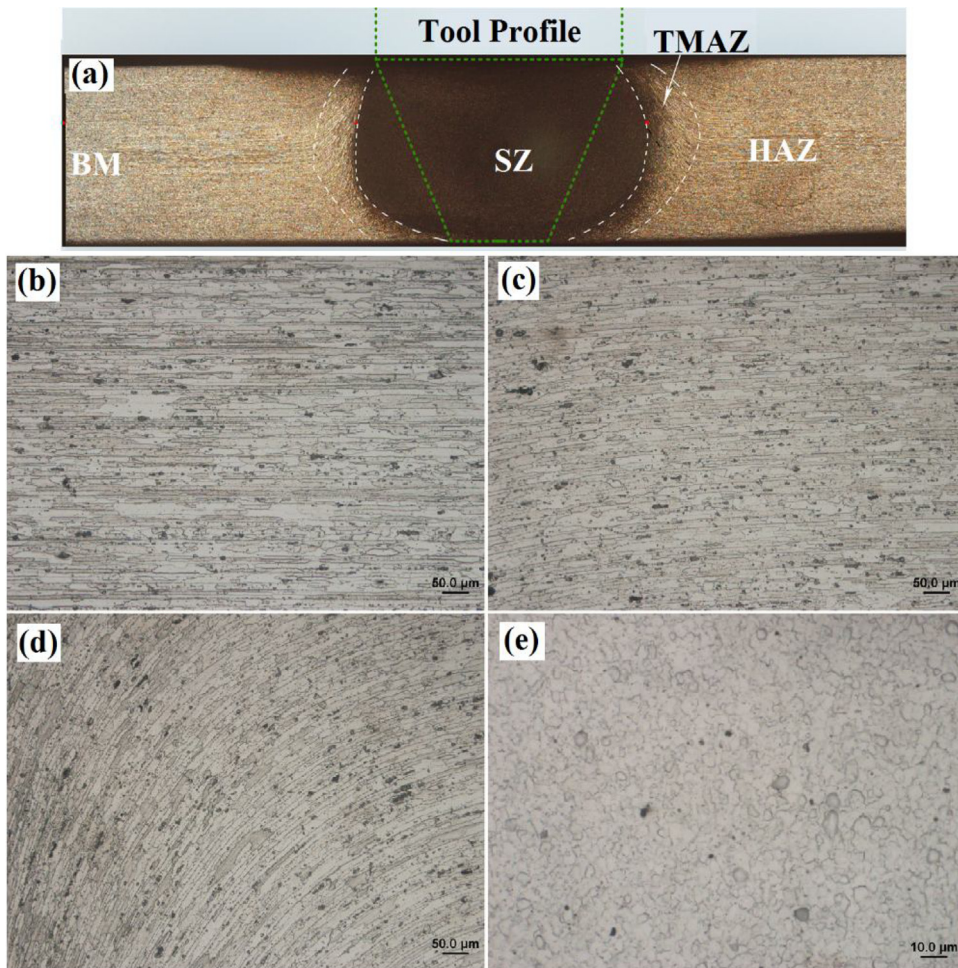


Fig. 7. Optical micrographs of SSFSWed Al 7075-T651 (a) macrograph, (b) BM, (c) TMAZ, (d) HAZ, (e) SZ [72].

between the abutting plates. The welding process starts with a slow travel speed until the start of plastic deformation, followed by an acceleration of the travel speed to a final steady state value [87]. In another method, the process starts by ensuring sufficient initial plasticization of workpiece surface in contact with the rotating bobbin before starting the traverse [86]. In BTFSW, the two shoulders generate sufficient frictional and deformation heat from either sides of the workpiece. This causes reactive forces to be contained within the tool, eliminating the possibility of compressive deformation of the pin [86].

The main process parameters in the BTFSW process are spindle rotation speed and tool traverse speed, though other variables such as dwell time, tool gap, support/clamp setting and plate condition may also influence the joint. The process conditions also depend upon variables such as tool geometry, features and other process settings. The recommended necessary parameters for BTFSW of Al alloys are rotation speeds of 450–600 rpm and travel speeds of 75–100 mm/min for thin aluminium plates (4–8 mm) and 170–300 rpm and 100–500 mm/min for thicker plates (about 25 mm) [88]. In BTFSW, increase in the ratio of the rotation speed to traverse speed increase the grain size while the weld quality and mechanical properties are improved with a low heat input, i.e., at lower rotation speeds or higher traverse speeds [89].

A typical weld macrograph of BTFSW process is shown in Fig. 10(a). The macrograph is typical of an FSW joint, constituting the SZ, TMAZ and HAZ. The SZ of BTFSW is dumbbell or hour-glass shaped, roughly presenting the association of two oppositely placed SZs of FSW with reduced shoulder width. The dumbbell

shape becomes unclear at higher traverse speeds [90]. The weld region has an upper SZ and a lower SZ, both recrystallized and equiaxed. The grain refinement is higher in the upper SZ. The TMAZ constitutes deformed, rotated and elongated grains, similar to the FSW. However, the onion ring region of FSW has been replaced by an ellipse-shaped region and a triangle-shaped region in the middle layer of SZ, as magnified in Fig. 10(b). These new regions in the BTFSW are due to insufficient deformation and stirring of the region. However, their sizes follow opposite trends with heat input [90–92]. With increase in traverse speed, the triangle size increases while the ellipse size decreases. Thus, these regions would be resulted due to mutually opposite effects.

BTFSW has been performed on Al, Mg and Fe alloys. This process is useful in overcoming several limitations of FSW process and can successfully weld thick sections. For example, the flexibility of the FSW process is restricted due to the backing plate support that carries the applied loads. As a result, FSW of closed hollow extrusions or complex shaped large structures becomes a daunting task. Also, root flaw defect can be formed during FSW if the tool pin is short or the shoulder plunge depth is incorrectly set [90]. On the other hand, no backing plate is necessary in BTFSW because the bobbin tool does not require an applied downward plunging force. A major part of the load is carried within the pin while the bottom shoulder of the bobbin can substitute the backing plate. Therefore, the BTFSW provides greater process flexibility and can be used for closed hollow extrusions and complex structures. In addition, the pin connecting the bobbin shoulders penetrates through the entire workpiece thickness, providing greater microstructure homogeneity.

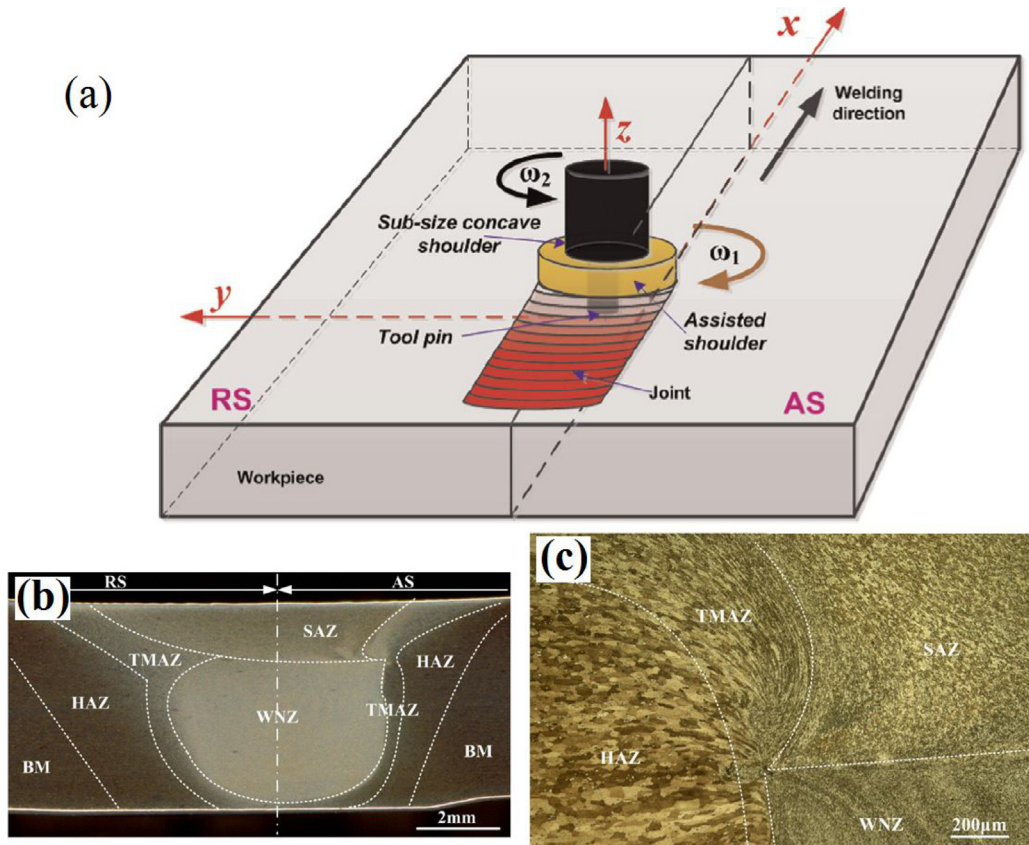


Fig. 8. (a) Schematic of RDRFSW; aluminium alloy 2219-T6 welded joint prepared by RDRFSW [77], (b) Macrograph [76], and (c) Microstructure [76].

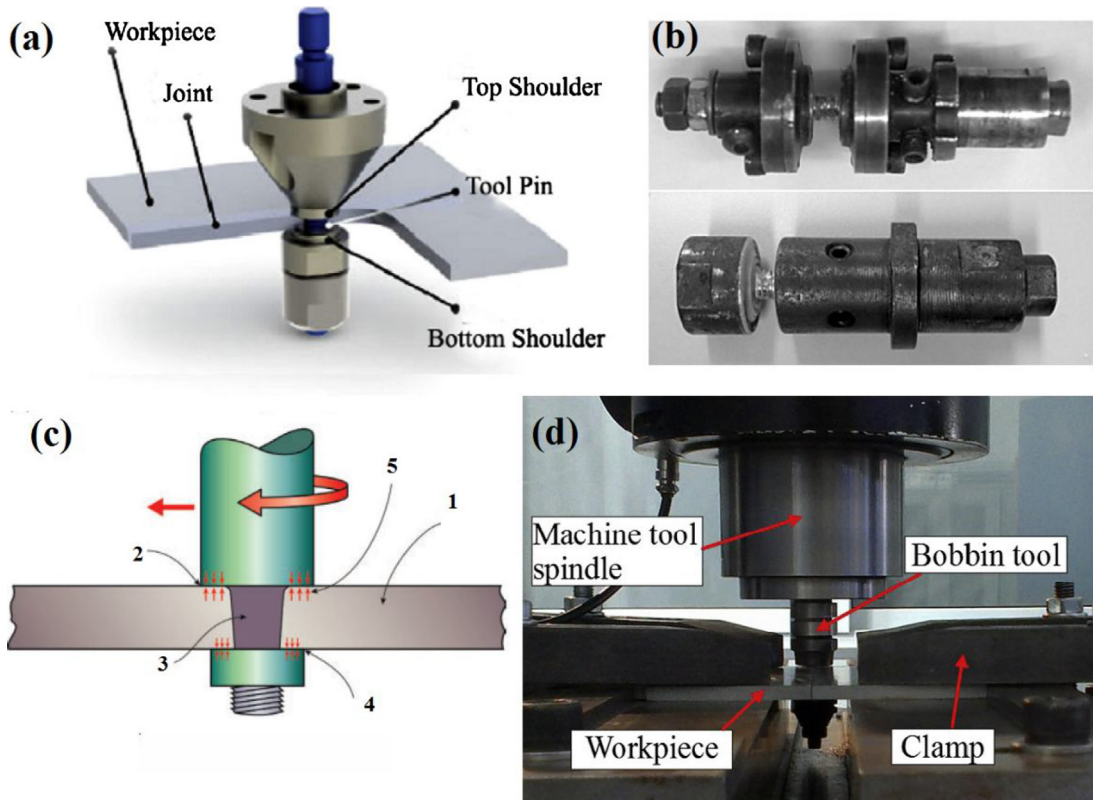


Fig. 9. Bobbin tool (a) Schematic [89], and (b) photograph [88]; BTFSW process (c) schematic, 1: workpiece, 2: top shoulder, 3: pin, 4: bottom shoulder, 5: acting forces [86], and (d) experimental setup [90].

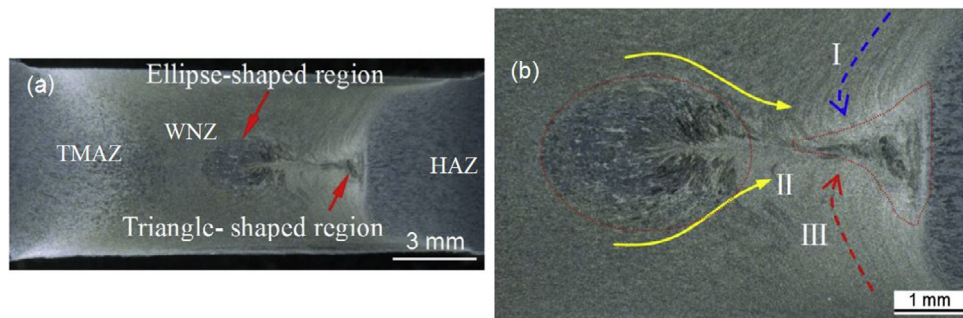


Fig. 10. Macrograph of weld in BTFSW process [90].

ity in thick section welding. Such ability of the BTFSW to weld a thick workpiece simultaneously from both sides ensures prevention of root flaw formation [90]. Some other developments include counter rotating twin tool and self-supporting tool based FSW processes [93–96]. In both cases, the weld quality is a function of tool rotation speed and traverse speed [93,94]. These processes are still in their infancy and further investigations are necessary for their evaluation.

Besides the above modified FSW processes, there are certain process variants of FSW which combine an auxiliary energy field such as a thermal energy field induced by electricity, laser, arc or plasma sources or a mechanical energy field induced by ultrasonic vibrations to FSW. The secondary energies have contributed to the improvement in material flow, process effectiveness, productivity and quality of the product of the FSW process either by complimenting the heat generation, as seen in thermally assisted FSW processes, or by inducing direct assistant softening of workpiece material, as in ultrasonically assisted FSW processes [17]. The experimental and numerical investigations of these processes are gradually emerging and would find more exploration in the near future. A detailed preliminary review on these auxiliary energy assisted FSW process variants has been presented elsewhere [17].

2.3. Friction stir spot welding (FSSW)

Friction stir spot welding (FSSW) is a variant of FSW, used mainly for the joining of difficult-to-weld sheets in lap configuration. This process is analogous to a process of FSW minus the lateral movement of tool. FSSW is a solid state joining process requiring no consumables, or shielding gas and is energy efficient [97]. FSSW was first performed by industries, Sumitomo Light Metal Industries, Ltd., Mazda, Kawasaki Heavy Industries, Ltd., and Norsk Hydro to eliminate the need for riveting and reduce the weight of component [98,99]. Since then, the process has found extensive application in the spot welding of a wide variety of metals and applications. At present, several types of FSSW processes such as the conventional FSSW [97–100], Refill FSSW (RFSSW) [101,102], and pin-less processes such as rotating anvil FSSW (RAFSSW) and double-sided FSSW [103–105] are in existence. Other variations of FSSW processes are short FSW processes known as 'stitch FSSW' [98,99,106–110] and 'swing FSSW' [98,99,111–113].

2.3.1. Process features of different variants of FSSW

2.3.1.1. FSSW. The various stages of FSSW process are shown in Fig. 11(a) [97–100]. At the plunge stage, the threaded pin of the rotating tool is plunged into the overlapping sheets. The friction heat generated between the tool and top workpiece softens the workpiece while the threading of the pin causes material flow. When the tool shoulder contacts the sheet surface, a high downward forging pressure is generated. Subsequently, the tool is fed further into the overlapping sheets and may be allowed to dwell

for a short period before being retracted. This produces a solid state bond at the interface between the two sheets, shown in Fig. 8(a).

During the plunge stage, material below the pin is extruded upward to the pin periphery [114], while the bonding occurs even before the pin plunges into the lower sheet due to deformation and diffusion of workpiece material at the pin tip. The material flow constitutes rotational, horizontal and vertical movement of the material [115]. Further actions of the pin establishes the bond formation. In FSSW, a dwell stage is not mandatory. One drawback of this process is the exit hole which is a dynamic imprint created by the tool on the joint during retraction. This exit hole can be filled with special tool design or by post-processing.

2.3.1.2. Refill FSSW. This is an improvised FSSW process which enables friction stir spot welding without an exit hole on the joint. Fig. 11(b) shows the various stages of refill FSSW process [98,101,102]. In refill FSSW, a purpose-built system creates a spot weld without an exit hole by nominally flushing it with the original workpiece surface. The system consists of three components, a clamp ring, a shoulder, and a pin, each acting independently during the welding.

During the welding, first, the clamp holds the overlapped workpieces. Subsequently, the rotating shoulder makes contact with the top workpiece while the pin remains retracted. Frictional heat at the shoulder-workpiece interface begins to heat and soften the workpiece. After sufficient heat generation, the pin is plunged into the workpiece while the shoulder is retracted enough to create a space to contain the workpiece material displaced by the pin. After a dwell period, the pin is retracted and the shoulder is gradually lowered towards the workpiece. This brings the displaced material back into the weld zone and fill the exit hole. The process is completed when the pin is completely retracted back into the shoulder.

2.3.1.3. RAFSSW and double-sided FSSW. Pin-less tools are low-cost alternatives of FSSW. Both the RAFSSW and double-sided FSSW processes adopt pin-less designs. RAFSSW is a one-sided pin-less FSSW process, which applies only a rotating shoulder for heat generation and massive forging loads for subsequent spot welding. An anvil is used to support the massive forging loads applied during the pin-less FSSW. This process leaves no exit hole, but the weldable sheet thickness is limited to 1 mm.

Double-sided FSSW, an improved variant of the single-sided RAFSSW, is meant to spot weld sheets of higher thickness. A schematic of the double-sided FSSW has been shown in Fig. 11(c). In this process, the workpieces clamped in a lap configuration are plunged from the top and bottom surfaces by a rotating pin-less tool shoulder and a rotating anvil, respectively. The rotation and forging from both sides are continued at the dwell stage which generate the required frictional heat and material deformation for the spot welding. It appears that the material flows from beneath the center of tool shoulder toward its edge, then downward and back towards

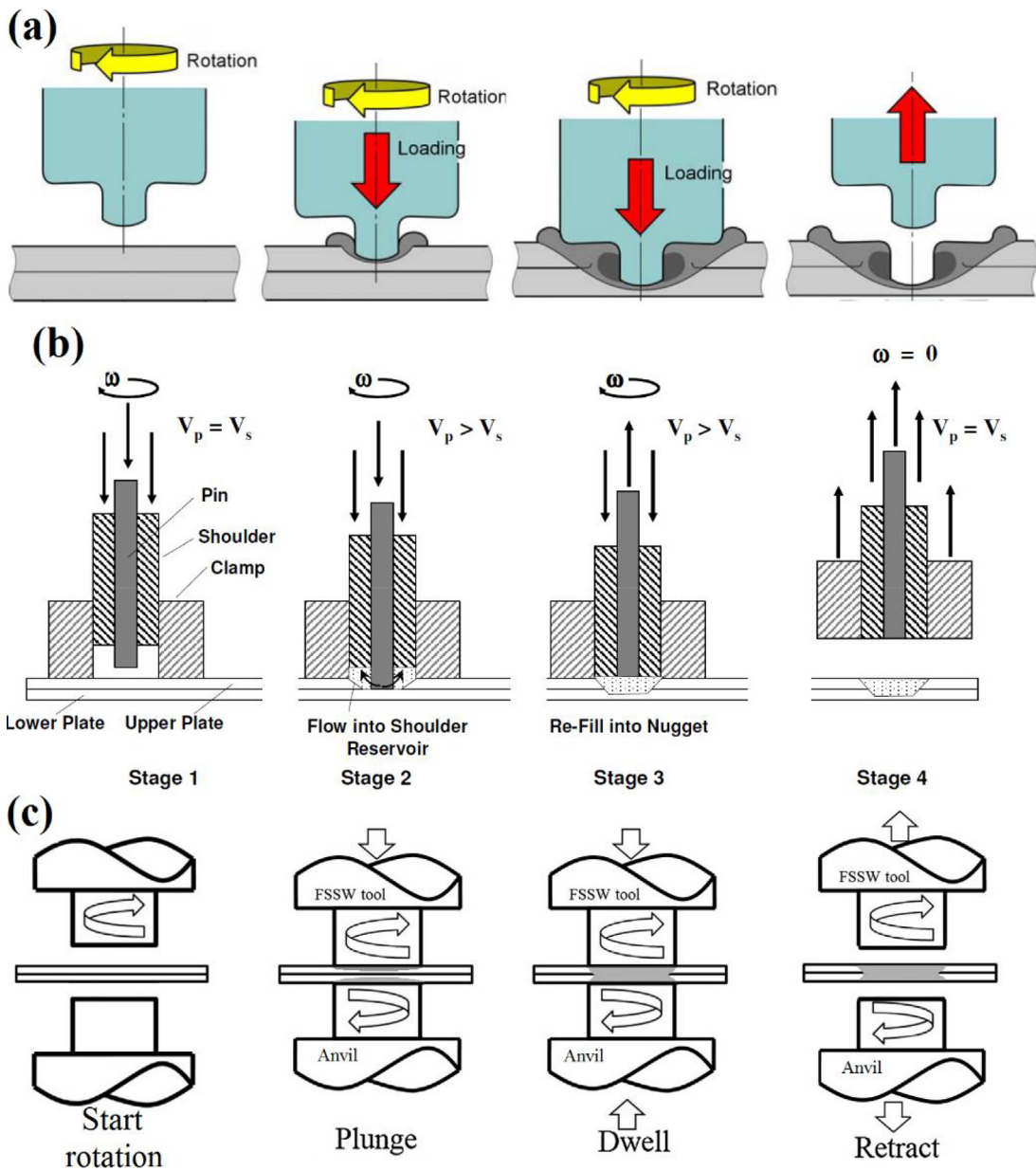


Fig. 11. Schematics of different process stages of (a) FSSW, (b) Refill FSSW [98], and (c) double sided FSSW.

the weld center [103]. The materials pushed down by the shoulder and pushed up by the rotating anvil meet along the interface to form the joint.

2.3.1.4. Short traverse FSSW processes. Other variants of FSSW such as stitch FSSW and swing FSSW use a very short tool traverse after the FSSW. The traverse is to produce a joints with larger joining area to achieve higher strength. The processes are illustrated in Fig. 12. Both the processes are designed for robotic operations. In the stitch FSSW, the tool holder follows a circular or octagonal path about an axis and produces a joint length of approximately 8 mm to 18 mm, as shown in Fig. 12(a) [98,106–110]. In swing FSSW, the tool swings in a small circular angle at the tool-holder axis via a cam drive system to generate a short 5 mm stitched FSSW joint, as shown in Fig. 12(b) [111–113]. The strength of joint made by swing FSSW is typically higher than that made by the non-swing FSSW [98].

2.3.2. Process parameters in FSSW

The main process parameters of FSSW affecting the joint quality are rotation speed, plunge rate, plunge depth and dwell time [116–121]. Lower rotation speeds produce more extensive stir in the material, larger stir zone and welds of higher weld interface, failure load and higher tensile shear strength. Heat input increases at higher rotation speed, higher plunge depth and lower plunge rate. The increase in dwell time also has a minor contribution towards improvement in joint strength [118].

Pin length and tool geometry are other important criteria that determine the nature of material flow, hook formation and the joint produced [121,122]. Pin length increases the size of stir zone and joint tensile strength. A hook is a partial metallurgical bond in the weld region between the overlapped metal sheets. Welds made with the cylindrical pin have a continuous hook pointing downwards while triangular pins produce an upward hook which is arrested at stir zone boundary [118]. To summarize, the process

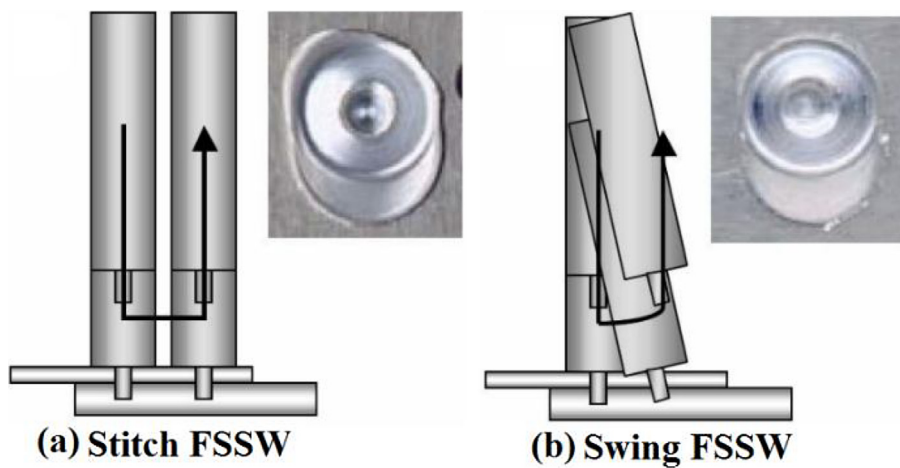


Fig. 12. Short traverse FSSW processes (a) stitch FSSW, and (b) swing FSSW [98].

parameters, and tool geometry must be optimized to achieve a sound friction stir spot weld.

2.3.3. Microstructure of friction stir spot weld

Fig. 13(a) shows the typical macrograph of a weld in FSSW. The weld constitutes an exit hole and stir zone. The exit hole is a dynamic indentation of pin and shoulder of the tool. In Fig. 13(a), the stir zone is separated from the rest of the weld by a dotted white line. The bottom surface of the stir zone is kept almost flat except near the central hole. In the SZ, the 'pin side' area shows the area where the upper and lower sheets are bonded. Outside the pin side area, the interfacial surface of the upper and lower sheets is slightly distorted into a macroscopic curved interface. Fig. 13(b–f) shows the microstructures of different zones of friction stir spot welded aluminium alloy. The refined grains of the pin bottom and pin side zones are highly recrystallized and equiaxed. Next to the SZ is the TMAZ which is followed by HAZ and BM. The grains in TMAZ are finer, distorted and elongated while those in HAZ are coarsened. These features are similar to those in the welds of FSW.

2.3.4. Feasibility and application

With proper selection of tool material, tool geometry and process parameters, FSSW is feasible to a wide variety of ferrous and nonferrous materials. The process combined with robotics has been applied for mass production in various industries such as aerospace, automotive and metal working industries. FSSW has been employed for the spot welding of a wide variety of materials which includes polymers, ferrous and nonferrous metals [97–109,95,107].

2.4. Friction stir riveting (FSR)

Mechanical fastening is an important area of material joining, fabrication and manufacturing which involves joining of two overlapped plates or components. Riveting is a globally accepted mechanical fastening process which goes well with most high strength metal alloys. However, mechanical fastening of the lightweight alloys such as aluminium and magnesium alloys and their joining to polymeric materials still throws many challenges. With the emergence and rapid advances in solid state technologies, realization of lightweight designs have become feasible, reliable and economic.

Solid state processes such as friction hydro pillar processing (FHPP) and friction taper stud welding (FTSW), self-piercing riveting (SPR) and friction stir spot welding (FSSW) are useful for the fastening of the lightweight materials [125–130]. However, the

above processes are associated with limitations such as pre-drilling of compromising holes, and absence of metallurgical bonding between the joined parts which make the fastening fully dependent on mechanical locking and rupture of material due to excessive deformation of bottom material at the riveting site. FSSW may solve these issues, but leave an undesirable exit hole [131–135] which would increase the cost of the fastening. In the efforts to simultaneously avoid the above limitations and reduce the process cost, several friction stir based fastening/riveting processes (FSR) have been developed in the recent years. This section provides an overview of these FSR processes.

2.4.1. FSR process features

It has been observed frequently in the literature that a solid state technology can be classified as a friction stir technology if rotational movement of one of the joining partners, particularly the consumable/non-consumable tools or fasteners generate frictional heat that provides the driving force for the process. Based on this criteria, the several types of friction stir riveting processes found in literature are friction riveting or FricRiveting (FR) [135–141], friction stir blind riveting (FSBR) [142–152], friction self-piercing riveting (FSPR) [130,153,154], rotation friction drilling riveting (RFDR) [155], and rotation friction drilling riveting (RFPR) [156].

Each of these riveting processes has been employed to fasten different combinations of joining partners in lap configuration. The types of rivets employed and the different stages involved in each of the FSR processes are shown in Fig. 14. Apart from these, recently, at the University of Toledo, a process has been developed in the name of friction stir riveting (FSR), that combines the principles of self-piercing riveting and friction stir welding. In this process, a rivet is drilled into overlaid workpieces by a rotating driver to a predefined depth [131–134]. It is evident that the working principle of each of these processes involve four basic stages, which are briefly discussed below.

2.4.1.1. Friction riveting or FricRiveting (FR).

FricRiveting is applied mainly to fasten polymer-metal combinations in lap configuration using cylindrical metallic rivets [137–139]. This process works on the principles of mechanical fastening and friction welding. FR constitutes four stages, initial feed, heating, forging and consolidation, as shown in Fig. 14 [137–142]. The initial feed stage involves pressing of a rotating rivet against the surface of plastic/polymer component partners which are lap-held against the metal partner(s) and the lap assembly is clamped (Fig. 14(a) of FricRiveting). Axial displacement of the rivet in the polymer is absent at this stage [138]. The heating stage involves gen-

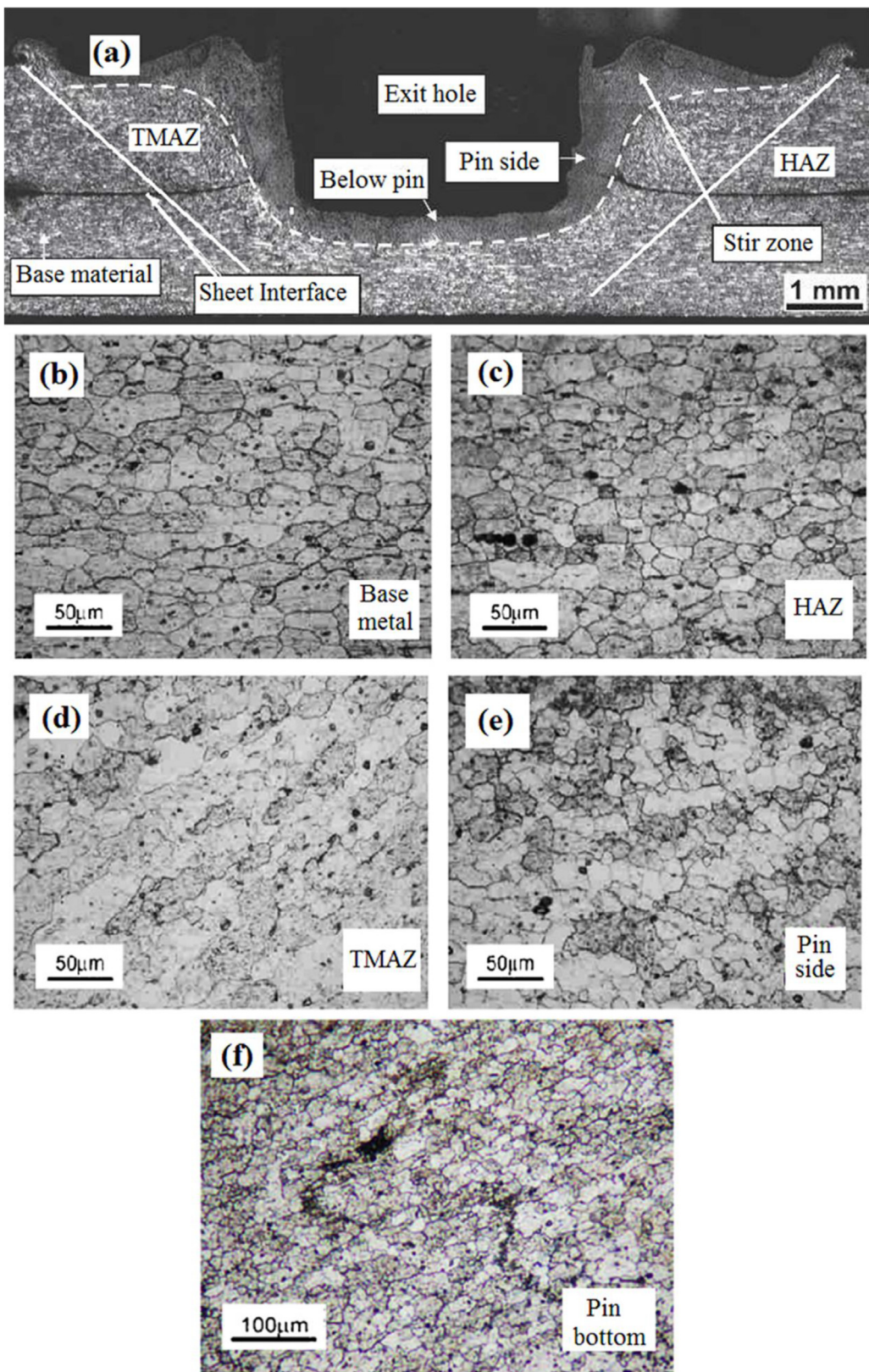


Fig. 13. Macrograph of a friction stir spot welded 7075-T6 alloy [123], and (b–f) Close up views of different regions in friction stir spot welded 6061-T6 alloy [124].

eration of a very thin plasticized/molten film on the polymer surface due to the frictional heat around the rivet tip by the high rotation speed and applied axial force, the penetration of the rivet into the polymer part, the ejection of a flash of plasti-

cized/molten polymer out of the joint and the softening of the rivet tip due to an increase in the local temperature combined with the low conductivity and high thermal expansion coefficient of the softened polymer (Fig. 14(b) of FricRiveting). Also, this stage

Process	Stages				Type of Rivet
	(a)	(b)	(c)	(d)	
FricRiveting					 M8 > M5
FSBR					 FSBR Conventional Rivet Modified Rivet
FSPR					 FSPR
RFDR					 RFDR Rivet cap Grip rod Shank 10mm
RFPR					 (a) Shank, Grip rod, Rivet cap, Plug (b) Rivet cross-section 10mm

Fig. 14. Schematic diagrams and types of rivets of the different FSR processes, FricRiveting [137,140], FSBR [142], FSPR [130], RFDR [155] RFPR [156].

marks the steady and unsteady states of viscous heat dissipation.

Increase in axial displacement of rivet with time is non-linear in the unsteady state, while it is linear in the steady state. In the forging phase, deceleration of rotation and increase of axial force causes the plasticized rivet tip to push the rest of the softened polymer to the flash and to encounter the resistance from the colder volumes of polymer. A sharp increase in the axial displacement rate occurs. These make the rivet tip to deform to diameters wider than the rivet shaft (Fig. 14(c) of FricRiveting). In the consolidation phase, the joint solidifies under pressure and it is subsequently held by the forces driving the deformed rivet tip into the plastic component and by the adhesive forces in the polymer/metal interface (Fig. 14(d) of FricRiveting). The axial displacement of rivet reaches a maximum and remains constant. The flash material can be either kept hidden into cavities placed in the rivet head or removed later. FricRiveting also allows fastening of metal-polymer-metal combinations where additional perforations in the metallic partners permit the penetration of the metallic rivet and allow formation of rivet-metal weld seams for extra anchoring [135,136,141].

2.4.1.2. Friction stir blind riveting (FSBR). FSBR process, a combination of friction stir riveting and blind riveting concepts, is recently developed mainly for one-sided joining of thick gauge sheets of similar and dissimilar alloys [127,142–152]. FSBR involves four basic stages of riveting process. At stage 1, a blind rivet along with its mandrel rotating at high speed ($\omega = 6000\text{--}12,000 \text{ rpm}$ [143]) is brought into contact with the top workpiece (Fig. 14(a) of FSBR).

At stage 2, the rotating blind rivet driven into the workpiece generates frictional heat between the rivet-workpiece interfaces and softens the workpiece material, thereby providing a friction stirrable path for the rivet to traverse through the workpiece. Under a lower driving force and torque, the rotating rivet along with its sharp mandrel can achieve full penetration into both workpieces (Fig. 14(b) of FSBR).

At stage 3, the rotation of the fully penetrated rivet is ceased and the setup is allowed to cool down to harden the soft phase. Subsequently, the rivet is pulled using the internal mandrel with sufficient outward axial force to upset the shank and fasten the workpieces together (Fig. 14(c) of FSBR). Once the withdrawing force surpasses the rated break-load of the mandrel, at stage 4, it notches and breaks the mandrel from the fastened rivet. In the process of pulling, creating the notch and fracturing the mandrel, both workpieces are locked tightly together (Fig. 14(d) of FSBR). Friction stir blind riveting, thus, do not require pre-drilled hole and has the advantage of one-sided accessibility [147].

2.4.1.3. Friction self-piercing riveting (FSPR). The FSPR is a recent technology and employs the concepts of self-piercing riveting (SPR) and friction stir spot welding. In this process the rivet constitutes a hollow semi-tubular shank and a sharp bottom. This process has been employed for the fastening of dissimilar alloys, 1 mm thick AA6061-T6 and 2 mm thick magnesium alloy AZ31 B [130,153]. Fastening by FSPR involves four stages as follows. At rivet feed stage, lap configured dissimilar alloy sheets are clamped onto a die. A rivet

rotating at constant set speed and moving downward contacts the surface of the top sheet (*Fig. 14(a)*) of FSPR.

At hot riveting stage, the rotating rivet pierces through the top sheet (Al alloy), causing friction heat generation and softening of the top sheet material, into the low ductility bottom sheet, such as Mg alloy (AZ31B) to form interlock (*Fig. 14(b)* of FSPR). At the in-situ friction stage, the downward feeding of the rivet stops, but its rotation continues for a fixed dwell time to generate additional heat for achieving solid state joining. The dwell time can be varied to control the temperature at the dissimilar interface (*Fig. 14(c)* of FSPR).

At off stage, the rotation motion of the rivet stops quickly to produce a stationary contact between the rivet and surrounding metal so that solid-state joining can be formed along the contact surfaces (*Fig. 14(d)* of FSPR). FSPR uses two types of rivets, one can be driven from the outside of the rivet, as shown in *Fig. 11* and the other, from the inside of the rivet [153].

2.4.1.4. Rotation friction drilling riveting (RFDR) [154]. RFDR is also a relatively new technology and is a partial combination of concepts of SPR and FSBR and is somewhat similar to the FSPR process. The rivet constitutes a semi-tubular shank, a rivet cap and a grip rod. As shown in *Fig. 14*, the rivet used in RFDR is similar to that in the FSPR with respect to its shank. However, the grip rod in the two processes are different. This process uses a drilling machine equipped with a steel die comprising of a small pipped cavity. A lone documented study on the RFDR process is the fastening of two or more Mg alloys.

As shown in *Fig. 14*, RFDR consists of the following four stages. Two or more overlapped magnesium alloy sheets are clamped firmly against a base plate with the pipped cavity die. The rivet, rotating at a pre-set speed (up to 6000 rpm), is brought to contact with the sheets-to-be-riveted by a drilling machine. Friction heat is generated at the rivet-sheet interface, as the sheet material is softened (*Fig. 14(a)* of RFDR). This enables the rivet to drill through the sheet. The rotating rivet is plunged into the sheets by applying a lower downward axial force. While being plunged, the rivet pierces through the top sheet and flares into the bottom sheet due to the action of the pip in the cavity die. This results in the formation of a mechanical interlock between the rivet and the sheets, fastening the sheets together.

After the full insertion, rotation of the rivet is stopped (*Fig. 14(b)* of RFDR). Immediately, a pre-set downward pressure is applied to the rivet for 3 s to further ensure a good interlocking (*Fig. 14(c)* of RFDR). The downward pressure is withdrawn, and the grip rod of the rivet is cut off to achieve the RFDR joint (*Fig. 14(d)* of RFDR). The difference in working principle between FSPR and RFDR lies at the later stages of the process. In the former method, feed force was withdrawn and rivet rotation was continued while in the later, it is the inverse.

2.4.1.5. Rotation friction pressing riveting (RFPR) [155]. The RFPR process, similar to the RFDR process combines the ideas of SPR and FSBR. The authors of RFDR have slightly improvised the rivet, the die of the RFDR process, improvised the method of flaring of rivet in the bottom sheet to develop the FSPR, and applied it to join Mg alloys. In RFPR, the rivet consists of a grip rod, a rivet cap, a semi-tubular shank and a separate plug, contrary to the rivet without a plug in RFDR processes, shown in *Fig. 14*. The process is conducted using a drilling machine equipped with a steel die. The die constituted a hole of 8 mm diameter at the middle and a punch in the hole to punch the plug.

The different stages of RFPR process, shown in *Fig. 14*, can be described as follows: 1) The rivet with its plug, driven at a pre-set high rotation speed, brought into contact with the to-be-riveted sheets for 3 s, thereby generating frictional heat between the rivet and the sheets, which softens the sheet materials (*Fig. 14(a)* of

RFPR). 2) The rotating rivet is driven into the softened sheets under reduced downward axial force and torque until it is fully inserted (*Fig. 14(b)* of RFPR). 3) After the full insertion, the rivet is stopped from rotating, and the plug is immediately pressed into the shank of rivet by pushing the punch upward. Under the plug action, the end of the rivet shank expands, forming a rivet-sheet mechanical interlock and fastening the sheets together (*Fig. 14(c)* of RFPR). 4) The downward pressure is withdrawn and the grip rod is cut off (*Fig. 14(d)* of RFPR). Like the RFDR, the RFPR process eliminates the need for pre-drilling a hole. Also, cracking of sensitive areas can be avoided due to the softening of metal sheets.

2.4.2. Process parameters in FSR

In FricRiveting, the main process parameters are the rivet rotation speed, joining time and joining pressure while heating time, rivet burn-off, burn-off rate, temperature and frictional torque are the process variables [137,139]. Rotation speed is responsible for the friction heat generation, molten polymer viscosity and thermal defect formation. Joining time corresponds to joining speed, volumetric defects and supply of heat energy to the softened polymeric film. The major role of joining pressure is to control the rivet forging and solidification while also contributing towards the control of joining speed and heating of the contacting interfaces.

In FSBR, spindle rotation speed and axial feed rate, off-axis angle and rivet cap diameter are the main process parameters [147]. Successful joint formation in dissimilar fastening process also depend upon the overlapping order [143]. Low ductility sheets (Mg sheets) at the top and high strength sheets (Al-sheets) at the bottom can produce sound fastening. In such an overlap, higher rotation speeds, 9000 rpm, produce more heat, reduce the penetration force, and thus, allow successful fastening even at higher feed rates (up to 780 mm/min). For lower and moderate rotation speeds, 2000 rpm–6000 rpm, low to moderate feed rates are ideal for sound fastening.

When the overlap is in the reverse order, fastening is successful at moderate rotation speeds and feed rates. If time is a constraint for parameter optimization, lower moderate rotation speeds (6000 rpm) and feed rates (270 rpm) would be ideal for the fastening of Mg/Al sheets, however, it is highly recommended to optimize the parameters. In the joining with carbon fiber-reinforced polymer composite on top and Al-alloy sheets at the bottom, low rotation speeds (3000 rpm) could produce good joining only up to low feed rates (120 mm/min), moderate rotation speeds (6000 rpm) up to 270 mm/min and high rotation speeds (9000 rpm) up to 420 mm/min [145]. In the FSBR of AZ31 B Mg alloys and high-strength DP600 steel, a rotation speed of 2200 rpm has caused increase in strength with increasing feed rates [148,149]. However, in the fastening of a non-heat treatable aluminium alloy, none of the above process parameters seem to affect the joint strength of the riveted component. Therefore, optimization of process parameter is essential in FSBR.

In FSPR, rivet feed rate, rivet rotation speed and dwell time are the main process parameters. Rivet feed rate and rivet rotation speed are mutually responsible for the mechanical connection between the rivet and the sheets while the dwell time affects the solid-state connection during the in-situ friction stage [130]. In a lap configuration with 2 mm thick AZ31 B at bottom and 1 mm AA6061-T6 at top, high rotation speeds have resulted better joints due to adequate frictional heat for deformation and rivet leg flaring, but, too high rivet feed rates would increase the propensity to crack [130]. Higher rivet feed rates increase the expansion value but allow shorter time for friction heat generation and induce insufficient deformation of the lower sheet. Also, the higher feed rates influence the stability of platform/die, leading to large gaps between rivet leg and bottom plate. Hence, lower feed rates are better for sound fastening [130,153,154].

In RFDR, rivet shank length, rivet rotation speed and downward pressure are the main process parameters. In the lone available study, this process is used to rivet 2 mm thick AZ31 alloy sheets. Shank length determines the appearance of the RDFR joint and partially contributes to the interlocking (i.e., amount of expansion of the radius of rivet shank), shear strength and integrity of the joint. The rivet rotation speed has no significant influence on the interlock and shear strength of the joint at given shank length and downward pressure [155]. Therefore, RFDR process is feasible over a large window of rivet rotation speeds. Increasing the downward pressure improves the interlocking and the shear strength to a certain extent. But excessive downward pressures should be avoided because they would increase the process cost without any improvement and even deteriorate the joint.

In RFPR, punch pressure is a decisive process parameter besides the rivet shank length, rotation speed, and downward pressure [156]. Rivet rotation speed has no visible effect on joint strength or integrity. But higher rotation speeds, producing more frictional heat during the RFPR operation, would soften the to-be-riveted sheets quickly and thus reduce the process time. A higher punch pressure increases the interlock but is not necessarily always beneficial for enhancing the shear strength of RFPR joints because excessive high punch pressure leads to heavy deformation of the punch, degradation of the bottom sheet and ultimately, failure of joint. In the FSR process investigated at the University of Toledo, interface curl, mixed zone, depth of penetration, volumes of dies and clamping force affect the quality of riveted joints significantly [131]. Use of die and clamping improves the riveting quality. Adequate penetration and small interface curl up presents a good riveting [132–135].

2.4.3. Metallurgical features of friction stir riveted parts

The FricRiveting process has been developed mainly for producing polymer-metal multi-metal structures such as polyether-imide/AA 2024-T351, Ti-6Al-4V/pultruded glass fiber reinforced thermoset polyester and Ti alloy/short-fibre reinforced polyether ether ketone hybrid joints [136–141]. Generally, the bulk of the virtual FricRiveting joint is supposed to contain a larger volume of the polymer, an intermediate sized volume known as the anchoring zone, defined by the volume of deformed rivet tip, and a much smaller volume of mechanical flaw/voids such as trapped air, volatile evolution and thermally charged content [139].

Fig. 15(a) shows the schematic of a FricRiveting joint microstructure. There are five different microstructural zones: the polymer heat-affected zone (PHAZ), the polymer thermo-mechanically affected zone (PTMAZ), the metal heat affected zone (MHAZ), the metal thermo-mechanically affected zone (MTMAZ) and the anchoring zone (AZ). Apart from these, two types of distinct interfaces exist in the joints, metal-polymer and polymer-polymer interfaces. The metal-polymer interface exists at the interface of PTMAZ and MTMAZ in the AZ while the polymer-polymer interface is the PTMAZ and PHAZ.

The MHAZ is affected only by heat, hence, recovery and age hardening re-precipitation are the main phenomena of microstructure evolution depending upon the alloy type and maximum temperature. PTMAZ receives both heat and plastic deformation. Hence recovery and recrystallization are inevitable. AZ is the region where the tip of the rivet is severely deformed due to the imposed loading. The load bearing through mechanical interference with the polymer base material produce the paraboloid AZ. PHAZ is effected by temperatures lower than its glass transition temperature or softening temperature. PTMAZ receives temperatures exceeding the softening point, and is evolved by shear deformation. The mechanical flaws in the polymer structure originate from volatile formation, cooling shrinkage and can be detrimental towards the joint [139].

The cross sectional view of joints in FSBR, FSPR, RFDR and RFPR are shown in **Fig. 15(b)** through e. It is clear that these consolidated joints have certain distinct features. However, it is surprising to learn that no dedicated study on the joint microstructure in these processes has been reported so far. It seems that the research interest revolves around improving the interlocking features of the joint which improve the shear strength, as shown in **Fig. 15(b)**. Some investigations on IMC formation, solid state connection and defect analysis has been carried out. In that particular study of FSPR [130], all the red dotted locations of **Fig. 15(c)** exhibit formation of intermetallic compound (IMC) layers. However, the location C, describing the interface of the riveted sheets, experiences the thickest intermetallic layer formation which further increase with increasing dwell time.

Solid state connection has been found at the rivet/Al and Al/Mg interfaces while the rivet/Mg interface has a gap. An EBSD study of Al 6111 alloy riveted by FSBR has shown a recrystallized SZ near the hole followed by three distinct TMAZs with different degrees of shear deformation and a HAZ next to the far-TMAZ [150]. In the FSR cross section, the region adjacent to the rivet is severely deformed and is known as the mixed zone as well as the TMAZ, as shown in **Fig. 15(f)** [131–134]. There is a need for more detailed studies on microstructure in these FSR processes to obtain comprehensive understanding of microstructure evolution in these processes and their effects on the joints.

2.4.4. Feasibility and application of FSR

As such, the FSR processes are employed to materials that are difficult to rivet, such as the softer (Al-alloys), low ductility (Mg-alloys), and brittle-but-low melting point (plastic polymers) materials. FricRiveting has been applied mainly to rivet thermoplastic polymers such as polyetherimide, pultruded glass fiber reinforced thermoset polyester and short-fibre reinforced polyether ether ketone with metals [135–141].

FSBR process has been used to rivet difficult-to-rivet separate dissimilar combinations of Mg alloy (AM60) – Al alloy (AA6022 and AA6082) [143], carbon fiber-reinforced polymer composite – Al alloy/Mg alloy [145,150], AA6111-T4 – AA6022-T4 [142,144], similar material joining of non-heat treatable Al 5052-H32 [147], Mg alloy (AZ31B-H32) – Al alloy (AA5754-O) [129] and various similar and dissimilar combinations of wrought Al-alloys (AA5005-H34, AA6013-T6, AA6260-T6 and AA6005A-T5), die cast Al-alloys (A380 and Aural-2 cast) and twin roll cast Mg alloy (AZ31B-O) [151]. An FSPR process, aimed at the riveting of low ductility materials, has been applied for the riveting of dissimilar alloys, AA6061-T6 and AZ31B. The FSPR should be considered successful because the joint has achieved 84% increase in shear strength [130,153,154].

Both the RFDR and RFPR processes have achieved successful riveting of 2 mm thick AB31 Mg alloy sheets, with improved shear strength and fatigue life as compared to conventional riveting processes [155,156]. The rivets used in these processes are mostly made of mild steel with a zinc coating. By adopting optimized process parameters, the aforesaid FSR processes seem to be reasonably successful and the properties of joints prove to be more attractive than the conventional solid state joining processes. The FSR processes have several advantages over the conventional solid state riveting processes. The FSR processes eliminate the need of a pre-drilled hole for rivet insertion. No external preheating is necessary with FSR process because the materials are simultaneously preheated in the process. Due to the softening of materials, the cracking of low ductility alloys can be effectively avoided. The softening reduces process loads and eliminates the requirement of preheating, holding these processes under economic check.

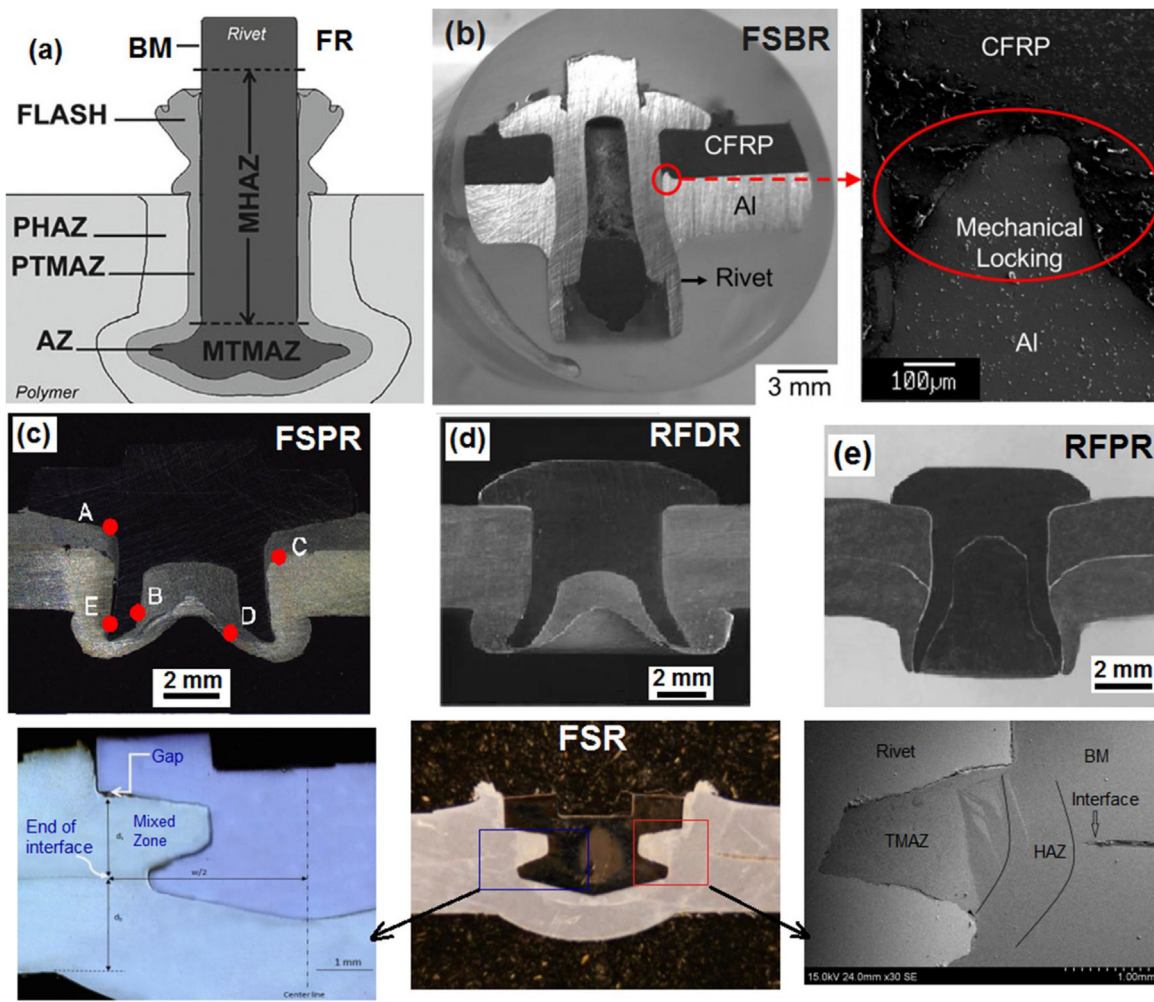


Fig. 15. Joint features in different types of FSR processes (a) FricRiveting [139], (b) FSBR [150], (c) FSPR [130], (d) RFDR [155], (e) RFPR [156], and (f) FSR [132].

2.5. Friction stir scribe (FSS)

Conventional FSW process of dissimilar materials with at least 20% difference in their melting points and 10% difference in their densities is unstable due to the large differences in flow stress. In conventional FSW of these materials, the material with lower melting point is plasticized much before the material with higher melting point and may flow away from the bonding area, causing insufficient bonding. Also, development of a brittle intermetallic compound layer at the interface of dissimilar materials is an issue [157].

Friction stir scribe (FSS) technology is developed recently for efficient lap joining of dissimilar materials that are chemically incompatible and have large difference in their melting points. FSS uses a specially designed tool where the tip of tool pin is integrated with a scribe cutter at a position off the center of the pin, as shown in Fig. 16(a) [158]. In a lap configuration where the softer metal is overlaid on the harder, a scribe cutter enables better stirring within the harder bottom metal [159]. The scribe cutter is a component of any material of higher strength and higher hardness than the two joining partners.

The scribe cutter is made of either the alloys of Ni, Ti, W, Rh, B, steel, carbide steel, polycrystalline cubic boron nitride (pCBN), Si₃N₄, or of combinations of these materials. A tool made of H13 steel integrated with a scribe cutter made of WC-Co complex has been reported [157–159]. In the lap dissimilar joining of materials where the material with low melting point is overlaid on that

with high melting point, the tool with the scribe cutter introduces a special mechanical interlocking geometry into the weld interface of the bottom material which enables effective dissimilar joining of the above incompatible materials.

2.5.1. Principle of the process

FSS is similar to the FSW in a lap configuration. The only difference is that FSS utilizes the innovative tooling that includes a tool with scribe cutter. FSS involves the same four stages of welding as FSW, i.e., plunging, dwelling, welding and retracting stages [160]. To lap-join a material combination with large difference in melting point and density, the tool with scribe cutter is plunged into the top material sheet in a manner that the scribe cuts through the top material in the lap stack and extends a distance 0.1–1.0 mm into the bottom material, as shown in Fig. 16(b). This plunge depth in the bottom material is less than or equal to the length of the scribe cutter.

In the plunge and dwell stages, the heat due to friction and deformation enables viscoplastic dissipation of the plasticized top material. On the other hand, the rotational movement of tool makes the scribe cutter to generate an interface of maximum width equal to twice its radial offset distance by cutting and forming mechanical interlocking features in the bottom materials. These interlocking features are simultaneously backfilled by the scribe-extruded plastic material of the top sheet to produce a lap joint of high shear strength [158]. The tool travel generates a lap weld of desired length and form. Without the scribe cutter, the tool pin

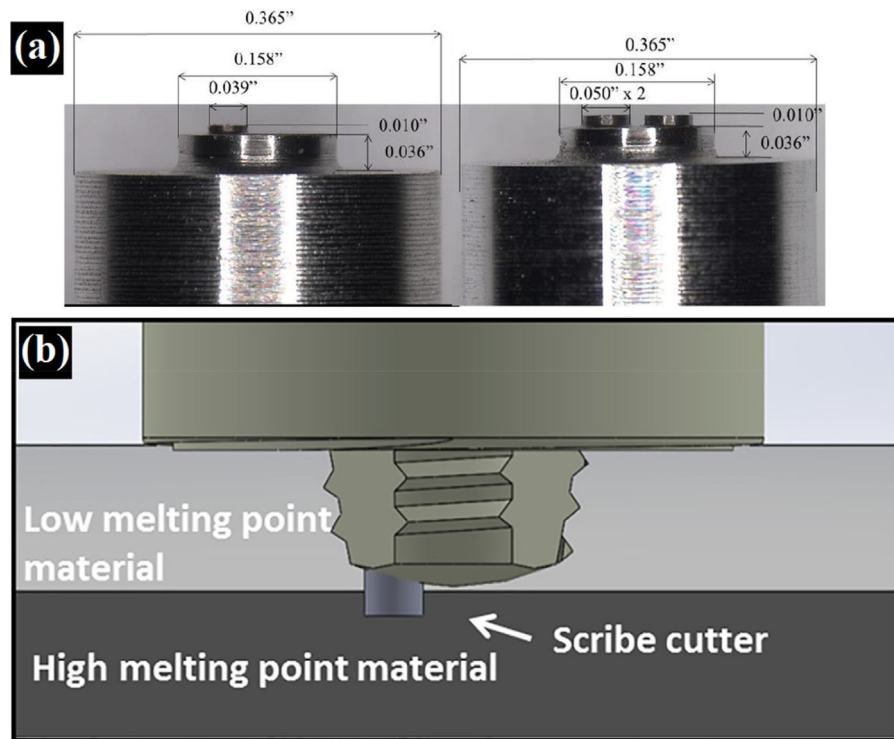


Fig. 16. (a) FSS tool with single and double scribe cutter [157], and (b) Schematic of FSS process [160].

would need to plunge deeper into the harder bottom alloy. This would require higher tool rotation speeds in order to achieve sufficient frictional heat to plasticize the harder material and cause tool wear [159,161–164].

2.5.2. Process parameters in FSS

The main process parameters in FSS are the tool rotation speed, traverse speed, tool plunge depth, and tool tilt angle are similar to those in the FSW. The FSS tool geometry requires careful design. For example, the single and double scribe cutter tool geometries and dimensions adopted for the welding of 1.0 mm thick 6022 aluminium and 0.7 mm thick low carbon electro galvanized steel alloy panels are shown in Fig. 16(a). It must be noted that the aim is to provide the tool with a position offset with the center of the tool in both the single and double scribe tools. Process and tooling parameters can influence the effectiveness of hook morphology and strength of the joint [160]. However, the studies available in this regard are too limited and more studies are needed to arrive at a thorough understanding on the effect of process and tooling parameters on the FSS joint.

2.5.3. Microstructural features in FSS welds

Fig. 17 shows the cross section of a typical lap FSS weld. The weld can be divided into four distinct regions with the weld zone (WZ) in the center followed by the TMAZ, HAZ and BM on the AS and RS. The WZ interface between the two alloys is depressed relative to the interface in the TMAZ, HAZ, and BM. Another distinct feature of FSS weld is the hook formation, i.e., mechanical bonding, which is due to the drawing up of the harder bottom material (steel in Fig. 18) into the top material (Al alloy in Fig. 18) on either side of the WZ [165]. The hooks are a result of the back filling of the softer top material into the mechanical interlocks and extrusion of the harder bottom material into the softer top material producing a composite-like structure.

In the lap joining of Al 6061 – (0.30 wt% C) RHA steel, chemical bonding is also feasible due to the temperature dependent diffusion of the two elements, Al and Fe, at the interface [165]. A thin IMC layer has been observed when the steel is uncoated [165], while a Zn-coated steel presents Al/Zn and Zn/Fe interfaces and no IMC layer [166], as shown in Fig. 18. The steel particles are dispersed in the region around the hook. These mechanical interlocking features would also appear in the joining of aluminium to various polymers [161]

2.5.4. Feasibility and application

FSS has been already employed in the joining of materials. Higher load tolerance and shear strength has been achieved in the Mg alloy/steel joining where the combinations attempted are 2.3 mm thick sheet of AZ31 magnesium alloy to 1.5-mm thick sheet of high strength, low alloy hot dipped galvanizing (HSLA-HDG) steel and to 0.8 mm thick sheets of DSTB-HDG steel, DSTB-HDG steel alloy and drawing Type B-Hot Dipped Galvanizing (DSTB-HDG) steel [158]. In the Al alloy/Steel joining, FSS joining has been conducted with 1.0 mm thick 6022 aluminium/0.7 mm thick low carbon electro galvanized steel alloy [157], 2.2-mm thick Al 6111-T4/1.5-mm thick dual phase (DP) galvannealed steel [159], and Al 6061 / (0.30 wt% C) RHA steel [165].

Recently, Al alloy/polymer joining has been also successfully conducted using FSS where, 1 mm thick AA6022 alloy could be welded to polyamide (6,6) (Nylon), High Density Polypropylene (HDPE), 50 wt% long carbon-fiber reinforced nylon (LCF50/PA66) and 40 wt% long glass fiber reinforced Nylon (LGF40/PA66) [161]. In FSS, the top material can be a softer or low melting point material such as the alloys of Al, Mg, Ti etc. while the harder bottom material can be a steel or a steel alloy. Also, ceramic/steel lap combinations would also be possible. With the current demand for weight reduction and emission control, FSS can easily penetrate into the automotive industry and can have applications in other sectors as well.

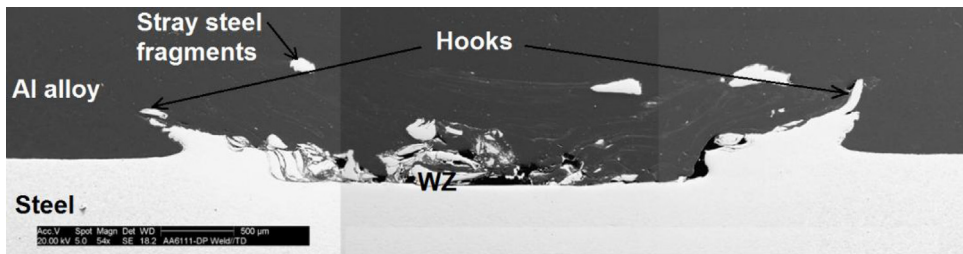


Fig. 17. Typical macro cross section of FSS weld [159].

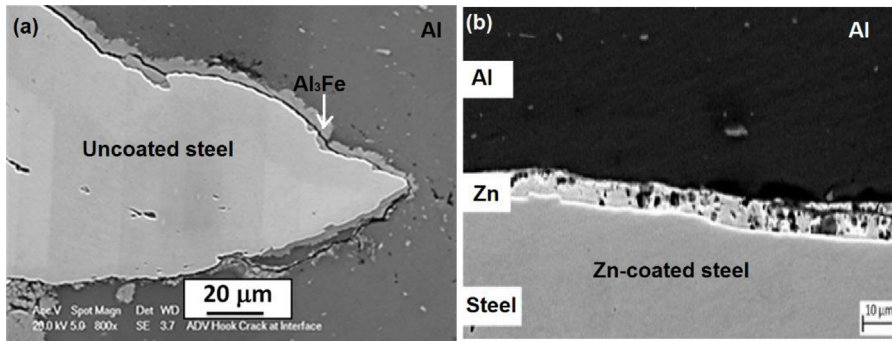


Fig. 18. Possibility of IMC layer formation (a) IMC in uncoated steel [165], and (b) IMC in coated steel [166].

3. Friction stir based processing technologies

3.1. Friction stir processing (FSP)

Friction stir processing (FSP) is analogous to FSW by the working principle. However, the purpose of its application is different. FSW is mainly intended for the joining of materials. Moreover, apart from being joined, it has been observed that the materials during FSW also undergo various useful microstructural modifications in their common stir zone or deformed zone due to severe plastic deformation during the process [6,7,167].

Therefore, the process, referred by the name FSP, has been applied for various other purposes such as for achieving ultra-fine-grains [167–184] and compositional/microstructural homogeneity [167,185,186], for modification and hardening of surface [167,187–192], for fabricating hybrid and in-situ surface [20,167,191–200] and bulk metal matrix composites of Al-alloys, high entropy alloys [20,167,182,192,201–227], Mg-alloys [20,167,191,192,228–236], Cu-alloys [20,167,191,192,237–243] and other high strength materials [20,167,191,192,244–246], for repairing cracked or defective components [20,167,247,248], for improving HAZ liquation cracking resistance [249,250], for additive manufacturing [20], for enhancing superplasticity [251–256] and many more.

In this particular section, the discussion is focussed on achieving grain refinement, microstructural and compositional homogeneity, surface and bulk composite fabrication, treatment of cracking and enhancement of superplasticity, using FSP.

3.1.1. Features of FSP procedure

The FSP procedure adopted for producing fine and ultrafine grains in cast alloys, for the modification of surface and for crack repair applications is similar to that used in FSW. Tools with or without pin are used. For desired ultrafine grain refinement, a rapid heat sink or cooling rate control appears to be extremely helpful [176–178]. FSP is tremendously useful for surface modification or surface hardness improvement and for the fabrication of surface and bulk level metal-matrix composites. The metal matrix and

the reinforcement material (particulate) in FSP can be ferrous or non-ferrous, compatible or non-compatible.

Different types of composites such as surface composites, bulk level micro-composites, nano-composites, in-situ composites and hybrid composites have been prepared by FSP [20,167,191–244]. For such fabrication, initial induction of the reinforcement material into the metal matrix before FSP is essential. In order to accomplish the initial induction, several methods such as stir casting, squeeze casting, molten metal infiltration, powder metallurgy etc. exist [191,192]. However, the commonly reported methods for the initial preparation of FSP are: (a) packing of the reinforcement particles tightly in a pre-machined groove on metal, and closing the groove with a capping pass by a tool with pin-less shoulder [198,206,245], (b) packing of the reinforcement material in predrilled holes of the metal so that the holes would be closed by the shoulder before its access to the pin [192,238,246], (c) covering the reinforcement particle filled holes or the groove with a thin sheet of the same metal to avoid the oozing of the particles [192,240], (d) applying a layer of reinforcement material slurry in a volatile or binding medium on the metal surface [187,192], (e) using a pin-less hollow tool with a concave shoulder prefilled with the reinforcement particles that flow to the processed surface during FSP [192,196], (f) depositing a layer of reinforcement particle-filled-consumable tool on the metal surface [192], (g) applying composite powder coating on the metal surface by plasma spraying or cold spraying or oxy-fuel spraying method [192,200], (h) mixing the powers or particles of metal and reinforcement in desired proportions, stirring and cold compacting the mixture into billets, heating for a desired time followed by hot pressing [202,203,218,225,226]. These techniques are also applied for modification of the surface or for surface hardening by FSP. Such particle reinforced metal is friction stir processed using a tool with a shoulder and a pin to fabricate a metal matrix composite.

For the repair of cracks generated by fusion joining, FSP has been used as a pre- or post-treatment method. FSP pre-treatment of BM before its fusion welding such as laser melting is used as an effective tool for avoiding the grain boundary liquation cracking [249,250] while FSP post-treatment is explored as a method for repairing or eliminating fusion weld defects [20,167,247,248]. Friction stir

processing the surface of GMAW joints changes the cast arc weld microstructure into a fully recrystallized fine grain structure and eliminates weld defects near the surface.

3.1.2. Process parameters in FSP

FSP produces temperatures in the range of 0.6–0.9 T_m (T_m = melting point of material), strain rates in the range of $1\text{--}10^3 \text{ s}^{-1}$ and strain up to ~ 40 [167,191]. Therefore, it causes intense thermal exposure, plastic deformation and material intermixing. The process parameters in FSP are mainly the machine variables such as rotation speed and traverse speed of the tool which govern heat generation, and the tool geometry. The heat input varies directly with rotation speed and inversely with traverse speed. Other variables such as tool tilt angle and penetration depth would also influence the process and the properties of processed zone, but, to a lower extent.

The documented reports show that heat input in the processed zone increases with rotation speed, causing grain coarsening and depression of hardness in the processed zone [167]. On the contrary, increase in traverse speed decreases the duration of high temperature exposure of processing zone, causing reduction in the grain size and increase in the hardness. However, these parameters should be optimized to achieve sufficient heat generation and material plasticization.

FSP reduces porosity and modifies the microstructure of processed material by breaking up the coarse second phase particles and respective dendrites of cast Mg and Al alloys [20,167]. Similarly, FSP causes breakup of the reinforcement particle clusters in the surface and bulk metal-matrix composites. In both these cases, homogenization or uniform distribution of the second phase particles or reinforcement particles in the metal matrix is a common phenomenon. Such homogenization and reduction in porosity increases with increase in rotation speed, increase in the number of passes [192] or decrease in tool traverse speeds due to favorable heat generation, viscosity and material flow [167,191,192,210,213,235,241].

In the fabrication of in-situ composites, lower traverse speeds are beneficial in producing finer and uniform grain size because they allows longer processing time. However, the above trends of rotation speed and traverse speed on grain refinement and particle distribution are not universal; these trends would reverse with the material and the reinforcement particle [167,191,192]. Surface composites would be left poorly bonded with higher traverse speed [187]. A Taguchi approach based investigation has showed that the effect of rotation speed is the highest (43.70%), followed by transverse speed (33.79%), pin profile (11.22%) and tool penetration depth (4.21%) [192,223].

3.1.3. Microstructures in FSP

The microstructure of a friction stir processed zone of 7075 Al-alloy is shown in Fig. 19(a). The typical distinct regions such as the BM, HAZ, TMAZ, the processed zone or SZ, onion rings, shoulder effected zone, pin effected zone as well as the pin bottom zone are clearly discernible [169,257]. The grain sizes through the thickness of the processed zone vary from 300 to 500 nm [169]. Grain refinement down to 30 nm has been achieved using FSP [187].

Fig. 19(b) shows the microstructure of a Al-Mg-Mn/SiC surface composite produced by FSP. It is evident that the surface has no porosity or defect and the SiC particles (black spots) are homogeneously distributed in the aluminium matrix. Also, the interface zone between the surface composite layer and the aluminium alloy substrate are perfectly bonded. As an example of homogeneous or uniform distribution, Fig. 19(c) shows the variation in the dispersion of Al_3Ti intermetallic compounds (bright area) in Al-Ti-Cu alloy after hot pressing, after extrusion and after FSP [186]. Initially, the intermetallics, Al_3Ti , in the hot pressed Al-Ti-Cu alloy are

largely localized and aluminium rich (black area) regions are visible. When this hot pressed material is extruded, the intermetallics as well as the aluminium rich regions are oriented along the extrusion direction. After FSP, however, the Al_3Ti particles are distributed homogeneously throughout processed zone, eclipsing all the Al rich region in the metal matrix. In another example, Fig. 19(d) shows the distribution of SiC particles in the Al 6061 matrix after extrusion and after FSW. Obviously, the distribution of SiC particles in the SiC/Al composite after the FSP is more uniform than that after the extrusion [167]. The homogenization of Al_3Ti particles in the Al-Ti-Cu alloy [186] and the SiC reinforcements in the Al 6061 alloy [167] are attributed to the intense stirring and intermixing of material in FSP which has caused breaking up of the coarse particles. The homogenization has improved the mechanical properties of the processed composites [167].

3.1.4. Application and feasibility

FSP has produced grain refinement and ultrafine grain structure and improved the local microstructure and corresponding mechanical properties of Al-, Cu-, Fe-, Mg-, and Ni-based alloy systems [167–190]. It has the potential to improve the grain size dependent properties such as superplasticity. For example, the superplasticity of friction stir processed 7075 Al alloy specimen is enhanced by an order of magnitude in strain rate at 490° , as shown in Fig. 20(a–c) [251]. Multi-pass processing of the alloy produced significant further improvement in the superplasticity of Al alloys in terms of the strain rate and temperature although the largest elongation has occurred in the single pass [251–256].

Many aluminium or magnesium based surface and bulk composites such as A390 alloy/graphite and A390 alloy/ Al_2O_3 composites, Al alloy/SiC, Al alloy/WC, Al alloy/NiTi, Al alloy/ SiO_2 , Al alloy/ TiO_2 , Al alloy/carbon nanotubes, AZ31/multiwall carbon nanotubes, AZ31/ Al_2O_3 and AZ31/SiC composite, AZ61/ TiO_2 ; AZ91 alloy/ Al_2O_3 composite, AZ91/SiC composite and the composites of Cu based alloys and SiC, TiC, B_4C , WC or Al_2O_3 particles have already been developed by FSP [167,185–246]. The details of composite preparation by FSP have been aptly and systematically reviewed elsewhere [167,191,192]. Moreover, FSP has been used as pre- or post-treatment procedure of fusion welds of some Al-, Fe- and Ni- alloys to avoid their potential failure due to fatigue cracking and liquation cracking [247–250].

3.2. Friction stir channeling (FSC)

Friction stir channeling (FSC) is an innovative single step method of manufacturing continuous and integral channels in monolithic plates in a single pass for heat exchanger applications. FSC is developed by smartly utilizing the mechanism of wormhole defect formation in FSW to produce continuous and integral channels [258–263]. Occurrence of wormholes in the FSW stir zone is because of flow inadequacies arising from non-optimized processing conditions such as an improper contact between the FSW tool shoulder and the surface of the workpiece or geometry of the tool features [260]. The wormhole formation mechanism was utilized with control over specific process parameters for the benefit of FSC technology development. Thus, the FSC may be seen as a process of deliberate creation of wormholes for beneficial purposes. At present, the FSC technology has been modified and improved for development of better channels in monolithic plates.

3.2.1. FSC features and principles

Three different concepts of FSC has been developed over the timeline although the foremost credit for development of the friction stirring channeling must be given to Mishra et al. [258–260]. In order to create channels of better shape, size, stability and integrity, alternate methods of FSC were developed by Vidal et al.

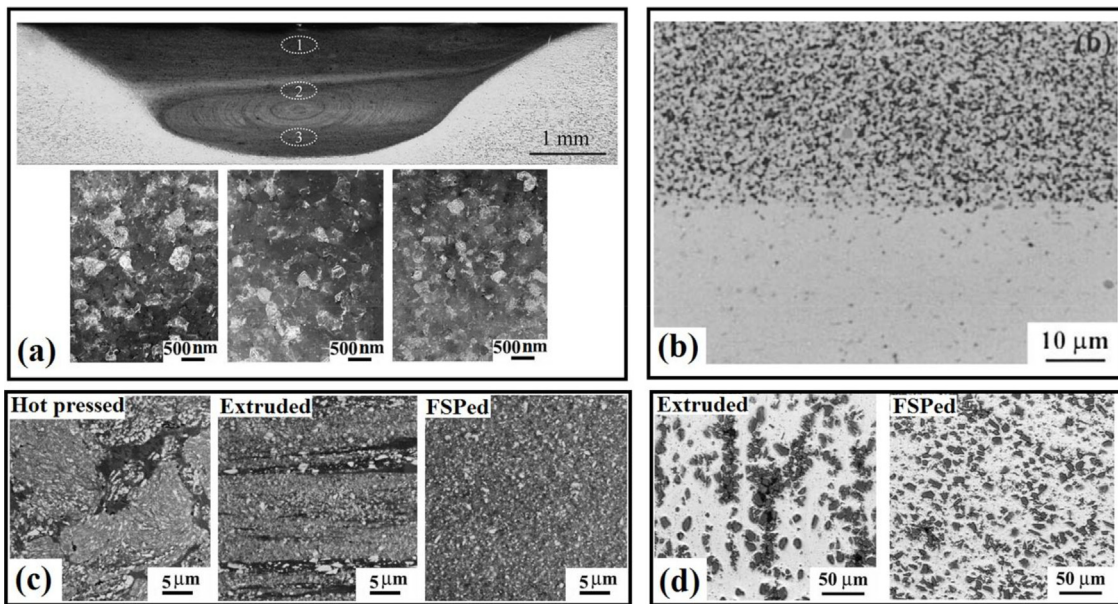


Fig. 19. Selected microstructures to show FSP causes (a) grain refinement in Al 7075 alloy [169] (b) Al-Mg-Mn/SiC surface composite formation with good bonding [187], (c) Al₃Ti intermetallic particle break up and homogenization on the surface of Al-Ti-Cu alloy [186] and (d) Uniform distribution of SiC reinforcement particles in Al-matrix in bulk scale [167].

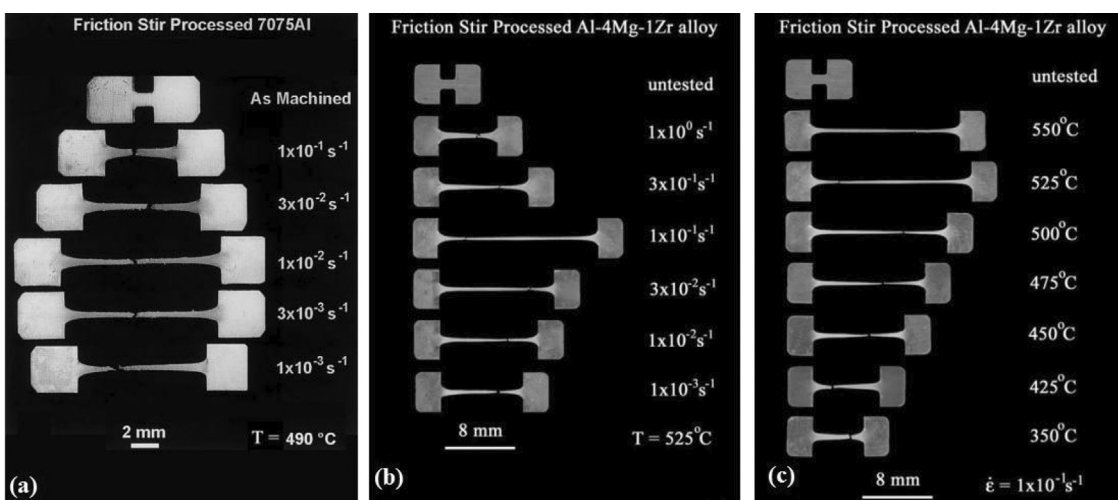


Fig. 20. Superplastic deformation in Al alloy after friction stir processing (a) at 490 °C, (b) at 525 °C, and (c) at a constant strain rate [251,252].

[20,264–274] and Rashidi et al. [275–279]. Hereinafter in this study, these three versions are referred to as FSC [258], alternate FSC (A-FSC) [20,264] and modified FSC (M-FSC) [275,276], respectively, for convenience. The principles of these processes are discussed below.

3.2.1.1. FSC [258–263]. The working principle of FSC is similar to that of FSW. Fig. 21(a) shows the schematic of the FSC process. FSC involves four stages, the plunging stage, dwelling stage, channeling stage and retraction. The channeling stage is analogous to the welding stage. Since the aim of FSC is to create a channel during the process, the tool geometry and its rotation direction during the process are important [261]. In addition to generating frictional heat to produce sufficient viscoelastic dissipation and material flow via its rotational movement, also important for the tool in the channeling stage of FSC (i.e., analogous of the welding stage of FSW) is to direct the material flow upwards, i.e., towards the tool shoulder, and to separate the plasticized material around the pin from that at the base of the pin. This requires specific designing of the tool and the process.

The upward flow is achieved by a rotating a right-hand threaded tool in clockwise direction or a left-hand threaded tool in counter clockwise direction. After the tool design, the mechanism of worm-hole formation is brought into practice. For this, an initial clearance, i.e., a deliberate gap, between the tool shoulder and the surface of workpiece is provided during the tool plunging stage and maintained throughout the dwelling and channeling stages. This clearance allows the material separated from the base of the pin and flown upwards to deposit on the top of the nugget underneath the shoulder surface. This action creates a continuous channel along the tool traverse direction. These channels are characterized by their shape, size, and hydraulic diameter and to some extent, the roof surface roughness [262].

3.2.1.2. A-FSC [20,264–274]. Schematic of AFSC is shown in Fig. 21(b). The concept and principles of A-FSC are slightly different from the FSC, although the objective is to produce internal channels. In A-FSC, a controlled amount of material, flowing from the interior processed zone of workpiece, is directed outside of the processed

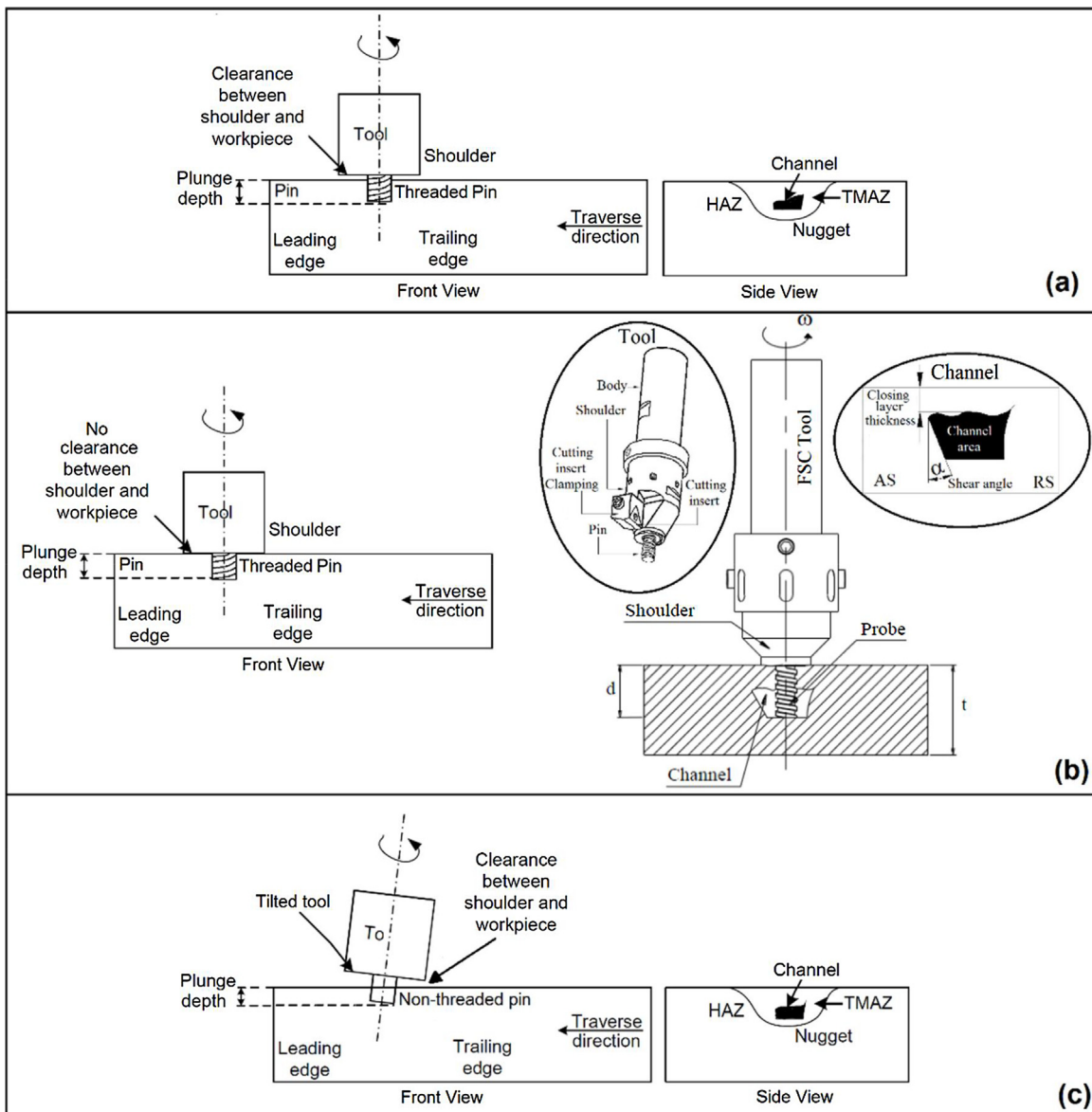


Fig. 21. Schematics of (a) FSC [260], (b) A-FSC [21,264], and (c) M-FSC [275,276] processes.

zone and extracted out in the form of self-detachable toe flash to produce internal channel [264]. This keeps the processed surface at the same initial level. This is contrary to the FSC, where the material flowing upwards is deposited in the processed zone underneath the shoulder, causing a slight bulging of the processed surface, only to be removed by milling later.

The major difference of A-FSC from FSC is that no initial clearance between the shoulder and the workpiece is provided [21]. Hence, the material from the base of the tool pin is deposited on the sides and back of the shoulder to create the channel. It is important to note that A-FSC employs a specially designed tool with a threaded pin, as is done in FSC [273,274]. Some new parameters defined to characterize the channel in A-FSC are channel area, closing layer thickness and shear angle, as shown in Fig. 21(b) [265,266]. Since there is no gap between the tool shoulder and the workpiece in A-FSC, a tool integrating surface finishing features has been modelled which, if possible, would simultaneously produce the required surface finish [21,268].

3.2.1.3. M-FSC [275–279]. A schematic of the M-FSC process has been shown in Fig. 21(c). In the M-FSC process, a non-threaded tool pin is employed [275]. The plunging, dwelling and channeling stages are conducted by applying a tilt angle to the tool and a clearance between the tool shoulder and workpiece surface. The idea behind tilting the tool at an angle is to better extract the material and create the channel. The non-threaded tool pin is used to achieve a steady state or constant material flow that would generate stable and possibly, more regular shaped channels [276,277].

In the M-FSC, direction of tool rotation is not a mandatory criteria for the formation of channel. However, a change in rotation direction shifts the location of channel from AS to RS or vice versa. These modifications have been proved vital for producing channels of larger size, more regular shape and better stability. This method has introduced the channel width as a parameter to characterize the channel [278,279]. Both the width and the height of the channel are increased in M-FSC as compared with the FSC.

3.2.2. Process parameters in FSC

In FSW, formation of a wormhole is undesirable and its prevention is of interest. In FSC, however, channels are the purposely created due to their potential in providing versatile service. The main process parameters in all the three versions of FSC are similar. The tool rotation and traverse speeds control the amount of heat generation from frictional dissipation and subsequent viscoplastic flow during the process. These two parameters, along with plunge depth affect the downward force applied on the workpiece and thus, affect the overall quality of the channel [21].

A typical channel formed by FSC is roughly elliptical in shape while those in A-FSC and M-FSC are far from conic sections and present a rough rectangle shape, as shown in Fig. 22(a). The shape, size, and integrity of the channel can be controlled by adjusting the clearance between the tool shoulder and workpiece and by controlling the heat index [260]. Heat index is a relative term defined as the ratio of the square of tool rotation speed to tool traverse speed. High heat index causes more material to flow upward [270]. It means, a high rotation speed and low traverse speeds create channels of better shape. The heat index also determines the integrity of the channel. Lower downward axial forces are beneficial towards the channel integrity.

Also, the channel cross-sectional area has increased at higher traverse speeds and lower rotation speeds. Channels are continuous over an optimized range of tool rotation speed, traverse speed and plunge depth. Too cold process conditions, i.e., too low rotation speed and plunge depths, create open channels which are not closed on the top underneath the shoulder due to insufficient plastic material while too hot process conditions lead to discontinuous channel, due to collapse of the channel roof [260]. Tool travel speed, tool rotation speed and the sizes of pin and shoulder can be adjusted to control the shape, size, and integrity of the channel [258–263]. In A-FSC, the channel area increases with an increase in the tool travel speed and decrease in tool rotation speed [266] while colder process conditions produce stable and better channels.

The A-FSC process parameters are not transferable from material to material and are strongly dependent on material thickness. Also, thermal conductivity of necessary accessories such as the clamping system, backing plate etc. in contact with the workpiece influence the process parameters. In M-FSC, rotation speed, traverse speed, plunge depth and tool tilt angle are important process parameters which have different influences across different regions of the channelled product owing to their strong tendency to effect the material flow [279].

Tilt angle effectively increases the downward forging action of material in AS. An increase in tilt angle causes increase in the amount of deposited material which creates large flash and decreases the area of the channel. Moreover, the area reduction leaves the channel with a more regular shape. The effect of transverse speed on the channel size and shape follows a similar trend as the tilt angle. Increase in the traverse speed tends to improve the channel size and shape. Lower rotation speeds are beneficial towards suppressing the groove on AS of channel roof and giving the channel a regular shape. However, the width of the channel is reduced [277–279]. In all the versions of friction stir channeling, the interior structure of the channel is also important because it can affect the heat exchange through the channel.

3.2.3. Microstructure of the channel and its vicinity

Understanding the channel formation requires identification of distinct flow regions in the channel cross section. Since FSC is similar to FSW except for the clearance or for the propensity to drive the viscoplastic material upward and create a channel, most of the thermomechanical actions in FSC follow the similar trait as in FSW. Therefore, the microstructures of the channel vicinity in FSC, A-FSC

and M-FSC are similar and also analogous to the weld microstructure in FSW except for the channel.

Fig. 22(a) shows the macrostructure of a channel and its surroundings achieved using the FSC [260]. The channel, the material flow pattern and the displacement of material from the pin bottom and its deposition at the channel roof along the advancing side are obvious. Regions A and B represent the stir zone, region C is the unprocessed parent material, and region D is the channel. Region E represents the region with deposits of material from the channel nugget region, flown upward above the original material surface underneath the shoulder. The stir zone in region A is partly processed by the pin and depicts the flow of the material from the pin base to the material surface underneath the shoulder. The deposit underneath the shoulder exerts a downward force at the trailing side of the pin on the channel roof, while the material near the workpiece surface is driven inward to get deposited in the retreating side, region B. The thermo-mechanically affected zone (TMAZ), presented by regions F and G, and the HAZ are not clearly visible.

Fig. 22(b) shows further classification of the SZ of a channel of M-FSC into SAZ, extrusion zone (EZ1 and EZ2) and channel zone (CZ). These stir zone features are important to control the channel structure and interior [279]. For instance, the roughness at the channel roof and base are important to achieve pressure drop in mini heat exchangers. In the A-FSC channel vicinity, shown in Fig. 22(c), the coarse grains are replaced by fine recrystallized and equiaxed grains surrounding the SZ and the channel. The TMAZ presents an increase in average grain size due to the tool stirring action that plastically deforms the material [268]. It appears that the SZ diameter and the channel height are respectively equal to the diameter and the used length of cylindrical pin in the process. The roughness of the channel is of particular significance.

Fig. 23(a) and (b) shows the interior surface features of channels produced in FSC and A-FSC, respectively. In FSC, the bottom and side walls of the channel are relatively smooth and flat while the channel roof is rough, undulated and oriented along the tool travel with a periodicity equal to the pitch (i.e., tool advance per rotation) of the process [260]. These roughness features are similar in A-FSC [269].

3.2.4. Feasibility and applications of FSC

So far, FSC versions have been conducted with monolithic metal plates of commercial 5 mm thick AA6061-T6, 10 mm thick Al 5083, 15 mm thick AA5083-H111, and 13 mm thick AA7178-T6 for production of linear and non-linear continuous channels [21,260,268,276]. With proper selection of tool material, FSC would allow production of such channels in other high strength materials such as Fe-, Ti- and Cu- alloys. FSC forms channels in a single step and is extremely useful in the manufacturing of commercial heat exchangers [257].

On the basis of recent testing and evaluation, FSC seems to have the potential to thrive in the heat exchanger and mould production industries [274]. The continuous internal channels produced by FSC has a variety of applications as heat exchangers which transfer thermal energy between multiple fluids, or between thermally contacted surfaces of a fluid and a solid at different temperatures. Heat exchangers are used for heating/evaporation or cooling/condensation of fluid stream to reject or recover heat. Surface compactness of heat exchangers make them candidates for application as vehicular heat exchangers, condensers and evaporators in air-condition and refrigeration industry, aircraft oil-coolers, automotive radiators, and intercoolers or compressors [274].

Channels for any type of heat exchangers can be manufactured by FSC. This process has been verified to be a potential alternative to conformal cooling and rapid prototyping processes such as drilling, EDM and milling in the mould production industries [20,273,274]. FSC has the potential to penetrate into the aerospace,

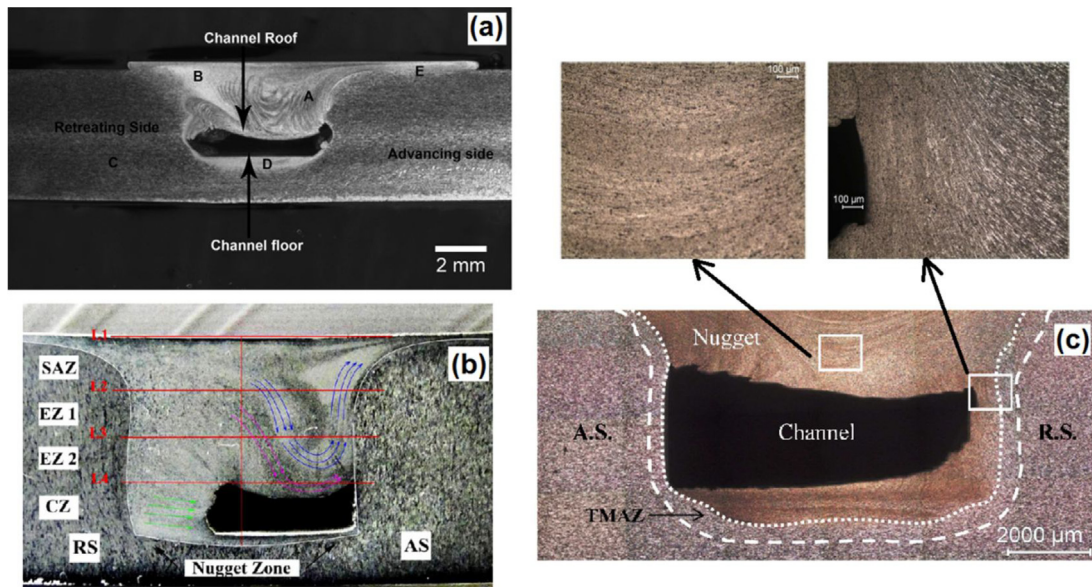


Fig. 22. Channelled cross section (a) in FSC, where A&B – channel nugget, C – parent material, D – channel, and E – material from the channel nugget deposited on the surface [260], (b) in M-FSC, where SAZ – shoulder affected zone, EZ – extrusion zone, CZ – channel zone [279], and (c) Channel in A-FSC, showing also the [268].

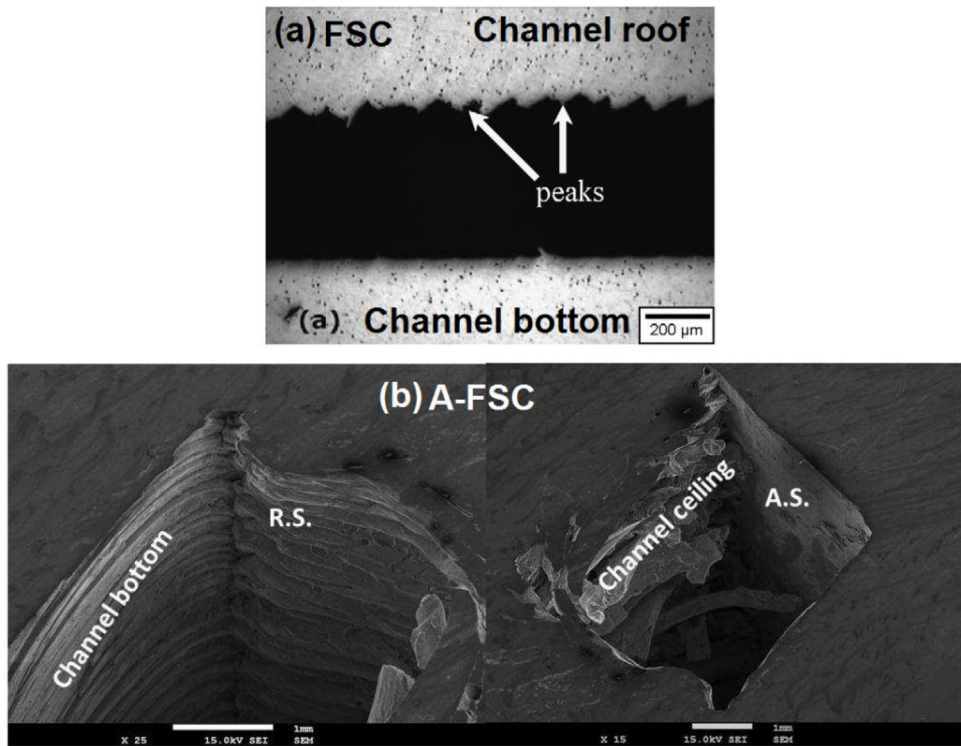


Fig. 23. Channel surface features in (a) FSC [251], and (b) A-FSC [266].

marine, ground transportation, automotive, defense (military) and biomedical industries [20,274].

3.3. Friction surfacing (FS)

Friction surfacing is probably the oldest among all the technologies based on the friction stir concept. The friction surfacing concept was first mentioned in a patent in 1941 and development on the process was reported in 1960s. However, the interest in friction surfacing and a commercially viable friction surfacing technology, FRICTEC, was developed only after 2–3 decades [280].

3.3.1. Process features and experimental setup

FS is listed among the friction stir technologies because it employs a rotating metal rod for the surfacing or application of a coating on a metal substrate. The metal rod in FS is generally referred to as mechtrode, a term probably coined parallel to the term electrode, because it is rotated under a mechanical load or pressure to generate heat and plasticized layers in the rod at the interface with the substrate. The position of mechtrode in the FS process is analogous to that of the tool in the FSW/FSP process. However, unlike the tool in FSW/FSP which is non-consumable, the mechtrode in FS is consumable and composed of the mate-

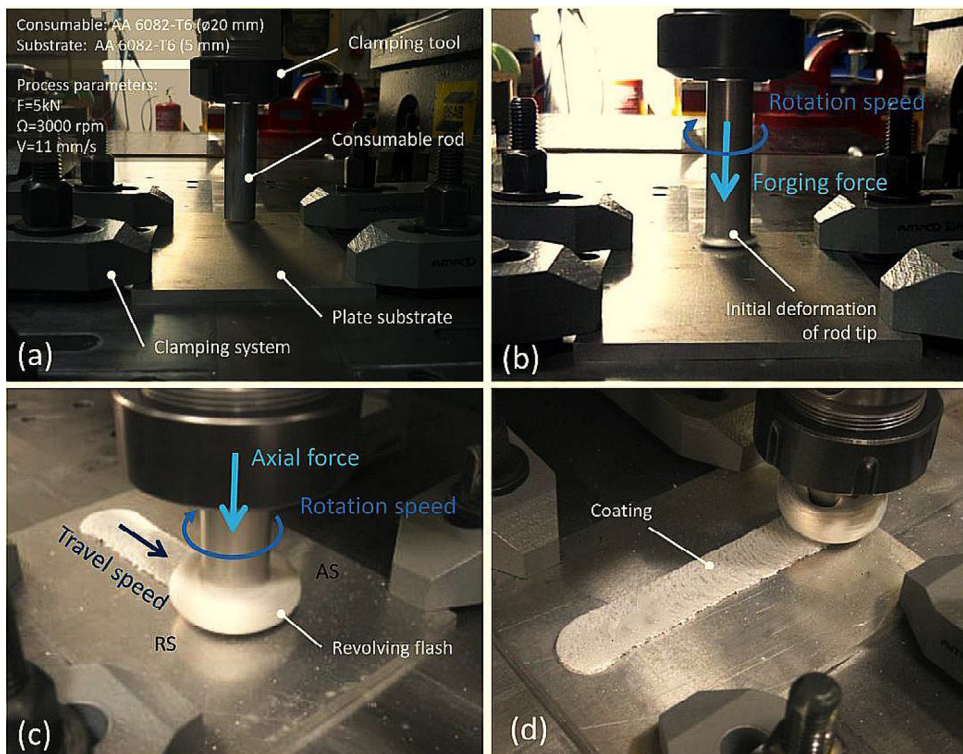


Fig. 24. Friction surfacing process (Figure adopted from [282]) (a) Fixture and set up, (b) Substrate-consumable contact and initial deformation of consumable tip, (c) Consumable deposition on substrate, and (d) Deposit.

rial which is desired to be coated on the substrate [281]. Based on the evolution of torque, force and temperature, the FS process involves two stages, the preheating or plasticization stage, and the deposition stage, as depicted in Fig. 24. In the plasticization stage, the rotating mechtrode without any lateral movement and under an applied axial contact force is pressed against the substrate (Fig. 24(a)). Frictional heat generated at the rod-substrate interface causes material softening, initial deformation and formation of a viscoplastic boundary layer at the rod tip (Fig. 24(b)). This is succeeded by the deposition stage, where, either the substrate or the mechtrode with its viscoplastic tip is travelled with respect to the other at a constant speed. During this stage, the tool feed rate and axial contact force are simultaneously controlled.

The thermo-mechanical actions result in metallic bonding between the viscoplastic layer and the substrate via an inter-diffusion process. Subsequent heat conduction into the substrate enables three successive phenomena: 1) consolidation of the viscoplastic layer near the bonded interface, 2) formation of a viscoplastic shearing interface between the rotating mechtrode and consolidated layer and, 3) movement of the viscoplastic shearing interface away from the substrate surface (Fig. 24(c)). These three phenomena lead to thickening of the layer [21,281]. The traverse of substrate or mechtrode produces a continuous deposition of mechtrode on the substrate surface due to the progressive consumption of the rod (Fig. 24(d)).

In the FS process, frictional heat generated at the mechtrode-substrate interface is the major heat source until the initial deformation stage. Beyond this stage, heat due to plastic deformation has the major contribution because the deformation lowers friction between the mechtrode and substrate surface [283]. Both the plasticization and the deposition stages can be either force/pressure or rod feed rate controlled [284]. A deviation of FS from the other friction stir based technologies is that FS does not involve a shoulder, i.e., the viscoplastic material at the mechtrode tip is pressed against the substrate without any lateral

restraint, because of its consumable nature. This obviously causes the viscoplastic material to flow outside the mechtrode periphery, resulting in a revolving flash of mushroom-shaped geometry as well as lack of bonding at the coating edges on both the advancing and retreating sides [285]. Hence, the width of fully bonded FS deposits is less than the diameter of the consumable [286]. It is to note that the bonding width is always smaller than the width of deposit in FS.

The deposited mechtrode layers are associated with ripples formation which are related to the material transfer in FS [281]. Ripple formation is due to the periodic deposition of distinct elliptical layers of the mechtrode [280,287,288]. The deposited layers, presenting an offset towards the advancing side from the middle, involve a smooth and straight advancing side and an uneven and ragged retreating side [289,290]. The deposited material comes mainly from the mechtrode center while the mechtrode boundary forms the flash [291]. The transfer of mechtrode material on to the substrate during FS occurs from the advancing to the retreating side, while bonding of the transferred material with the surface occurs on the back of the mechtrode, and from the retreating to the advancing side [292,293]. The microstructures of the advancing and retreating sides, however, are similar [294].

3.3.2. Process parameters in FS

The process parameters determining the FS efficiency are the rotation speed, travel speed, tilt angle of the mechtrode, the rod consumption and hot-working pressure. The rod consumption can be adjusted by controlling the axial force or contact stress applied on the consumable and/or the rod axial feed rate [281]. In FS, the effect of process parameters on the surfaced product is complex and vary with the substrate-mechtrode combination. For example, although a higher rotation speed would produce more heat, too high rotation and/or travel speeds allow less time for interfacial interaction between the mechtrode and the substrate and thus, reduce the bonded width [295]. The rotation speed affects

the mechtrode-deposit contact area as well as the interfacial shear between the deposited and viscoplastic layers. Thus, a lower rotation speed is considered better [296]. The bonding efficiency also depends upon the relative speeds between the substrate and the mechtrode. Higher mechtrode tilt angle can cause better confinement of viscoplastic material and thus increase the bond width [291].

The mechtrode diameter, rotation and travel speeds and axial force significantly influence the characteristics of the deposit. It has been reported that both axial force and rotation speed affect the bond quality. For example, large axial forces yield inhomogeneous deposits with a depressed center [295] while inadequate axial forces yield poor consolidation of the deposit [291]. Therefore, the axial force has to be optimized for effective bonded width and wider and thinner deposits. Also, the increase in axial force improves the mechanical properties of deposits [288]. However, it produces deeper heat effected zones in the substrate [297].

Figs. 25 and 26 show the influence of mechtrode rotation speed and substrate travel speed on the nature of deposit. Mechtrode rotation speed significantly influences the width and roughness of the deposit [289,294], as shown in Fig. 25. Very high rotation speeds reduce the depth of substrate HAZ, produce flatter and regular deposits with good surface finish, narrower bonding width and lower thickness [288,289,298,299]. Lower and intermediate rotation speeds improve the bonding strength and width, but the deposit becomes irregular. Further, the bonding strength increases with travel speed, however, excessive travel speeds decrease both thickness and width [290].

Deposits made with lower travel speeds fail under lower shear forces while higher shear forces are necessary to fail the deposits made at higher travel speeds. Also, the former deposits fail at the interface while the latter fail in the deposit [289]. At higher travel speeds, the HAZ is smaller because of shorter periods of heat exposure and limited grain growth [281,292,300]. Too high travel speeds show an adverse effect on the bonding at the edges of the deposit [281,300]. The virtual interacting surface is elliptical and it experiences longer exposures with increasing mechtrode diameter, at a given travel speed [281,287]. Therefore, the process parameters should be carefully optimized for effective FS.

3.3.3. Metallurgical features of deposit

The thermomechanical actions involved in the mechetrode of FS are too complex. Fig. 27.1 schematically outlines the various thermomechanical events experienced by the mechetrode. Accordingly, the axial direction of mechetrode before deposition involves several thermomechanical zones of variable microstructures [281,289]. As stated earlier, consolidation of mechetrode on the substrate precedes heat conduction into the substrate and heat convection and radiation to the surroundings. Therefore, the cooling of deposit is rapid and the deposits experience smaller periods of heat exposure, resulting in a continuous layer of fine grained microstructure [287]. While the microstructure evolution is mainly due to CDRX and DDRX by shearing deformation [291], other mechanisms such as phase transformation and second phase particle distribution gradients also contribute [281,287].

Fig. 27.2 shows the microstructures evolved along the mechetrode axis and in the deposit. It is interesting to compare the mechetrode microstructures in Fig. 27.2 with the thermo-mechanical scheme in Fig. 27.1. The cold worked or preheated region in Fig. 27.2(b) can be compared to the HAZ where grains are slightly coarsened as compared to the BM in Fig. 27.2(a). The thermo-mechanically affected zone (TMAZ) in regions Fig. 27.2(c) and (d) appear due to compression in the center and torsion at the periphery of the mechetrode. The TMAZ can be compared to the electroplastic region while the recrystallized and fine grained

microstructures in Fig. 27.2(e) and (f) are from the hot worked viscoplastic region.

3.3.4. Feasibility and application of FS

The initial purpose and applications of FS were to repair or rehabilitate or resurface the worn or damaged surfaces through building up or crack sealing within localized areas [279,281]. At present, FS is continuously explored for producing fine grained deposits/coatings, which offer superior wear and corrosion resistance on metal surfaces [286]. Being a solid state process with no melting of material, FS has application potential in the deposition of dissimilar alloys and materials containing hard phases such as tool steels and Co-based alloys which would otherwise be incompatible or difficult to deposit by conventional fusion based methods. Lack of melting and lower heat input also reduces HAZ and residual stresses of the deposits due to lowered grain growth, and solidification shrinkage [281].

FS has been applied to improve surface properties and produce metal matrix composites in certain areas of manufacturing of parts and tools. A wide range of successful depositions by FS includes tool steels, stainless steels, mild steel, alloys of copper, nickel, titanium, aluminium and magnesium over similar and dissimilar substrates. Among the investigated combinations, carbon steel is the most versatile substrate accepting deposits of a variety of steels such as stainless steels, high speed steels, tool steels, mild steel, alloy steels, Co-Cr based alloys, Ni-Cr based alloys, AA1100 and bronze. Next versatile substrates are the alloys of aluminium. Deposition of Pure Ti and Pure Cu is incompatible with both ferrous and non-ferrous substrates except for deposition of Cu on Cu substrate [281,302–304]. Other successful mechetrode-substrate combinations for FS are detailed by Gandra et al. [281].

3.4. Friction stir surface cladding (FSSC)

Friction stir surface cladding (FSSC) is a recent solid state surface modification methodology, applying the principles of FSW and FS, which aims to deposit thin layers of a clad material on a substrate by breaking up the surface oxide layers and forming metallic bond between the substrate and the cladding material. The clad material extends through a hollow rotating tool onto the substrate. Two versions of this process have been studied where the bottom of the tool may or may not be in contact with the substrate [301,305,306]. The features of tool and process parameters are discussed below.

3.4.1. Process features and experimental setup

The FSSC tool constitutes one or more circular openings that host the consumable cladding rods, as shown in Fig. 28(a–d). The hosted pins are pushed by a steel piston on to the substrate. In FSSC, cladding is possible only if the heat generation is adequate enough to sufficiently soften the cladding rods. As shown in Fig. 28(b–d), two approaches, i.e., with or without the tool bottom touching the substrate, are adopted [305–313]. In the first approach, the rotating tool is lowered until its bottom contacts the surface of the substrate at a fixed force. This allows rupture of the oxide layers on the surface and initial heat generation due to friction at tool-substrate interface and substrate-cladding rod interface. In the dwelling phase, the tool rotation and downward force on the substrate heat up the substrate and the FSSC tool. End of the dwell phase starts the deposition phase where the piston driven cladding rods, while rotating together with the tool, are pressed down at a constant feed rate and pushed out towards the substrate. Simultaneously, the substrate is linearly moved under the tool at a constant speed and a clad layer is formed on the substrate.

In the second approach, shown in Fig. 28(c) and (d), the tool does not contact the substrate surface, but, the cladding rods do. The numbers in the figures indicate the order of action during

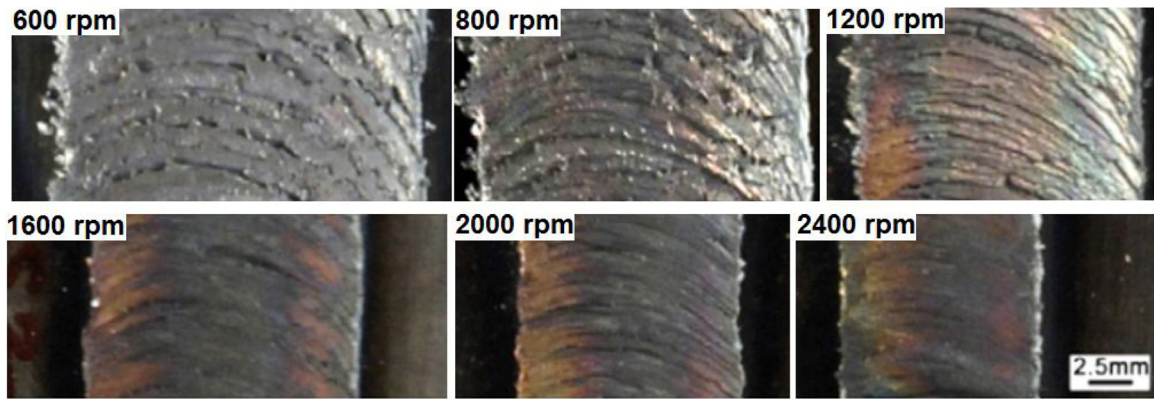


Fig. 25. Variation in width and surface finish of deposit with rotation speed [289].

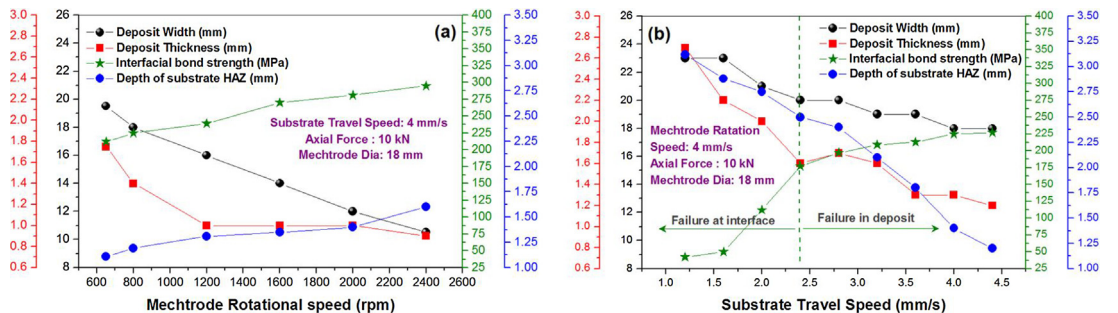


Fig. 26. Variation in quality of H13 mild steel deposit on low carbon steel due to (a) rotation speed, and (b) Travel Speed (Replotted using the data adopted from [294]).



Fig. 27. (.1) Thermo-mechanical events in the FS [287], (.2) Microstructural transformations during the FS of 6XXX Al on 2XXX Al on (a) Consumable base material, (b) heat affected zone, (c) compression-driven TMAZ, (d) torsion-driven TMAZ, (e and f) fully recrystallized microstructure, (g) deposited material and (h) bonding interface [21].

the process. Therefore, the heat generation is only by the friction between the substrate and cladding rods. In the deposition phase, the cladding rods are provided with a constant feed rate while the substrate is moved relative to the tool. This forms a clad layer on the tool. Throughout the FSSC process, a negative tool tilt angle is given to the tool. It can be seen clearly in Fig. 28(c) and (d) that either single or multiple cladding rods can be used.

3.4.2. Parameters of the process [305,306]

Clad layer quality is characterized by width, thickness and nature of bonding between the clad layer and the substrate [306]. The aim of cladding is to provide the substrate surface with additional properties of the clad material. Hence, no intermixing between the clad material and substrate is desirable, because it

would deteriorate the surface properties of both the clad and the substrate materials. Therefore, a proper process selection comprising of the choice between the processes with or without the clad-substrate contact and between the tools with single or double cladding rod openings is important.

Important process parameters of FSSC, numbered in Fig. 28(c), are tool rotation speed, substrate translation speed, tool tilt angle, rod feed rate and tool gap. The cladding depends upon the force exerted by the tool/cladding rod on the substrate which can be varied by varying the rod feed rate or the substrate translation speed. The degree of mixing of the substrate with the clad material depends, among other things, on the downward force of the FSSC tool on the substrate and the tool gap. The clad layer quality is highly dependent on the frictional and plastic deformation heat generated

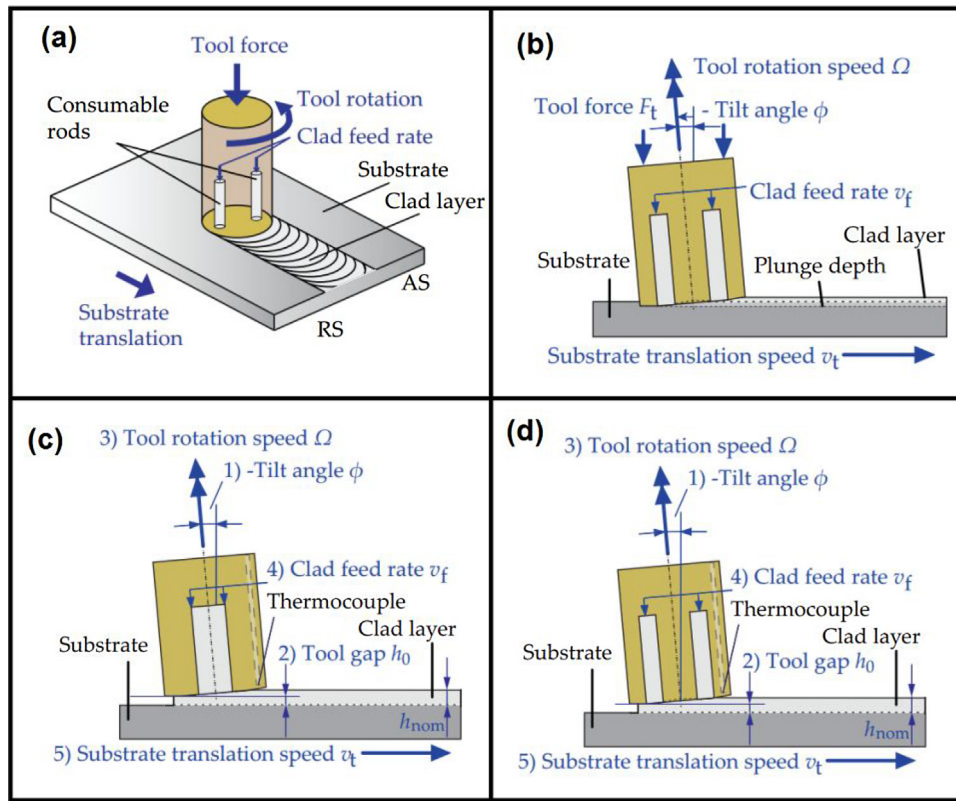


Fig. 28. FSSC process (a) schematic of first approach, (b) side view first approach, (c) schematic of second approach with one cladding rod, and (d) schematic of second approach with two cladding rods [305].

during the deposition process. The heat generated is shown to be strongly related to the tool rotation rate and the supply rate, i.e. the volume of the clad material supplied per unit time. For higher tool rotation rates and/or supply rates, the generated heat is larger, as also revealed by the temperature in the FSSC tool bottom [309,310].

3.4.3. Microstructure of cladded surface

In the FSSC process, the clad layer interface is of interest. Fig. 29 shows the macro and microstructure of clad layer interface of AA1050 deposited on the AA2024 substrate for three process conditions at a low tool force [305]. Fig. 29(a) shows that the clad layer interface consists of a clad-substrate mixed region and a heat affected region when the FSSC tool is in contact with the substrate during the FSSC process. This allows a healthy intermixing between the clad and the substrate surface and develops bands of substrate-rich and clad-rich regions. The degree of intermixing and width of cladded layer depend on the process conditions. The larger is the applied tool force, the larger is the width and depth of the intermixed clad layer and heat affected region in the substrate. Grain orientation of the layer is parallel to the substrate surface with relatively large grains found under the clad layer. Fine grains in the intermixing region indicate strong mechanical deformation.

When the FSSC tool is not in contact with the substrate (tool gap), no large intermixing of the substrate with the clad material occurs, as can be seen in Fig. 29(b). The intermixing is further limited at higher tool forces. When the tool gap is applied with a single rod of clad material, the clad-substrate intermixing at the clad layer interface is virtually nil and the substrate is deformed only slightly, as evident from Fig. 29(c).

3.4.4. Feasibility and application

One of the advantages of FSSC is no flash formation during the cladding. At present, FSSC has been applied at laboratory scale to

produce thin clad layers on an AA2024-T3 substrate using AA1050 clad material. FSSC process seems suitable for hard-to-weld highly alloyed AA2000 and AA7000 aluminium series [305–313]. Cladding is a useful method of corrosion protection of the weld region of the Al alloys [313,314]. FSSC is considered to be a future prospect for Al cladding in buildings because a building cladded with aluminium is quieter than the one covered with other metals due to the sound cushioning nature of aluminium [313]. A different version of FSSC has been recently reported where a series of lap-joints of copper cladding sheets to a steel substrate has been staggered using FSW lap welding to clad copper on steel [314–316]. The cladded component has offered better quality than that prepared by fusion welding.

3.5. Friction stir additive manufacturing (FSAM)

Additive manufacturing is a method of manufacturing parts by successive deposition of layers or deposition of layer upon layer to make an object [317]. It is the opposite of the subtractive manufacturing processes such as machining. The parts manufactured are derived by slicing models from three dimensional computer-aided-design. Although the FSAM technique has been introduced a decade ago [318], and its potential in achieving higher productivity and lower material loss has been predicted immediately afterwards [319,320], its performance in lightweight constructions for structural applications has been seriously explored and evaluated only recently. FSAM, being a solid state technology, obviously has several advantages over its fusion counterparts.

3.5.1. Features of FSAM process

Based on the combining processes, two types of friction stir additive manufacturing (FSAM) processes are reported in the literature. Type 1 is a combination of additive manufacturing and friction sur-

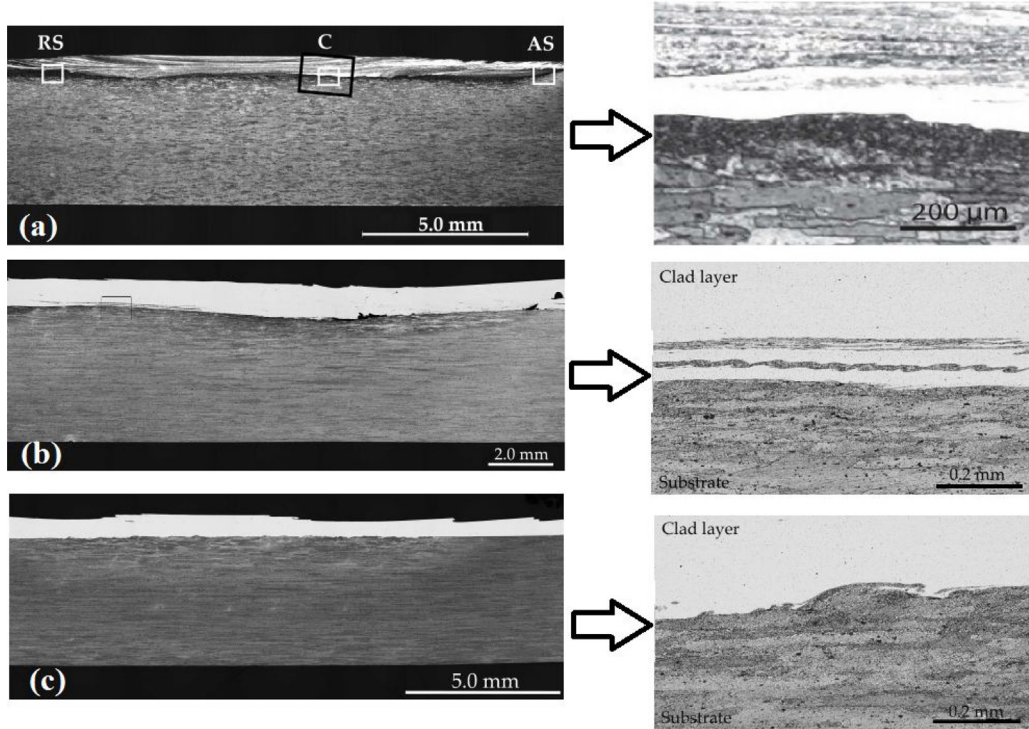


Fig. 29. Microstructure of clad layer interface of AA1050 deposited on the AA2024 substrate (a) double rod cladding and approach 1, (b) double rod cladding and approach 2 and (c) single rod cladding and approach 2 [305].

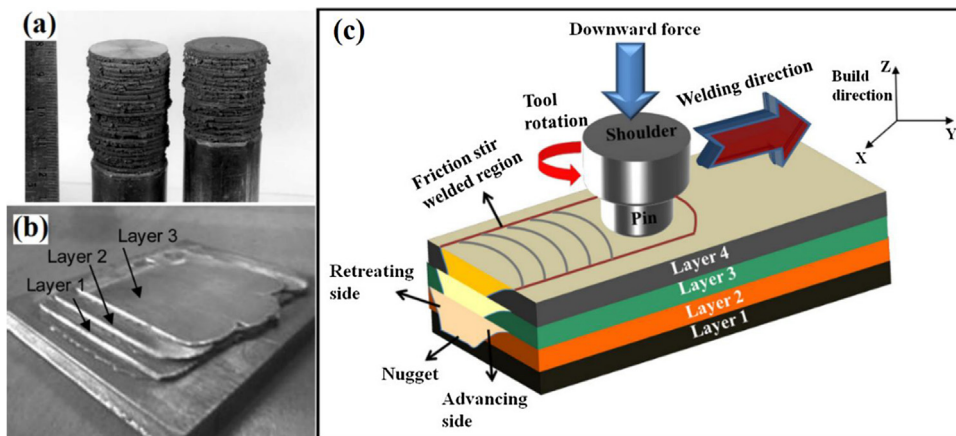


Fig. 30. Schematics of FSAM (a) rotary friction welding and friction deposition [321], (b) friction deposition and additive manufacturing [322], and (c) additive manufacturing and FSW [323].

facing or rotary friction welding and friction deposition [321,322] while the type 2 is a combination of additive manufacturing and friction stir welding [311]. Fig. 30(a) and b shows the products of type 1 FSAM while Fig. 30(c) shows the schematic of type 2 FSAM process. In the type 1 FSAM, rotary friction welding is combined with friction deposition process. It is important to note that friction deposition and friction surfacing work basically on the same principle, solid state material transfer from a consumable rod onto the substrate by rubbing [321].

In friction deposition, the material transfer occurs in a single step where rubbing of a rotating consumable rod against a substrate with a predefined load generates frictional heat, plasticizing the material at the rubbing end of the consumable rod. The rotation of the consumable rod develops a torsional shear between the plasticized material and the rotating rod leading to material transfer onto the substrate. Continuation of this process builds up plasti-

cized material of desired thickness, leaving a layer of deposit on the substrate. In friction surfacing, the principle of material plasticization is similar, i.e., the rotating consumable rod, referred to as mechtrrode, is rubbed against the substrate to generate plasticized material. However, the material transfer is due to the traverse of the substrate with respect to the mechtrrode.

The type 1 FSAM involves multiple repetitions of the friction deposition on an already friction deposited substrate [321], as shown in Fig. 30(a), or systematic multiple repetition of the friction surfacing on multiple tracks of the substrate [322], as shown in Fig. 30(b). Single track multilayer and multitrack multilayer approaches can be adopted to fabricate the desired parts.

The type 2 FSAM, shown in Fig. 30(c), involves producing a lap joint of two sheets by FSW and adding more sheets to the lap joint in lap configuration using successive FSW operations [323]. In the first step of the type 2 FSAM process, a lap joint of overlapping sheets

or plates is produced by traversing a non-consumable rotating tool. The heat generation and joining in FSW has been discussed earlier in this paper. In the succeeding steps of the process, the lap joining is repeated by sequentially stacking sheets over the previously welded layers and performing the lap joining to produce a multi-layered build. Number of succeeding steps in FSAM depends upon the desired final thickness of the joint and thickness of the overlaid plate.

Apart from the above, friction stir processing is used in conjugation with several fusion based additive manufacturing processes such as laser-engineered near net shaping (LENS), thermal spray, laser-assisted direct metal deposition etc. and solid-state additive processes such as cold spray, kinetic metallization, selective laser sintering (SLS) etc. to improve the physical properties, microstructure and mechanical properties of the product and to achieve desired integrity of the product [20]. In this method, a desired overlay is deposited on the substrate using one of the above mentioned fusion or solid-state process, followed by friction stir processing of the overlay.

3.5.2. Parameters involved in FSAM process

The process parameters of FSAM are similar to those in the friction surfacing or friction stir welding. The process parameters, the tool geometry or the consumable rod dimensions are chosen on the basis of the net thickness of the layer to be manufactured and the materials of the consumable rod and the deposit. The required net layer thickness and its shape decides the number of layers to be deposited and the method to be followed, i.e., either single track multilayer or multitrack multilayer deposition [321,322].

In type 2 FSAM, hotter welding conditions produce hooking defect and cracking along the interface of TMAZ and SZ of the builds due to decrease in forging forces and high residual stresses, respectively [323]. The variations in microstructure is also more within the build produced at higher heat input. The process parameters are found playing important roles in the material flow and thus, towards the mechanical properties of the build. The sheet thickness and the position of interfaces from the tool shoulder determine the microstructure. For type 1 FSAM, however, no dedicated study on the effect of process parameters is available at present.

3.5.3. Microstructural features of FSAM builds

Fig. 31(a) shows the microstructure of the center of friction deposited layer of austenitic stainless steel on mild steel. The microstructure indicates equiaxed fine grains due to dynamic recrystallization. Also, the multiple deposition of new layers causes sensitization in the previously deposited layers (3 layers below from the new layer) due to high temperature and cooling within the critical rate conducive for sensitization [311].

Fig. 31(b) shows the microstructure of multi-track multilayer deposit of mild steel rod on a mild steel plate, produced by type 1 FSAM (friction surfaced build). Good inter-track and inter-layer bonding can be achieved by proper choice of consumable-substrate combination, process parameters and positioning of consumable rod [322]. The deposit of stainless steel friction surfaced on mild steel in **Fig. 31(b)** shows fine grains with a mixture of ferrite and pearlite. Also, during subsequent deposition, the middle layers are reheated, causing a tempered microstructure in the middle layers and martensite in the upper later.

Fig. 31(c) shows the microstructure of a four layer lap build of the Mg alloy made by type 2 FSAM. The layer 4 is the top most layer of the build followed by layers 3, 2 and 1. The microstructure is complex, containing a number of distinct regions such as the different layers, layer interfaces, one pass SZs, two pass SZs, TMAZ, HAZ etc. [323]. Obviously, the number of these regions in a FSAM build vary depending upon the number of layers. Banding regions, analogous to onion rings, are also available below the interfaces.

Analysis has shown that the banding regions differ in the composition of alloying elements, while the weight% of the parent metal shows no noticeable change. The interface banding regions show formation of intermetallic compounds and precipitates with varied sizes and shapes such as fine spherical, fine globular, fine plate and coarse irregular [323]. Also, the top layer constitutes the shoulder dominated region and the subsequent lower layers comprise of pin dominated regions. The layers and the interfaces constitute a mixture of coarser, finer and very fine recrystallized and equiaxed grains while the TMAZ constitutes coarse grains and fine grained necklace features.

3.5.4. Feasibility and application

Application of friction joining for the purpose of additive manufacturing is patented in 2004 by White [318]. With proper selection of the technique, materials, tool and geometry, several friction stir technologies can be used in conjugation with FSAM, which would be feasible to both ferrous and non-ferrous alloys and also for dissimilar alloys [321]. Possible use of FSAM in aerospace applications has been claimed by Boeing [319] and Airbus 2006 [320] to achieve higher productivity and lower material loss. In FSAM, an entire layer can be deposited in one step and the achievable layer thicknesses is higher compared to that in other additive manufacturing processes. Strong metallurgical bonding between layers, and good mechanical and microstructural properties are some additional advantages. Distinctive characteristics of FSAM has a competitive edge over the existing fusion and other solid state additive manufacturing techniques.

3.6. Friction stir forming (FSF)

Friction stir forming (FSF) is a process which makes use of the friction stirring technology to achieve improved formability and form transfer for micro-forging and mechanical interlocking of materials into desired new shapes and structures, hence making its application potential versatile and interesting [324–329]. Developed by Nishihara [330,331], FSF has been used for different applications such as to draw a material into a desired form, join a thin metallic wire to plate/sheet(s), lap joining or mechanical fastening of dissimilar metal sheets and generation of composites of difficult-to-mix materials etc.

3.6.1. Process features and experimental setup

FSF is an improved method which combines the concepts of friction stirring process and forming process. The objective of the process is to generate sufficient thermal softening in the workpiece material to enable its flow into a die or an analogous structure and micro-forge into the shape of die [329]. FSF utilizes a non-consumable tool consisting of a shoulder and with or without a pin and a shaped die to receive the transferred soft material intended for micro-forging [332–338]. The die can be a distinct component of the FSF equipment [320] or can be a guide slit or a cavity or of any other artificial shape on the base material itself, depending upon the requirement [329,330,339–341]. If the die is a distinct component of the FSF equipment, the tool and the die are positioned vertically opposite to each other and the workpiece is placed on the die prior to the FSF [332]. If the die is a pre-machined shape on the workpiece, such as a slit or a cavity for enclosing a dissimilar material, the objective then is to guide the plastic material into the shape [329,330,339,340]. For the mechanical fastening of dissimilar materials by FSF, a hole of smaller diameter than the die is pre-drilled in the bottom sheet for allowing the flow of deformed top sheet material through the hole into the die to achieve interlock of the flown material with the bottom sheet [333].

The working stages of FSF are as follows. 1) The rotating FSF tool is pressed vertically opposite to the die in the desired area of

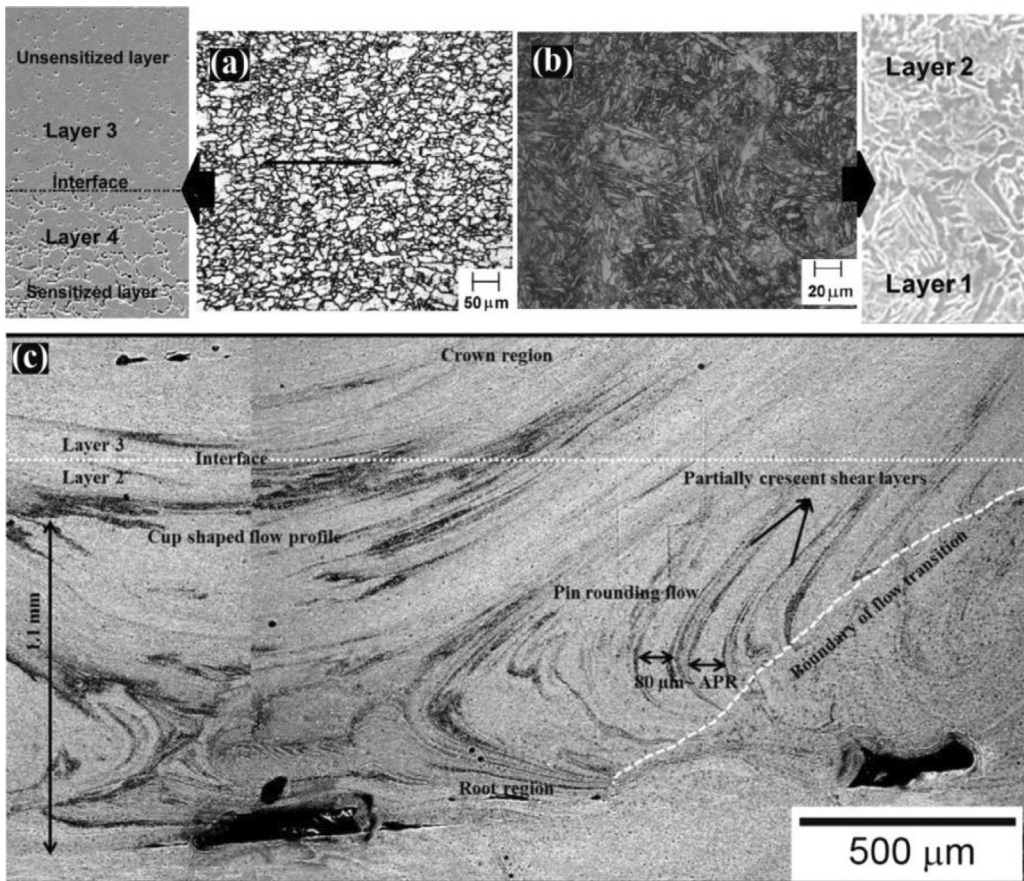


Fig. 31. Microstructure of (a) mild steel deposit on mild steel substrate in Type 1 FSAM [321], (b) stainless steel friction surfaced on mild steel in Type1 FSAM multitrack multilayer surfacing [322], and (c) Partial macrostructure of Type 2 FSAM build of Mg alloy [323].

the to-be-formed workpiece to generate sufficient frictional heat and degree of plasticization of workpiece. The tool makes a dip and slightly penetrates into the workpiece. 2) As the tool is traversed, friction stirring occurs and the workpiece flows into the die under or in the workpiece as a result of plastic flow. Thus, the shape of the die is transferred to the workpiece, or the workpiece and the die are mechanically fastened by the anchor effect or mechanical interlocking. 3. At the end, the tool is retracted to obtain the formed shape or joint or interlocking or mixing.

3.6.2. Process parameters in FSF

The process parameters of FSF vary depending upon the application. Common process parameters of all the FSF processes are the tool rotation speed, tool traverse speed, feed rate or plunge speed, tool geometry and tool tilt angle [329,330,332,340]. Investigating the formability of A6061P-T6 aluminium alloy on a grooved S45C steel bar and cladding of the grooves by FSF, Nishihara have shown that travel speed has a reasonable influence on the surface temperature of the die which corresponds to filling rate, concluding that the die temperature increases with rotation speed and plunge depth, but decreases with travel speed [331]. These parameters contribute to the frictional heat generation and plastic flow in FSF. Tool tilt angle contributes to the confinement of the plastic material and control of material loss in terms of flash. The above parameters along with plunge depth cause significant variations in the plastic material flow in the fabrication of Cu-W composite by FSF [329].

In the mechanical fastening of 1.4 mm 6014 Al alloy to 0.7 mm GMW2 mild steel by FSF process, tool diameter and tool plunge depth are reported to be important parameters by Lazarevic et al. from their design of experiment (DOE) study [334–336]. Interaction

of these two parameters contribute to the total energy. Apart from the above, the remaining thickness of the top sheet is an important process parameter in the fastening of 1.4 mm thick AA6014 and 1.0 mm thick AISI 5182 aluminium alloys with 0.7 mm GMW2 mild steel by FSF [336]. Generally, the top sheet is thicker than the bottom sheet. The top sheet is the one to be deformed and thinned during the FSF and the remaining thickness has to withstand the compressive axial load during the forming. The plunge depth should be kept minimum to reduce the thinning of the top sheet. Large plunge depth and the resulting insufficient remaining thickness of top sheet would lead to failure of the structure. These DOE studies, however, have shown that effect of plunge speed on joint strength and joint failure are negligible [333,334]. The set up geometry such die geometry, positioning etc. are also important parameters to achieve sound results with FSF.

3.6.3. Microstructures of formed product

The FSF studies reported in the literature has been aimed at different purposes, such as to mechanically interlock a wire in a bulk metal [330] or to make a composite by encapsulating a metal insert in another metal block [329] or to mechanically fasten two dissimilar metals [332] etc. The thermomechanical scenario in these FSF processes are different from each other. Hence it is not possible to arrive at some generalization on microstructure evolution in FSF. However, it is seen that the microstructures of the formed components constitute the typical SZ, TMAZ, HAZ and BM depending upon the thermomechanical actions exerted.

In a study, an insulated thin Cu-wire has been mechanically interlocked to Zn-22Al superplastic alloy by placing the wire in a guide slit in between overlapping plates [340]. The microstruc-

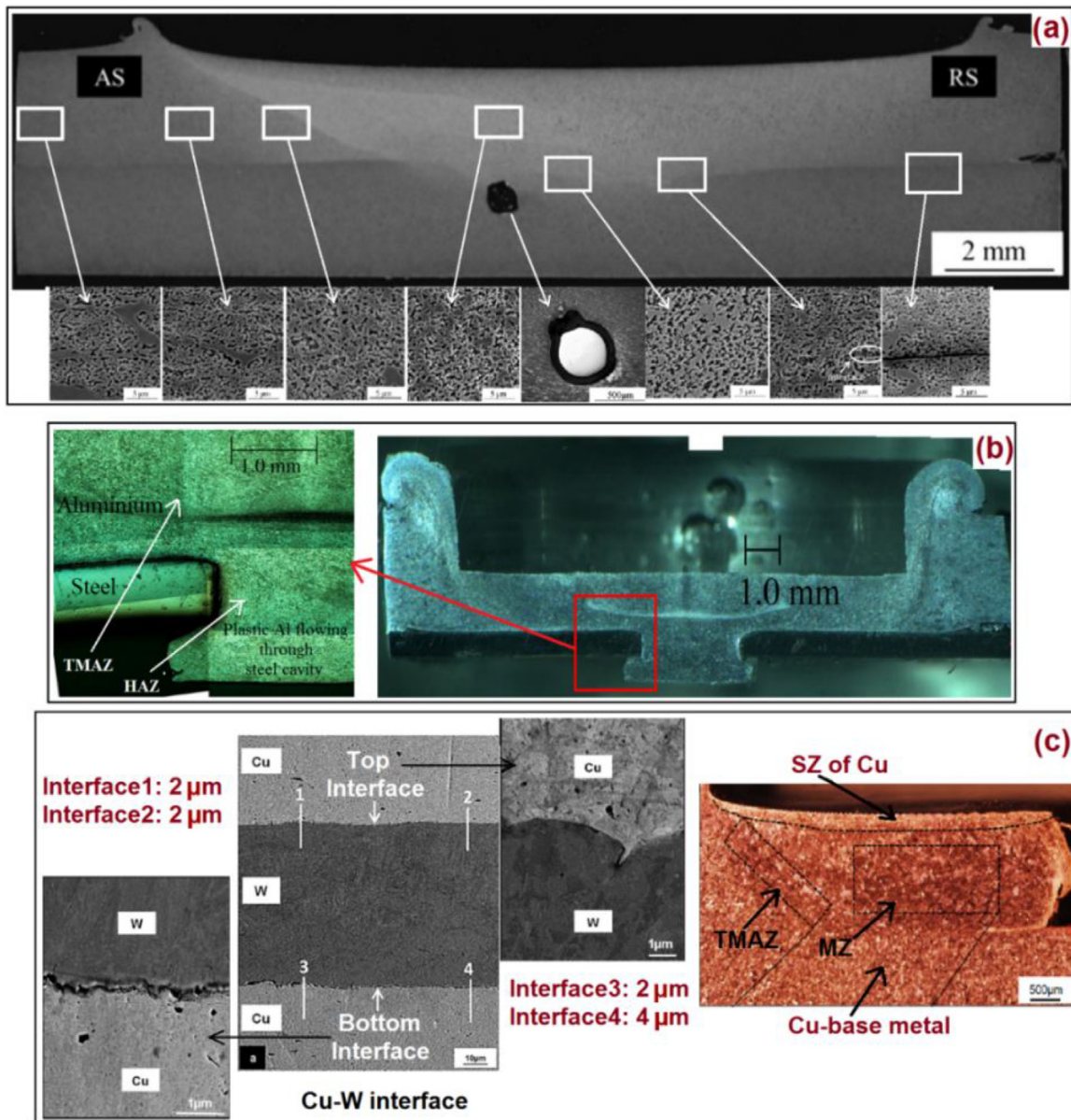


Fig. 32. Macro and microstructures of FSF products (a) Interlocked Cu-wire between superplastic Zn-22Al plates [340], (b) Joining of Al 6014/Mild steel [334], and (c) Fabrication of Cu-W composite [329].

ture in Fig. 32(a) shows that the superplastic alloy completely fills its slot. Also, the macrostructure shows no interface between the two alloy plates. The marked areas in the macrostructure show SZ, TMAZ and HAZ in their typical positions with the grain structure getting finer towards the stir zone.

Fig. 32(b) presents micrographs of the FSF joint of Al-alloy and [334]. The magnified microstructure shows the flow of the deformed aluminium from top plate through a hole in the bottom plate. It is clear that the aluminium formed around the edge of the steel has been pushed into the die cavity through the hole in the bottom sheet. A distinct boundary can be seen between the material under the tool and the material formed into cavity. The portion of the boundary rotating with the tool represents the TMAZ while that forged into the cavity without rotation represents the HAZ [334].

Fig. 32(c) shows the interface of a Cu-W composite fabricated by placing W-inserts in a machined cavity of a Cu block and processed by FSF [329]. The top and bottom interface regions exhibit no IMC layer due to lack of diffusion, but a continuous interlock of width 2 μm between Cu and W has been observed. The Cu block processed

under the FSF tool exhibits three distinct regions, 1) fine, recrystallized and equiaxed Cu-grains of SZ immediately below the tool, 2) elongated Cu-grains of TMAZ from the edge of the tool towards the machined cavity, and 3) slightly larger and deformed Cu-grains in the mixed zone (MZ).

3.6.4. Feasibility and application of FSF

Using FSF, Nishihara et al. has cladded A7074P, A2024P, A2017P and A6061P aluminium alloys in the grooves of a carbon steel plate to find that 6061 is the best candidate for cladding [330,331]. Balakrishnan et al. have used FSF to successfully join aluminium to nylon by a mechanical interlock and found the interlock stronger than adhesively bonded joints [328]. FSF has been used to produce mechanical interlocks between an A6061P-T6 aluminium alloy plate and various types of thin metallic wires such as piano wire, ultrathin stainless steel strand, super elastic alloy wire and shape memory alloy wire [339].

Tabatabaei adopted the above concept to mechanically interlock a thin insulated copper wire sandwiched between two Zn-22Al

superplastic alloy plates by causing superplastic deformation in the later [340]. Mechanical interlocking of the thin metallic wire extends the application potential of FSF to microfabrication of composite materials, smart materials and micro-processed materials for electronic and electrical sectors. Ostu et al. used FSF to form 2017-T3 sheets into frustum of pyramids by a hemispherical tool [341,342]. Liu et al. employed similar FSF method as Lazrevic et al. [332] to successfully join low carbon 1010–1018 steel/Al 6014, AZ31B-H23 (Mg alloy)/mild steel, and Al 6014/carbon fiber reinforced nylon matrix [336,337]. FSF has been successfully employed to fabricate Cu-W composite by placing W-inserts in the cavity of a Cu-block and then processing with a flat tool to achieve sound intermixing of copper and tungsten [329]. The above successful applications of FSF opens up a wider path for the process.

3.7. Friction stir extrusion (FSE)

Extrusion of material by friction stirring or the friction stir extrusion (FSE) process has at least three different applications documented in the literature [343–359]. One of the applications, by the name friction extrusion (FE), applies the friction stir principles to join dissimilar materials, e.g. aluminium alloy to steel, by extruding the softer into a predesigned groove or hole of the harder material such that mechanical interlocking and chemical bonding between the two materials can be realized [344]. An improved version of this process has been reported, by the name “two-sided friction stir extrusion riveting” where a harder material is sandwich joined between two softer materials [345]. Both these processes are similar to one of the applications of friction stir forming reported earlier [334].

The second type of the FSE is a solid state material synthesizing process that produces extruded products by direct conversion of scraps into useful bulk rod/wire via thermomechanical processing [346–353]. This process is dedicated to extract wires from metallic chips or wastes. The third type of the process, known as friction stir back extrusion (FSBE), produces tubes from bulk rod materials [354–359]. The above three types of FSE process are referred to as FSE-joining, FSE-wire drawing and FSE-tubing, respectively, in this study. Apart from those listed here, two more such processes based on extrusion via friction stirring include rotation of a rod or a billet material while being forced through a die to draw it into wire, and cladding of a solid rod from a tube by rotating and forcing it through a die, as discussed by Nicholas et al. [359].

3.7.1. Process features and experimental setup

3.7.1.1. FSE-wire drawing [346–353]. The schematic of FSE-wire process is shown in Fig. 33(a). The main components used in the FSE experiments are a stationary billet chamber and a rotating plunge die with a scrolled face, both made of hard materials. The plunge die has an outer diameter almost equal to or slightly smaller than the internal diameter of the chamber to facilitate the stirring action of the process. The plunge die constitutes an inner hole of a fixed length and diameter for extrusion of the wire. During the process, the rotating plunge die is pushed into the container, which is filled with the metal chip/waste. The rotation and translation of the plunge die relative to the container causes stirring and mixing of the chips. The increasing contact and pressure between the rotating plunge die and the chips lead to plasticization of the chips and their flow towards the plunge die hole. In the end, a consolidated wire is formed in the die hole. The wire can be easily extracted from the plunge die due to its small length of contact.

3.7.1.2. FSE-tubing [354–358]. The setup of FSE-tube process consists of two components, the stirring tool and the die, as shown schematically in Fig. 33(b). The stirring tool is a polished solid rod prepared from a hard metal such as H13 tool steel [354,355]. The

tool end is tapered to facilitate penetration while the stirring surface of the tool end is kept flat and without a tool pin. The extruding die is made of pre-hardened steel. The die cavity is a blind hole of diameter larger than the diameter of the tool. This is to provide an obvious clearance between the outer surface of the stirring tool and the inner surface of the die. The die is made in two halves in order to facilitate extraction of tube [356]. The extruding die is securely planted on a machining center with its cavity centred with respect to the stirring tool in order to ensure axisymmetric deformation conditions.

During the process, the stirring tool, rotating at a selected speed, is driven downwards at a fixed feed rate against a metallic bar specimen placed in the die cavity. The downward motion of tool forces the material of metallic bar radially outwards, analogous to back extrusion. Also, high load imposition and friction at the tool–specimen interface generates sufficient frictional heat and softens the bar, facilitating its deformation. This also allows penetration of the tool into the bar, leaving it back extruded as well as producing a tube. After reaching a desired depth, the rotating tool is retracted. Release of the extruding die retrieves the tube.

3.7.1.3. FSE-Joining [343–345]. In the FSE-joint process, shown in Fig. 34(a), dissimilar materials such as aluminium and steel can be lap joined without intermetallic compound layer issues. The harder material, which is also the bottom sheet, is provided with a pre-machined concave groove such as slit saw or O-ring dovetail groove or any other groove that would facilitate mechanical interlocking between the softer top sheet and the bottom sheet. The FSE-joint process is similar to FSW. In the plunge stage, it is ensured that the rotating tool always remains in the softer top sheet and the shoulder is engaged in the weld. The top material is plasticized and extruded into the concave groove of the bottom sheet. A profiled shoulder and pin are preferred in this process because, these features force the plasticized material down and extrude into the groove. Once extruded, the specially designed concave grooves mutually fix the dissimilar materials and allow mechanical interlocking to produce a dissimilar joint.

Double-sided FSE-joining is another extrusion-joining method that combines the elements of FSE-joining, i.e., extruding the material into a preformed cavity to join both materials is combined with the concept of rotating anvil friction stir spot welding (RAFSSW) which is based on imposing deformation of the participating materials from the top and the bottom with the help of a pair of rotating anvils [345]. Schematics of the double sided FSE-joining is shown in Fig. 34(b). In this process, the harder material constituting a predrilled hole is placed in the middle of a triple lap configuration. The triple lap is placed under oppositely rotating anvils which cause deformation of the top and bottom sheets, backward and forward extrusion of the deformed top and bottom materials into the predrilled hole of the middle material and joining of the extruded materials. Also, a diffusion bonding is produced between the middle material and the top and bottom materials.

3.7.2. Process parameters in FSE

In FSE-wire drawing, the tool geometry, extrusion parameters, i.e., tool rotation speed, plunge rate, extrusion hole, and material characteristics are the main parameters, affecting the material flow pattern and temperature distribution and thus, influencing the microstructure evolution and mechanical properties of the recycled wires [345,352,353]. A variation in rotation speed leads to a change in extrusion temperature. Too high temperature leads to grain growth and results hot cracking of the wire while too low temperatures lead to formation of voids, cold cracks, tearing and twisting in the extruded wire [347,348,350,352]. Therefore, intermediate rotation speeds are suitable. Increasing plunge rate also increases the temperature and the grain size and lead to hot crack-

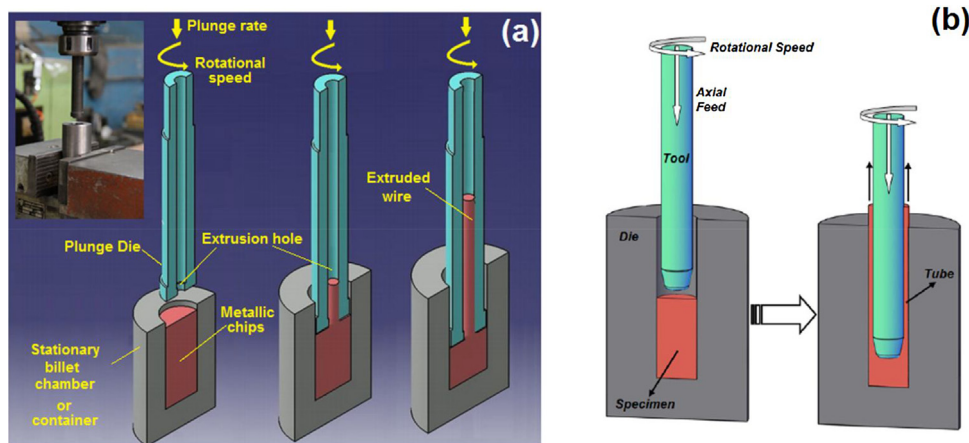


Fig. 33. (a) Schematic of FSE-wire drawing process [352], (b) Schematic of FSE-tubing process [354].

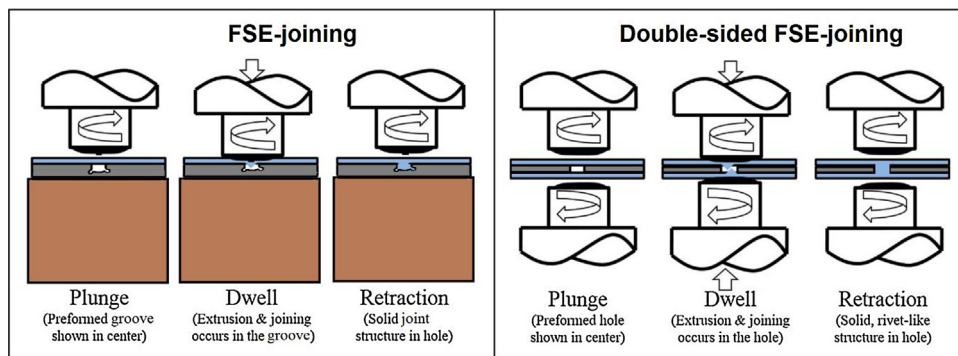


Fig. 34. (a) Schematic of FSE-joining process, (b) Schematic of double-sided FSE-joining process [345].

ing [352,353]. Unfortunately, so far, no information about the effect of process parameters on the FSE-tubing processes or on their products is available in the literature for further comment. In the FSE-joining process, dwell time, specimen hole diameter and number of holes affect the feasibility of welding and the strength and quality of the joint [345]. The higher are these values, the stronger is the bond. However, this process also needs a wider investigation on the process parameters.

3.7.3. Metallurgy of FSE product

The product of FSE process have been claimed to perform better than those produced using conventional fusion processes. In both the wire drawing and the tubing, grain refinement is a common phenomenon and the location of grain refinement is the location within the wire or the tube that undergoes severe plastic deformation [348,356]. In the tubing process, the tube basal center which is also the stirring zone, has refined grains while the basal periphery have grains with elongated morphology and higher aspect ratio. Away from the base, on the wall of the tube, grain growth is evident, however, the coarsening is not severe [356,357]. The grain refinement features are approximately independent of the material.

Some special features such as elongation in Al alloys or twinning in Mg alloys at the basal periphery have been reported. These features are clear from Fig. 35(a) and (b), which show the microstructures of various regions of an extruded Al-tube, and an extruded Al-wire, respectively. The fine recrystallized and equiaxed stir zone microstructure in the tubing process can be attributed mainly to dynamic recrystallization while static recrystallization, partial recrystallization, and heat extrusion etc. also play minor roles [358]. Away from the stir zone, the contribution of dynamic

recrystallization seems to dip slightly and gradually with the elongated grains indicating tendency for partial recovery. In the FSE (single and double-sided)-joining processes, the joints show no evidence of intermetallic compound layer.

3.7.4. Feasibility and application

Friction extrusion processes are attractive prospects for dissimilar joining, recycling of machining waste and other industrial waste, and consolidation of powder product potentially as a method of mechanical alloying. In the tubing process, it saves almost an unbelievable amount of energy (~99%), hence it is an energy efficient tubing method. The FSE-wire drawing and FSE-tubing has been applied mainly to the Al and Mg alloys while the FSE-joining processes have been applied for the dissimilar joining of aluminium to steel without intermetallic compound layers [346,351,355,357].

4. Summary and outlook

This review points out that although friction stir concept is time-worn, it has been put into routine practice only after the invention of friction stir welding and found remarkable success in the welding of Al-alloys and rapidly emerging as a candidate joining technique for other ferrous and non-ferrous alloys. Over the timeline of past 26 years, several new technologies based on the friction stir concept have been developed, simply by maneuvering, modifying, exploiting and improvising each and every criteria of the process, such as the machine, the tool design, the workpiece, the process, the positions of the workpiece and the tool, the position of the backing plate or die, the size and shape of the die, by the selection of consumable and non-consumable tools, the heat generation, material flow and

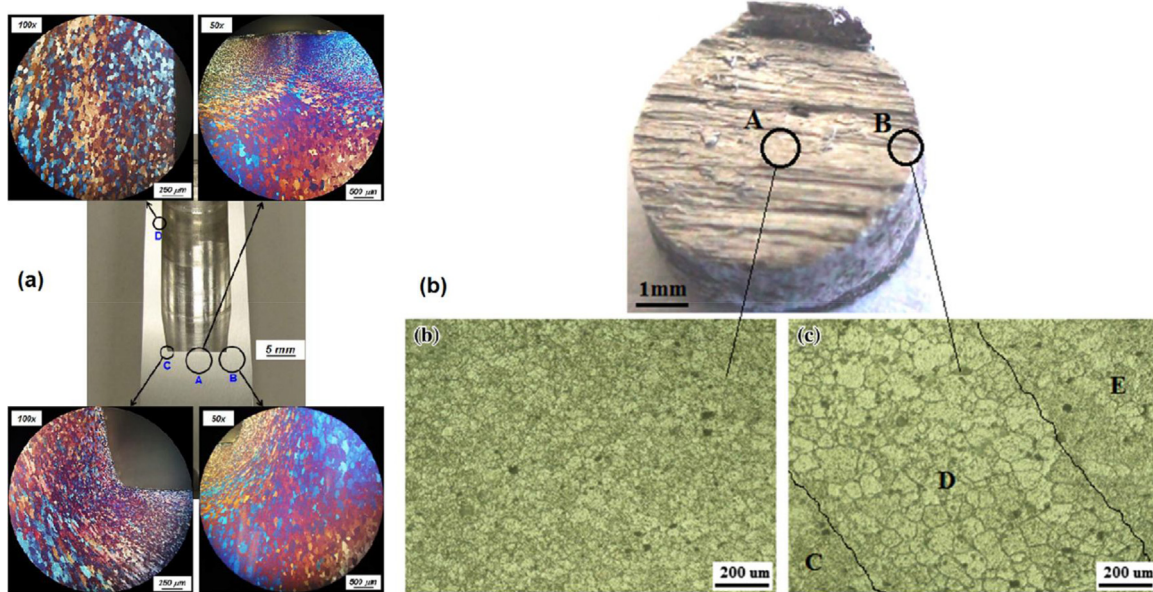


Fig. 35. Microstructure of (a) Al-tube produced in FSE-tubing [356], and (b) Al wire produced in FSE-wire drawing [348].

other mechanisms of the process to join and process materials to the desire.

Development of the processes discussed in this review shows that a reasonable degree of understanding about the friction stir physics and the related mechanisms is already available. The main aim of the friction stir based technologies is to achieve a sufficient degree of material plasticization or the third body region, which allows diffusion and intermixing of material irrespective of their compatibility. To achieve a sufficient plasticization, adequate amount of heat generation is essential. The heat generation, material deformation, process effectiveness, product quality and productivity depend upon the process parameters.

The main process parameters in the friction stir based joining and processing technologies are those which drive the heat generation and material plasticization, and subsequent material transfer, i.e., the tool rotation speed, tool traverse speed, feed rate or plunge speed, tool geometry and tool tilt angle. Therefore, careful optimization of process parameters is vital to achieve sustainable results. The microstructure of the friction stir joined or processed zone typically constitutes a recrystallized and refined region which exhibits relatively better mechanical and microstructural properties.

At present, the friction stir concept appears to have been utilized in most of the metal working operations and to a wide range of ferrous and non-ferrous materials. With minor manipulations in the equipment, tool or the process, a wide range of materials can be manufactured for a variety of purposes. Although some of these friction stir based metal working processes are still in the preliminary stages of their development, the conducted investigations indicate that these solid state processes are either similar or better than their fusion counterparts in terms of technological feasibility and product quality with respect to the fabrication of light weight metals. The issues to look into are the adaptability and cost of these processes.

Also, significant progress should be made in the modelling aspect of these processes which would help monitor and control the process while yielding better products at lower costs. At present, although the induction of robotics has significantly improved the flexibility of the equipment, large loads are applied on the tool to achieve the tool stability in the friction stir metal working operations. This makes the friction stir equipment immobile and also

results tool wear. Developments should be made to compact the friction stir equipment so that it can be transported for minor in-field applications. This would help ultimately materialize the lightweight design concept and its further benefits.

Acknowledgements

The authors gratefully acknowledge the financial support on this work from the National Natural Science Foundation of China (Grant Nos. 51475272 and 51550110501). One of the authors, G. K. Padhy, thanks Shandong University for the Postdoctoral fellowship.

References

- [1] W.M. Thomas, E.D. Nicholas, J.C. Needham, M.G. Murch, P. Templesmith, C.J. Dawes, Friction stir butt welding, GB Patent 9125978.8, International Patent PCT/GB92/02203, 1991.
- [2] P.L. Threadgill, A.J. Leonard, H.R. Shercliff, P.J. Withers, *Int. Mater. Rev.* 54 (2009) 49–93.
- [3] P.S. De, R.S. Mishra, *Sci. Technol. Weld. Join.* 16 (2011) 343–347.
- [4] O.S. Salih, H. Ou, W. Sun, D.G. McCartney, *Mater. Des.* 86 (2015) 61–71.
- [5] G. Çam, S. Mistikoglu, *J. Mater. Eng. Perform.* 23 (2014) 1936–1953.
- [6] R.S. Mishra, Z.Y. Ma, *Mater. Sci. Eng. R* 50 (2005) 1–78.
- [7] R. Nandan, T. DebRoy, H.K.D.H. Bhadeshia, *Prog. Mater. Sci.* 53 (2008) 980–1023.
- [8] M.B. Uday, M.N.A. Fauzi, H. Zuhailawati, A.B. Ismail, *Sci. Technol. Weld. Join.* 15 (2010) 534–558.
- [9] G. Çam, *Int. Mater. Rev.* 56 (2011) 1–48.
- [10] T. DebRoy, H.K.D.H. Bhadeshia, *Sci. Technol. Weld. Join.* 15 (2010) 266–270.
- [11] T. Watanabe, H. Takayama, A. Yanagisawa, *J. Mater. Process. Technol.* 178 (2006) 342–349.
- [12] J. Defalco, *Weld. J.* 88 (2009) 44–48.
- [13] B.T. Gibson, D.H. Lammlein, T.J. Prater, W.R. Longhurst, C.D. Cox, M.C. Ballun, K.J. Dharmaraj, G.E. Cook, A.M. Strauss, *J. Manuf. Process.* 16 (2014) 56–73.
- [14] H.K.D.H. Bhadeshia, T. DebRoy, *Sci. Technol. Weld. Join.* 14 (2009) 193–196.
- [15] W.M. Thomas, P.L. Threadgill, E.D. Nicholas, *Sci. Technol. Weld. Join.* 4 (1999) 365–372.
- [16] X.C. Liu, C.S. Wu, G.K. Padhy, *Sci. Technol. Weld. Join.* 20 (2015) 345–352.
- [17] G.K. Padhy, C.S. Wu, S. Gao, *Sci. Technol. Weld. Join.* 20 (2015) 631–649.
- [18] W.J. Arbegast, in: R.S. Mishra, M.W. Mahoney (Eds.), *Friction Stir Welding and Processing*, ASM International, New York, 2007, pp. 273–308.
- [19] F. Nascimento, L. Quintino, *Biul. Inst. Spaw.* 58 (2014) 12–23.
- [20] M.K. Kulekci, U. Esme, B. Buldum, *Int. J. Adv. Manuf. Technol.* 85 (2016) 1687–1712.
- [21] P. Vilaça, C. Vidal, J. Gandra, in: Z. Ahmed (Ed.), *Aluminium Alloys – New Trends in Fabrication and Applications*, Intech Open Access Publisher, 2012, pp. 159–197.
- [22] W.M. Thomas, *An Investigation and Study into Friction Stir Welding of Ferrous-based Material*, PhD Thesis, University of Bolton, 2009.

- [23] W.M. Thomas, D.G. Staines, I.M. Norris, R. de Frias, *Weld. World* 47 (2003) 10–17.
- [24] R. Rai, A. De, H.K.D.H. Bhadeshia, T. DebRoy, *Sci. Technol. Weld. Join.* 16 (2011) 325–342.
- [25] Y.N. Zhang, X. Cao, S. Larose, P. Wanjara, *Can. Metall. Quart.* 51 (2012) 250–261.
- [26] C.E. Rowe, W.M. Thomas, Advances in Tooling Materials for Friction Stir Welding, TWI and Cedar Metals Ltd., 2005 (Web link: http://www.innovatec.com/downloads/rowe_matcong.pdf).
- [27] A. Arora, M. Mehta, A. De, T. DebRoy, *Int. J. Adv. Manuf. Technol.* 61 (2012) 911–920.
- [28] T. DebRoy, A. De, H.K.D.H. Bhadeshia, V.D. Manvatkar, A. Arora, *Proc. R. Soc. A* 468 (2010) 3552–3570.
- [29] A. Arora, A. De, T. DebRoy, *Scr. Mater.* 64 (2011) 9–12.
- [30] M. Mehta, A. De, T. DebRoy, *Sci. Technol. Weld. Join.* 19 (2014) 534–540.
- [31] V. Buchibabu, G.M. Reddy, A. De, *J. Mater. Process. Technol.* 241 (2017) 86–92.
- [32] R.S. Mishra, P.S. De, N. Kumar, *Friction Stir Welding and Processing*, Springer International Publishing, 2014, pp. 95–108.
- [33] S.K. Selvam, T.P. Pillai, *Int. J. Chem. Technol. Res.* 5 (2013) 1346–1358.
- [34] M.L. Rao, P.S. Babu, T. Rammohan, Y. Seenaiah, *AKGEC Int. J. Technol.* 3 (2012) 15–18.
- [35] M. Mijajlović, D. Milčić, in: R. Kovacevic (Ed.), *Welding Processes*, Intech Publications, 2012, pp. 247–274.
- [36] Y.B. Zhong, C.S. Wu, G.K. Padhy, *J. Mater. Process. Technol.* 239 (2017) 273–283.
- [37] G.Q. Chen, Q.Y. Shi, Y.J. Li, Y.J. Sun, Q.L. Dai, J.Y. Jia, Y.C. Zhu, J.J. Wu, *Comp. Mater. Sci.* 79 (2013) 540–546.
- [38] H. Su, C.S. Wu, A. Pittner, M. Rethmeier, *Energy* 77 (2014) 720–731.
- [39] X.C. Liu, C.S. Wu, *J. Mater. Process. Technol.* 225 (2015) 32–44.
- [40] K.N. Krishnan, *Mater. Sci. Eng. A* 327 (2002) 246–251.
- [41] R.W. Fonda, J.F. Bingert, *Scr. Mater.* 57 (2007) 1025–1052.
- [42] P.B. Prangnell, C.P. Heason, *Acta Mater.* 53 (2005) 3179–3192.
- [43] S. Mironov, Y.S. Sato, H. Kokawa, in: A.J. Schwartz, M. Kumar, B.L. Adams, D.P. Field (Eds.), *Electron Backscattered Diffraction in Materials Science*, Springer Science, New York, 2009, pp. 291–300.
- [44] S. Gourdet, F. Montheillet, *Acta Mater.* 51 (2003) 2685–2699.
- [45] R.W. Fonda, K.E. Knippling, *Sci. Technol. Weld. Join.* 16 (2011) 288–294.
- [46] R.W. Fonda, J.F. Bingert, K.J. Colligan, *Scr. Mater.* 51 (3) (2004) 243–248.
- [47] J.Q. Su, T.W. Nelson, C.J. Sterling, *Mater. Sci. Eng. A* 405 (2005) 277–286.
- [48] R.W. Fonda, K.E. Knippling, J.F. Bingert, *Scr. Mater.* 58 (2008) 343–348.
- [49] B. Heinz, B. Skrotzki, *Metall. Mater. Trans. B* 33 (2002) 489–498.
- [50] T.R. McNeiley, S. Swaminathan, J.Q. Su, *Scr. Mater.* 58 (2008) 349–354.
- [51] S. Mironov, K. Inagaki, Y.S. Sato, H. Kokawa, *Metall. Mater. Trans. A* 46 (2015) 783–790.
- [52] G.K. Padhy, C.S. Wu, S. Gao, L. Shi, *Mater. Des.* 92 (2016) 710–723.
- [53] G.K. Padhy, C.S. Wu, S. Gao, *Mater. Lett.* 183 (2016) 34–39.
- [54] G.K. Padhy, C.S. Wu, S. Gao, *Mater. Des.* 116 (2017) 207–218.
- [55] S. Gao, C.S. Wu, G.K. Padhy, L. Shi, *Mater. Des.* 99 (2016) 135–144.
- [56] Y. Yue, Z. Li, S. Ji, Y. Huang, Z. Zhou, *J. Mater. Sci. Technol.* 32 (2016) 671–675.
- [57] Z.H. Zhang, W.Y. Li, Y. Feng, J.L. Li, Y.J. Chao, *Sci. Mater. A: Eng.* 598 (2014) 312–318.
- [58] Z.H. Zhang, W.Y. Li, J. Shen, Y.J. Chao, J. Li, Y.E. Ma, *Mater. Des.* 50 (2013) 551–557.
- [59] B.B. Wang, F.F. Chen, F. Liu, W.G. Wang, P. Xue, Z.Y. Ma, *J. Mater. Sci. Technol.* 33 (2017) 1009–1014.
- [60] C. Sharma, D.K. Dwivedi, P. Kumar, *Mater. Des.* 43 (2013) 134–143.
- [61] X.Q. Lv, C.S. Wu, G.K. Padhy, *Mater. Lett.* 203 (2017) 81–84.
- [62] G.M. Karthik, G.J. Ram, R.S. Kottada, *Mater. Sci. Eng. A* 684 (2017) 186–190.
- [63] P.M. Krishna, D. Simhachalam, N. Ramanaiah, *J. Appl. Sci.* 12 (2012) 1053–1057.
- [64] W. Woo, L. Balogh, T. Ungár, H. Choo, Z. Feng, *Mater. Sci. Eng. A* 498 (2008) 308–313.
- [65] D. Lohwasser, Z. Chen, *Friction Stir Welding: From Basics to Applications*, first ed., Elsevier, 2009.
- [66] R. Rahbarpour, T. Azdast, H. Rahbarpour, S.M. Shishavan, *Sci. Technol. Weld. Join.* 19 (2014) 673–681.
- [67] M.M.Z. Ahmed, B.P. Wynne, W.M. Rainforth, P.L. Threadgill, *Scr. Mater.* 64 (2011) 45–48.
- [68] J.Q. Li, H.J. Liu, *Mater. Des.* 43 (2013) 299–306.
- [69] S.D. Ji, X.C. Meng, J.G. Liu, L.G. Zhang, S.S. Gao, *Mater. Des.* 62 (2014) 113–117.
- [70] D. Li, X. Yang, L. Cui, F. He, H. Shen, *Mater. Des.* 64 (2014) 251–260.
- [71] C.A. Maltin, L.J. Nolton, J.L. Scott, A.I. Toumpis, A.M. Galloway, *Mater. Des.* 64 (2014) 614–624.
- [72] D. Li, X. Yang, L. Cui, F. He, X. Zhang, *J. Mater. Process. Technol.* 222 (2015) 391–398.
- [73] P.S. Davies, B.P. Wynne, W.M. Rainforth, M.J. Thomas, P.L. Threadgill, *Mater. Mater. Trans. A* 42 (2011) 2278–2289.
- [74] S.D. Ji, X.C. Meng, Z.W. Li, L. Ma, S.S. Gao, *J. Mater. Eng. Perform.* 25 (2016) 1228–1236.
- [75] J. Martin, *Friction Stir Welding*, The Welding Institute, UK, 2017 <http://www.manufacturingchampions.in/Document/presentaion-9%202016%20Robotic%20FSW%20-20Future%20Trends%20CI%20Conference%20of%20Welding.pdf>.
- [76] J.Q. Li, H.J. Liu, *Mater. Des.* 45 (2013) 148–154.
- [77] L. Shi, C.S. Wu, H.J. Liu, *Int. J. Mach. Tool Manuf.* 91 (2015) 1–11.
- [78] J.Q. Li, H.J. Liu, *J. Mater. Sci. Technol.* 31 (2015) 375–383.
- [79] L. Shi, C.S. Wu, H.J. Liu, *Weld. World* 59 (2015) 629–638.
- [80] L. Shi, C.S. Wu, H.J. Liu, *Int. J. Adv. Manuf. Technol.* 74 (2014) 319–334.
- [81] L. Shi, C.S. Wu, H.J. Liu, J. Mater. Eng. Perform. 23 (2014) 2918–2929.
- [82] J.Q. Li, H.J. Liu, *Int. J. Adv. Manuf. Technol.* 76 (2015) 1469–1478.
- [83] H. Montazerolghaem, M. Badrossamay, A.F. Tehrani, S.Z. Rad, M.S. Esfahani, *Mater. Manuf. Process.* 30 (2015) 1109–1114.
- [84] H.J. Liu, J.Q. Li, W.J. Duan, Proceedings of the 1st International Joint Symposium on Joining and Welding, Osaka, Japan 6–8 Nov, 2013, pp. 25–32.
- [85] J. Hilpert, H.N. Schmidt, J.F. Dos Santos, N. Huber, *J. Mater. Process. Technol.* 211 (2011) 197–204.
- [86] W.M. Thomas, C.S. Wiesner, D.J. Marks, D.G. Staines, *Sci. Technol. Weld. Join.* 14 (2009) 247–253.
- [87] S.S. Chaudhury, K.S. Bhavsar, *Int. J. Sci. Technol. Eng.* 2 (2016) 630–633.
- [88] M.K. Sued, D. Pons, J. Lavroff, E.H. Wong, *Mater. Des.* 54 (2014) 632–643.
- [89] W.Y. Li, T. Fu, L. Hütsch, J. Hilpert, F.F. Wang, J.F. Dos Santos, N. Huber, *Mater. Des.* 64 (2014) 714–720.
- [90] H. Zhang, M. Wang, X. Zhang, G. Yang, *Mater. Des.* 65 (2015) 559–566.
- [91] L. Zhou, G.H. Li, C.L. Liu, J. Wang, Y.X. Huang, J.C. Feng, F.X. Meng, *Sci. Technol. Weld. Join.* 22 (2016) 438–445.
- [92] P.L. Threadgill, M.M. Ahmed, J.P. Martin, J.G. Perrett, B.P. Wynne, *Mater. Sci. Forum* 638 (2010) 1179–1184.
- [93] K. Kumari, S.K. Pal, S.B. Singh, *J. Mater. Process. Technol.* 215 (2015) 132–141.
- [94] Y.X. Huang, L. Wan, S.X. Lv, *Sci. Technol. Weld. Join.* 18 (2013) 239–246.
- [95] L. Wan, Y.X. Huang, W.Q. Guo, *J. Mater. Sci. Technol.* 30 (2014) 1243–1250.
- [96] L. Wan, Y.X. Huang, Z.L. Lv, *Mater. Des.* 55 (2014) 197–203.
- [97] R.S. Mishra, M.W. Mahoney, *Friction Stir Welding and Processing*, ASM, International, Ohio, 2007, pp. 235–272.
- [98] T.Y. Pan, SAE Technical Paper No. 2007-01-1702, 2007.
- [99] A.P. Gerlich, T.H. North, in: R. Schwartz (Ed.), *Innovations in Materials Manufacturing, Fabrication, and Environmental Safety*, CRC Press, 2010.
- [100] T. Iwashita, Method and apparatus for joining, US Patent 6601751 B2, 2003.
- [101] C. Schilling J.F. dos Santos, Method and device for joining at least two adjoining work pieces by friction welding, US Patent 6,722,556, 2004.
- [102] M. Kumagai, S. Tanaka, Method of spot joining for aluminum alloy, Japan Patent 2001-259863, 2001.
- [103] C.D. Cox, B.T. Gibson, D.R. DeLapp, A.M. Strauss, G.E. Cook, *J. Manuf. Process.* 16 (2014) 241–247.
- [104] D. Bakavos, Y. Chen, L. Babout, P. Prangnell, *Metall. Mater. Trans. A* 42 (2011) 1266–1282.
- [105] Y. Tozaki, Y. Uematsu, K. Tokaji, *J. Mater. Process. Technol.* 210 (2010) 844–851.
- [106] C. Schilling, A.V. Strombeck, J.F. dos Santos, N.V. Heesen, Proceedings of 2nd Symposium on Friction Stir Welding, May 26–28, Gothenburg, Sweden, 2000.
- [107] A. von Strombeck, C. Schilling, J.F. dos Santos, *Biul. Inst. Spaw.* 45 (2001) 49–52 (in Polish).
- [108] A.C. Addison, A.J. Robelou, Proceedings of the 5th International Friction Stir Welding Symposium, Metz France, September 14, 2004.
- [109] B.M. Tweedy, C.A. Widener, J.D. Merry, J.M. Brown, D.A. Burford, SAE Technical Paper, 2008-01-1135.
- [110] G. Buffa, L. Fratini, M.A. Piacentini, *J. Mater. Process. Technol.* 208 (2008) 309–317.
- [111] F. Hunt, H. Badarinarayan, K. Okamoto, SAE Technical Paper 2006-01-0970, SAE 2006 World Congress, April 3–6, Detroit, MI, USA, 2006.
- [112] K. Okamoto, F. Hunt, S. Hirano, SAE Technical Paper 2005-01-0730, SAE 2005 World Congress, April 11–14, Detroit, MI, USA, 2005.
- [113] K. Okamoto, F. Hunt, S. Hirano, SAE Technical Paper 2005-01-1254, SAE 2005 World Congress, April 11–14, Detroit, MI, USA, 2005.
- [114] Q. Yang, S. Mironov, Y.S. Sato, K. Okamoto, *Mater. Sci. Eng. A* 527 (2010) 4389–4398.
- [115] P. Su, A. Gerlich, T.H. North, G.J. Bendzsak, *Sci. Technol. Weld. Join.* 11 (2013) 61–71.
- [116] R. Karthikeyan, V. Balasubramanian, *Int. J. Adv. Manuf. Technol.* 51 (2010) 173–183.
- [117] Y. Tozaki, Y. Uematsu, K. Tokaji, *Fatigue Fract. Eng. Mater. Struct.* 30 (2007) 143–148.
- [118] W. Yuan, R.S. Mishra, S. Webb, Y.L. Chen, B. Carlson, D.R. Herling, G.J. Grant, *J. Mater. Process. Technol.* 211 (2011) 972–977.
- [119] M.K. Bilici, A.I. Yükler, *Mater. Des.* 33 (2012) 145–152.
- [120] Y. Tozaki, Y. Uematsu, K. Tokaji, *Int. J. Mach. Tool Manuf.* 47 (2007) 2230–2236.
- [121] J.F. Hinrichs, C.B. Smith, B.F. Orsini, R.J. DeGeorge, B.J. Smale, P.C. Ruehl, Proceedings of the 5th International Symposium of Friction Stir Welding, September 14–16, Metz, France, 2004.
- [122] H. Badarinarayan, Q. Yang, S. Zhu, *Int. J. Mach. Tool Manuf.* 49 (2009) 142–148.
- [123] A. Gerlich, G. Avramovic-Cingara, T.H. North, *Metall. Mater. Trans. A* 37 (2006) 2773–2786.
- [124] D.A. Wang, S.C. Lee, *J. Mater. Process. Technol.* 186 (2007) 291–297.
- [125] I. Stol, W. Thomas, P. Threadgill, Friction plunge riveting process, US Patent No. 10/792,409, 2004.
- [126] R. Stevenson, P.C. Wang, Rivet with sliding cap for friction stir riveting, US Patent No. 7013768 B2, 2006.
- [127] P.C. Wang, R. Stevenson, Friction stir rivet method of joining, US Patent No. 7862271, 2011.

- [128] S.R. Banait, A.K. Raut, B.G. Nerkar, J. Tejani, *Int. J. Res. Appl. Sci. Eng. Technol.* 3 (2015) 192–196.
- [129] J. Li, S. Lazarevic, S. Miller, W.M. Wang, W. Cai, L. Xi, K. Wang, M. Banu, Proceedings of 9th International Workshop on Microfactories, October 5–8, 2014, Honolulu, USA, 2017, pp. 195–201.
- [130] Y. Li, Z. Wei, Z. Wang, Y. Li, *J. Manuf. Sci. Eng.* 135 (2013) 061007.
- [131] Z. Wang, Characterization of Friction-stir Riveting AA5754, Master Thesis, The University of Toledo, 2014.
- [132] Y. Hu, Friction-stir Riveting: Mechanical Testing of Friction Stir Riveting, Ph.D Thesis, The University of Toledo, 2015.
- [133] S.J. Durbin, Friction-Stir Riveting: An Innovative Process for Joining Difficult-to-Weld Materials, Master Thesis, The University of Toledo, 2012.
- [134] G. Ma, Friction-Stir Riveting Characteristics of Friction-stir Riveted Joints Master Thesis, The University of Toledo, 2012.
- [135] N.Z. Borba, Friction Riveting of Ti-6Al-4V and Pultruded Glass Fiber Reinforced Thermoset Polyester Hybrid Joints, Master Thesis, Universidade Federal de São Carlos, 2015.
- [136] J. Altmeyer, J.F. dos Santos, S.T. Amancio-Filho, *Mater. Des.* 60 (2014) 164–176.
- [137] S.T. Amancio-Filho, Friction riveting: development and analysis of a new joining technique for polymer-metal multi-material structures, Technical University Hamburg-Harburg / GKSS Research Center, Germany 2007, ISSN 0344-9629.
- [138] S.T. Amancio Filho, M. Beyer, J.F. dos Santos, Method of connecting a metallic bolt to a plastic piece, US Patent, No. 7,575,149 B2, 2009.
- [139] S.T. Amancio-Filho, *Weld. World* 55 (2011) 13–24.
- [140] M.F. Borges, S.T. Amancio-Filho, J.F. dos Santos, T.R. Strohaecker, J.A. Mazzaferro, *Comp. Mater. Sci.* 54 (2012) 7–15.
- [141] L. Blaga, J.F. Dos Santos, R. Bancila, S.T. Amancio-Filho, *Constr. Build. Mater.* 80 (2015) 167–179.
- [142] J. Min, Y. Li, B.E. Carlson, S.J. Hu, J. Li, J. Lin, *CIRP Ann. Manuf. Technol.* 64 (2015) 13–16.
- [143] J. Min, J. Li, B.E. Carlson, Y. Li, J.F. Quinn, J. Lin, W. Wang, *J. Manuf. Sci. Eng.* 137 (2015) 051022.
- [144] J. Min, J. Li, Y. Li, B.E. Carlson, J. Lin, W.M. Wang, *J. Mater. Process. Technol.* 215 (2015) 20–29.
- [145] J. Min, Y. Li, J. Li, B.E. Carlson, J. Lin, *Int. J. Adv. Manuf. Technol.* 76 (2015) 1403–1410.
- [146] J. Min, J. Li, Y. Li, B.E. Carlson, J. Lin, *J. Manuf. Sci. Eng.* 138 (2016) 054501.
- [147] D. Gao, U. Ersoy, R. Stevenson, P.C. Wang, *J. Manuf. Sci. Eng.* 131 (2009) 061002.
- [148] C.Q. Zhang, X.J. Wang, B.Q. Li, *Adv. Mater. Res.* 183–185 (2011) 1616–1620.
- [149] C.Q. Zhang, B.Q. Li, X.J. Wang, *Adv. Mater. Res.* 228–229 (2011) 427–432.
- [150] W.M. Wang, H.A. Khan, J. Li, S.F. Miller, A.Z. Trimble, *J. Manuf. Sci. Eng.* 139 (2017) 021005.
- [151] S. Lathabai, V. Tyagi, D. Ritchie, T. Kearney, B. Finnin, S. Christian, A. Sansome, G. White, *SAE Int. J. Mater. Manuf.* 4 (2011) 589–601.
- [152] A.Z. Trimble, B. Yamamoto, J. Li, *J. Manuf. Sci. Eng.* 138 (2016), 095001.
- [153] Y. Ma, M. Lou, Z. Yang, Y. Li, *J. Manuf. Sci. Eng.* 137 (2015), 054501.
- [154] Y. Ma, Y. Li, W. Hu, M. Lou, Z. Lin, *J. Manuf. Sci. Eng.* 138 (2016), 061007.
- [155] G. Han, M. Wang, Z. Liu, P.C. Wang, *J. Manuf. Sci. Eng.* 135 (2013), 031012.
- [156] H. Duan, G. Han, M. Wang, X. Zhang, Z. Liu, *Mater. Des.* 54 (2014) 414–424.
- [157] R. Justman, M. West, B. Jasthi, C. Widener, A. Boysen, Friction Stir Lap Welding Aluminum to Steel Using Scribe Technology. Master Thesis, Dakota School of Mines, USA, 2013 <http://met.sdsmt.edu/reu/2013/6/2/Report/Final%20Report.pdf>.
- [158] Y. Hovanski, G.J. Grant, S. Jana, K.F. Mattlin, Friction stir welding tool and process for welding dissimilar materials. US patent 8,434,661, 2013.
- [159] E.E. Patterson, Microstructural Characterization of Friction Stir Welded Aluminum-steel Joints. Master Thesis, Washington State University, USA, 2013.
- [160] P. Upadhyay, Y. Hovanski, S. Jana, L.S. Fifield, *J. Manuf. Sci. Eng.* 139 (2017), 034501.
- [161] P. Upadhyay, Y. Hovanski, L.S. Fifield, K.L. Simmons. In: Friction Stir Welding and Processing VIII, 2015; 16 pp. 153–161.
- [162] H.H. Cho, S.H. Kang, S.H. Kim, K.H. Oh, H.J. Kim, W.S. Chang, H.N. Han, *Mater. Des.* 34 (2012) 258–267.
- [163] S. Jana, Y. Hovanski, G.J. Grant, *Metall. Mater. Trans. A* 41 (2010) 3173–3182.
- [164] S. Jana, Y. Hovanski, G.J. Grant, K. Mattlin, Friction Stir Welding and Processing VI, 2011, pp. 205–211.
- [165] E.E. Patterson, Y. Hovanski, D.P. Field, *Metall. Mater. Trans. A* 47 (2016) 2815–2829.
- [166] T. Curtis, W. Christian, M. West, B. Jasthi, Y. Hovanski, B. Carlson, R. Szymanski, W. Bane, in: R.S. Mishra, M.W. Mahoney, Y. Sato, Y. Hovanski (Eds.), Friction Stir Welding and Processing VIII, 2015, pp. 163–169.
- [167] Z.Y. Ma, *Metall. Mater. Trans. A* 39 (2008) 642–658.
- [168] Z.Y. Ma, R.S. Mishra, *Scr. Mater.* 53 (2005) 75–80.
- [169] J.Q. Su, T.W. Nelson, C.J. Sterling, *Scr. Mater.* 52 (2005) 135–140.
- [170] Z.Y. Ma, S.R. Sharma, R.S. Mishra, *Scr. Mater.* 54 (2006) 1623–1626.
- [171] J.Q. Su, T.W. Nelson, C.J. Sterling, *Phil. Mag.* 86 (2006) 1–24.
- [172] C.I. Chang, X.H. Du, J.C. Huang, *Scr. Mater.* 57 (2007) 209–212.
- [173] E.A. El-Danaf, M.M. El-Rayes, M.S. Soliman, *Mater. Des.* 31 (2010) 1231–1236.
- [174] I. Charit, R.S. Mishra, *Acta Mater.* 53 (2005) 4211–4223.
- [175] A. Orozco-Caballero, M. Álvarez-Leal, P. Hidalgo-Manrique, C.M. Cepeda-Jiménez, O.A. Ruano, F. Carreño, *Mater. Sci. Eng. A* 680 (2017) 329–337.
- [176] C.I. Chang, C.J. Lee, J.C. Huang, *Scr. Mater.* 51 (2004) 509–514.
- [177] C.I. Chang, X.H. Du, J.C. Huang, *Scr. Mater.* 59 (2008) 356–359.
- [178] Z.Y. Ma, A.L. Pilchak, M.C. Juhas, J.C. Williams, *Scr. Mater.* 58 (2008) 361–366.
- [179] L. Karthikeyan, V.S. Senthilkumar, V. Balasubramanian, S. Natarajan, *Mater. Des.* 30 (2009) 2237–2242.
- [180] L. Karthikeyan, V.S. Senthilkumar, K.A. Padmanabhan, *Mater. Des.* 31 (2010) 761–771.
- [181] K. Nakata, Y.G. Kim, H. Fujii, T. Tsumura, T. Komazaki, *Mater. Sci. Eng. A* 437 (2006) 274–280.
- [182] Z.Y. Ma, S.R. Sharma, R.S. Mishra, *Mater. Sci. Eng. A* 433 (2006) 269–278.
- [183] A.H. Feng, Z.Y. Ma, *Acta Mater.* 57 (2009) 4248–4260.
- [184] A.H. Feng, Z.Y. Ma, *Scr. Mater.* 56 (2007) 397–400.
- [185] Y. Morisada, H. Fujii, T. Nagaoka, M. Fukusumi, *Scr. Mater.* 55 (2006) 1067–1070.
- [186] P.B. Berbon, W.H. Bingel, R.S. Mishra, C.C. Bampton, M.W. Mahoney, *Scr. Mater.* 44 (2001) 61–66.
- [187] R.S. Mishra, Z.Y. Ma, I. Charit, *Mater. Sci. Eng. A* 341 (2003) 307–310.
- [188] H.S. Grewal, H.S. Arora, H. Singh, A. Agrawal, *Appl. Surf. Sci.* 268 (2013) 547–555.
- [189] A. Kurt, I. Uygur, E. Cete, *J. Mater. Process. Technol.* 211 (2011) 313–317.
- [190] E.R. Mahmoud, M. Takahashi, T. Shibayanagi, K. Ikeuchi, *Wear* 268 (2010) 1111–1121.
- [191] V. Sharma, U. Prakash, B.M. Kumar, *J. Mater. Process. Technol.* 224 (2015) 117–134.
- [192] H.S. Arora, H. Singh, B.K. Dhindaw, *Int. J. Adv. Manuf. Technol.* 61 (2012) 1043–1055.
- [193] S. Soleimani, A. Abdollah-Zadeh, S.A. Alidokht, *Wear* 278 (2012) 41–47.
- [194] A. Shafeei-Zarghani, S.F. Kashani-Bozorg, A. Zarei-Hanzaki, *Wear* 270 (2011) 403–412.
- [195] A. Shafeei-Zarghani, S.F. Kashani-Bozorg, A. Zarei-Hanzaki, *Mater. Sci. Eng. A* 500 (2009) 84–91.
- [196] Y. Huang, T. Wang, W. Guo, L. Wan, S. Lv, *Mater. Des.* 59 (2014) 274–278.
- [197] Y. Mazaheri, F. Karimzadeh, M.H. Enayati, *J. Mater. Process. Technol.* 211 (2011) 1614–1619.
- [198] Y. Morisada, H. Fujii, T. Nagaoka, M. Fukusumi, *Mater. Sci. Eng. A* 419 (2006) 344–348.
- [199] A. Ghasemi-Kahrizsangi, S.F. Kashani-Bozorg, *Surf. Coat. Technol.* 209 (2012) 15–22.
- [200] B. Zahmatkesh, M.H. Enayati, *Mater. Sci. Eng. A* 527 (2010) 6734–6740.
- [201] D. Yadav, R. Bauri, *Mater. Lett.* 64 (2010) 664–667.
- [202] I.S. Lee, C.J. Hsu, C.F. Chen, N.J. Ho, P.W. Kao, *Compos. Sci. Technol.* 71 (2011) 693–698.
- [203] Z.Y. Liu, B.L. Xiao, W.G. Wang, Z.Y. Ma, *Carbon* 50 (2012) 1843–1852.
- [204] D.R. Ni, J.J. Wang, Z.N. Zhou, Z.Y. Ma, *J. Alloy. Compd.* 586 (2014) 368–374.
- [205] C.J. Hsu, P.W. Kao, N.J. Ho, *Mater. Lett.* 61 (2007) 1315–1318.
- [206] Y. Morisada, H. Fujii, T. Nagaoka, K. Nogi, M. Fukusumi, *Composites A* 38 (2007) 2097–2101.
- [207] H. Izadi, A.P. Gerlich, *Carbon* 50 (2012) 4744–4749.
- [208] S.A. Alidokht, A. Abdollah-Zadeh, S. Soleimani, H. Assadi, *Mater. Des.* 32 (2011) 2727–2733.
- [209] A.H. Byung-Wook, C.H. Don-Hyun, K.I. Yong-Hwan, J.U. Seung-Boo, *Trans. Nonferrous Metal. Soc. China* 22 (2012) s634–s638.
- [210] A. Dolatkhah, P. Golbabaei, M.B. Givi, F. Molaikeiya, *Mater. Des.* 37 (2012) 458–464.
- [211] M. Bahrami, K. Dehghani, M.K. Givi, *Mater. Des.* 53 (2014) 217–225.
- [212] M. Bahrami, M.K. Givi, K. Dehghani, N. Parvin, *Mater. Des.* 53 (2014) 519–527.
- [213] M. Zohoor, M.B. Givi, P. Salami, *Mater. Des.* 39 (2012) 358–365.
- [214] J. Qian, J. Li, J. Xiong, F. Zhang, X. Lin, *Mater. Sci. Eng. A* 550 (2012) 279–285.
- [215] L. Ke, C. Huang, L. Xing, K. Huang, *J. Alloy. Compd.* 503 (2010) 494–499.
- [216] C.J. Hsu, C.Y. Chang, P.W. Kao, N.J. Ho, C.P. Chang, *Acta Mater.* 54 (2006) 5241–5249.
- [217] R. Bauri, D. Yadav, G. Suhas, *Mater. Sci. Eng. A* 528 (2011) 4732–4739.
- [218] Q. Zhang, B.L. Xiao, W.G. Wang, Z.Y. Ma, *Acta Mater.* 60 (2012) 7090–7103.
- [219] M. Sharifatabar, A. Sarani, S. Khorshidian, M.S. Afarani, *Mater. Des.* 32 (2011) 4164–4172.
- [220] M. Bahrami, M.K. Givi, K. Dehghani, N. Parvin, *Mater. Des.* 53 (2014) 519–527.
- [221] W. Wang, Q.Y. Shi, P. Liu, H.K. Li, T. Li, *J. Mater. Process. Technol.* 209 (2009) 2099–2103.
- [222] H. Izadi, A.P. Gerlich, *Carbon* 50 (2012) 4744–4749.
- [223] M. Salehi, M. Saadatmand, J.A. Mohandesi, *Trans. Nonferrous Metal. Soc. China* 22 (2012) 1055–1063.
- [224] M. Dixit, J.W. Newkirk, R.S. Mishra, *Scr. Mater.* 56 (2007) 541–544.
- [225] Q. Zhang, B.L. Xiao, Q.Z. Wang, Z.Y. Ma, *Mater. Lett.* 65 (2011) 2070–2072.
- [226] Q. Zhang, B.L. Xiao, D. Wang, Z.Y. Ma, *Mater. Chem. Phys.* 130 (2011) 1109–1117.
- [227] N. Kumar, M. Komarasamy, P. Nelaturu, Z. Tang, P.K. Liaw, R.S. Mishra, *J. Miner. Metal. Mater. Soc.* 67 (2015) 1007–1113.
- [228] B.M. Darras, M.K. Khraisheh, F.K. Abu-Farha, M.A. Omar, *J. Mater. Process. Technol.* 191 (2007) 77–81.

- [229] L.S. Raju, A. Kumar, Defence Technol. 10 (2014) 375–383.
- [230] M. Azizieh, A.H. Kokabi, P. Abachi, Mater. Des. 32 (2011) 2034–2041.
- [231] G. Faraji, P. Asadi, Mater. Sci. Eng. A 528 (2011) 2431–2440.
- [232] P. Asadi, G. Faraji, M.K. Besharati, Int. J. Adv. Manuf. Technol. 51 (2010) 247–260.
- [233] P. Asadi, R.A. Mahdavinejad, S. Tutunchilar, Mater. Sci. Eng. A 528 (2011) 6469–6477.
- [234] C.J. Lee, J.C. Huang, P.J. Hsieh, Scr. Mater. 54 (2006) 1415–1420.
- [235] Y. Morisada, H. Fujii, T. Nagaoka, M. Fukusumi, Mater. Sci. Eng. A 433 (2006) 50–54.
- [236] C.H. Chuang, J.C. Huang, P.J. Hsieh, Scr. Mater. 53 (2005) 1455–1460.
- [237] M. Barrouz, M.K. Givi, Composites A 42 (2011) 1445–1453.
- [238] H.R. Akramifard, M. Shamanian, M. Sabbaghian, M. Esmailzadeh, Mater. Des. 54 (2014) 838–844.
- [239] M. Sabbaghian, M. Shamanian, H.R. Akramifard, M. Esmailzadeh, Ceram. Int. 40 (2014) 12969–12976.
- [240] M.N. Avettand-Fènoël, A. Simar, R. Shabadi, R. Taillard, B. de Meester, Mater. Des. 60 (2014) 343–357.
- [241] C.A. Leon-Patiño, E.A. Aguilar-Reyes, M. Braulio-Sánchez, G. Rodríguez-Ortiz, E. Bedolla-Becerril, Mater. Des. 54 (2014) 845–853.
- [242] M. Barrouz, P. Asadi, M.K. Givi, M. Taherishargh, Mater. Sci. Eng. A 528 (2011) 1740–1749.
- [243] M. Barrouz, M.K. Givi, J. Seyfi, Mater. Charact. 62 (2011) 108–117.
- [244] A. Ghasemi-Kahrizsangi, S.F. Kashani-Bozorg, Surf. Coat. Technol. 209 (2012) 15–22.
- [245] S. Mironov, Y. Sato, H. Kokawa, Acta Mater. 56 (2008) 2602–2614.
- [246] B. Li, Y. Shen, L. Luo, W. Hu, Mater. Sci. Eng. A 574 (2013) 75–85.
- [247] S. Mukherjee, A.K. Ghosh, Mater. Sci. Eng. A 528 (2011) 3289–3294.
- [248] C.B. Fuller, M.W. Mahoney, Metall. Mater. Trans. A 37 (2006) 3605–3615.
- [249] S.M. Mousavizadeh, F.M. Ghaini, M.J. Torkamany, J. Sabbaghzadeh, A. Abdollah-Zadeh, Scr. Mater. 60 (2009) 244–247.
- [250] J.R. Rule, J.M. Rodelas, J.C. Lippold, Weld. J. 92 (2013) 283s–290s.
- [251] R.S. Mishra, M.W. Mahoney, S.X. McFadden, N.A. Mara, A.K. Mukherjee, Scr. Mater. 42 (1999) 163–168.
- [252] Z.Y. Ma, R.S. Mishra, M.W. Mahoney, R. Grimes, Mater. Sci. Eng. A 351 (2003) 148–153.
- [253] Z.Y. Ma, R.S. Mishra, M.W. Mahoney, Acta Mater. 50 (2002) 4419–4430.
- [254] L.B. Johannes, R.S. Mishra, Mater. Sci. Eng. A 464 (2007) 255–260.
- [255] Z.Y. Ma, R.S. Mishra, F.C. Liu, Mater. Sci. Eng. A 505 (2009) 70–78.
- [256] V.V. Patel, V. Badheka, A. Kumar, J. Mater. Process. Technol. 240 (2017) 68–76.
- [257] T.R. McNeley, S. Swaminathan, J.Q. Su, Scr. Mater. 58 (2008) 349–354.
- [258] R.S. Mishra, Integral channels in metal components and fabrication thereof, US Patent No. 6923362, 2005.
- [259] R.S. Mishra, Integral channels in metal components and fabrication thereof, US Patent No. 7354657, 2008.
- [260] N. Balasubramanian, Friction Stir Channeling: an Innovative Technique for Heat Exchanger Manufacturing, Ph.D Thesis, Missouri University of Science & Technology, 2008.
- [261] N. Balasubramanian, R.S. Mishra, K. Krishnamurthy, J. Mater. Process. Technol. 209 (2009) 3696–3704.
- [262] N. Balasubramanian, R.S. Mishra, K. Krishnamurthy, J. Manuf. Sci. Eng. 132 (2010), 054504.
- [263] N. Balasubramanian, R.S. Mishra, K. Krishnamurthy, J. Mater. Process. Technol. 211 (2011) 305–311.
- [264] P. Vilaca, C. Vidal, Ferramenta Modular Ajustavel e Respectivo Processo de Abertura de Canais Internos Contínuos em Componentes Macicos (Modular adjustable tool and correspondent process for opening continuous internal channels in solid components); National patent pending No. 105628 T, 2011.
- [265] C. Vidal, V. Infante, P. Vilaca, Key Eng. Mater. 488 (2012) 105–108.
- [266] C. Vidal, V. Infante, P. Vilaca, Mater. Sci. Forum 730 (2013) 817–822.
- [267] C. Vidal, V. Infante, P. Vilaca, Proc. Eng. 66 (2013) 264–273.
- [268] C. Vidal, V. Infante, V. Lage, P. Vilaca, Key Eng. Mater. 577 (2014) 37–40.
- [269] C. Vidal, V. Infante, Adv. Mater. Res. 891 (2014) 1494–1499.
- [270] C. Vidal, V. Infante, P. Vilaca, Int. J. Fatigue 62 (2014) 85–92.
- [271] C. Vidal, V. Infante, P. Vilaca, Int. J. Fatigue 62 (2014) 77–84.
- [272] C. Vidal, V. Infante, P. Vilaca, Eng. Fail. Anal. 56 (2015) 204–215.
- [273] M. Ferraz, Friction stir channeling-Industrial applications and prototype development. <https://fenix.tecnico.ulisboa.pt/downloadFile/395144527869/Extended%20Abstract.pdf>.
- [274] M. Ferraz, Friction Stir Channeling Industrial Applications. Master Thesis, Universidade Técnica de Lisboa, 2012.
- [275] A. Rashidi, A. Mostafapour, S. Salahi, V. Rezazadeh, Appl. Mech. Mater. 302 (2013) 365–370.
- [276] A. Rashidi, A. Mostafapour, V. Rezazadeh, S. Salahi, Appl. Mech. Mater. 302 (2013) 371–376.
- [277] A. Rashidi, A. Mostafapour, Proc. Inst. Mech. Eng. B: J. Eng. Manuf. (2015) 0954405415598943. 10.1177/0954405415598943.
- [278] A. Rashidi, A. Mostafapour, Int. J. Adv. Manuf. Technol. 80 (2015) 1087–1096.
- [279] A. Rashidi, A. Mostafapour, Int. J. Mater. Form. 9 (2016) 1–8.
- [280] A.W. Batchelor, S. Jana, C.P. Koh, C.S. Tan, J. Mater. Process. Technol. 57 (1996) 172–181.
- [281] J. Gandra, H. Krohn, R.M. Miranda, P. Vilaca, L. Quintino, J.F. dos Santos, J. Mater. Process. Technol. 214 (2014) 1062–1093.
- [282] J. Gandra, D. Pereira, R.M. Miranda, P. Vilaca, Proc. CIRP 7 (2013) 341–346.
- [283] X.M. Liu, Z.D. Zou, Y.H. Zhang, S.Y. Qu, X.H. Wang, Surf. Coat. Technol. 202 (2008) 1889–1894.
- [284] V.I. Vitanov, N. Javaid, Surf. Coat. Technol. 204 (2010) 2624–2631.
- [285] E.D. Nicholas, Weld. J. 65 (1986) 17–27.
- [286] E.D. Nicholas, in: D. Olson, T. Siewert, S. Liu, G. Edwards (Eds.), ASM Handbook-Welding Brazing and Soldering, ASM, International, Ohio, 1993, pp. 321–323.
- [287] G.M. Bedford, V.I. Vitanov, I.I. Voutchkov, Surf. Coat. Technol. 141 (2001) 34–39.
- [288] H. Sakihama, H. Tokisue, K. Katoh, Mater. Trans. 44 (2003) 2688–2694.
- [289] H.K. Rafi, G.J. Ram, G. Phanikumar, K.P. Rao, Surf. Coat. Technol. 205 (2010) 232–242.
- [290] H.K. Rafi, G.J. Ram, G. Phanikumar, K.P. Rao, Proceedings of the World Congress on Engineering, London, 2010 (Vol. 2).
- [291] K. Fukakusa, Weld. Int. 10 (1996) 524–529.
- [292] J. Gandra, R.M. Miranda, P. Vilaca, J. Mater. Process. Technol. 212 (2012) 1676–1686.
- [293] H.K. Rafi, G. Phanikumar, K.P. Rao, Metall. Mater. Trans. A 42 (2011) 937–939.
- [294] H.K. Rafi, G.J. Ram, G. Phanikumar, K.P. Rao, Mater. Des. 32 (2011) 82–87.
- [295] T. Shinoda, J.Q. Li, Y. Katoh, T. Yashiro, Surf. Eng. 14 (1998) 211–216.
- [296] M.L. Kramer de Macedo, G.A. Pinheiro, J.F. dos Santos, T.R. Strohaecker, Weld. Int. 24 (2010) 422–431.
- [297] A.M. Kalken, Friction Surfacing of Stainless Steel on Mild Steel with a Robot, Master Thesis, Delft University of Technology, 2001.
- [298] V.I. Vitanov, I.I. Voutchkov, J. Mater. Process. Technol. 159 (2005) 27–32.
- [299] H. Tokisue, K. Katoh, T. Asahina, T. Usiyama, Mater. Trans. 47 (2006) 874–882.
- [300] V.I. Vitanov, I.I. Voutchkov, G.M. Bedford, J. Mater. Process. Technol. 107 (2000) 236–242.
- [301] U. Subhuddin, S. Mironov, H. Krohn, M. Beyer, J.F. Dos Santos, Metall. Mater. Trans. A 43 (2012) 5224–5231.
- [302] I. Voutchkov, B. Jaworski, V.I. Vitanov, G.M. Bedford, Surf. Coat. Technol. 141 (2001) 26–33.
- [303] M. Chandrasekaran, A.W. Batchelor, S. Jana, J. Mater. Process. Technol. 72 (1997) 446–452.
- [304] K.P. Rao, A.V. Sreenu, H.K. Rafi, M.N. Libin, K. Balasubramaniam, J. Mater. Process. Technol. 212 (2012) 402–407.
- [305] A.A. van der Stelt, Friction Surface Cladding: Development of a Solid State Cladding Process, Ph.D Thesis, University of Twente, The Netherlands, 2014.
- [306] S. Liu, Friction Surface Cladding of AA1050 onto AA2024: Parameter Study and Process Window Development, Ph.D. Thesis, Universiteit Twente, 2016 (Thesis&).
- [307] A.A. van der Stelt, T.C. Bor, H.J. Geijsselaers, R. Akkerman, A.H. van den Boogaard, Key Eng. Mater. 554 (2013) 1014–1021.
- [308] S. Liu, T.C. Bor, A.A. van der Stelt, H.J. Geijsselaers, C. Kwakernaak, A.M. Kooijman, J.M. Mol, R. Akkerman, A.H. van den Boogaard, J. Mater. Process. Technol. 229 (2016) 769–784.
- [309] S. Liu, T.C. Bor, H.J. Geijsselaers, R. Akkerman, Parameter Study for Friction Surface Cladding of AA1050 on AA2024-T351. <http://doc.utwente.nl/101884/1/FSC-university%20of%20Twente%20S%20Liu.pdf>.
- [310] S. Liu, T.C. Bor, H.J. Geijsselaers, R. Akkerman, FSWP International Conference, October 1–2, 2015.
- [311] M.V. Kumar, S. Satish, Proc. of NCRIST-2015 & Indian J. Scient. Res. 12 (2015) 217–220.
- [312] Local cladding of advance aluminium alloys employing friction stir welding. <https://www.utwente.nl/en/et/tm/research/projects/FSC/#duration>.
- [313] D. Christoulis, (Local) Alloying and Cladding of Advanced Aluminium Alloys Employing Friction Stir Welding. <http://www.narcis.nl/research/RecordID/OND1334605>.
- [314] D. Lohwasser, Z. Chen (Eds.), Friction Stir Welding: From Basics to Applications, Elsevier, 2009.
- [315] M. Gruppelaar, Friction stir welding technology for new cladding solutions in buildings. <https://www.linkedin.com/pulse/friction-stir-welding-technology-new-cladding-melle-gruppelaar>.
- [316] Z. Shen, Y. Chen, M. Haghshenas, T. Nguyen, J. Galloway, A.P. Gerlich, Mater. Charact. 104 (2015) 1–9.
- [317] J.J. Dilip, G.D. Janaki Ram, B.E. Stucker, Int. J. Rapid Manuf. 3 (2012) 56–69.
- [318] D. White, Object consolidation employing friction joining: US Patent, No. 6,457,629. 2002-10-1.
- [319] J.A. Baumann, Production of Energy Efficient Preform Structures (PEEPS) (No. Final Technical Report- DE-EE0003483, The Boeing Company, 2012.
- [320] P.H. Lequeux, R. Muzzolini, J.C. Ehrstrom, F. Bron, R. Maziarz, High Performance Friction Stir Welded Structures Using Advanced Alloys (Powerpoint Presentation), Aeromat Conference, Seattle, 2006.
- [321] J.J. Dilip, H.K. Rafi, G.J. Ram, Trans. Indian Inst. Metal. 64 (2011) 27–30.
- [322] J.J. Dilip, S. Babu, S.V. Rajan, K.H. Rafi, G.J. Ram, B.E. Stucker, Mater. Manuf. Process. 28 (2013) 189–194.
- [323] S. Palanivel, P. Nelaturu, B. Glass, R.S. Mishra, Mater. Des. 65 (2015) 934–952.
- [324] R.S. Forrest, D.J. Waldron, Stir forming apparatus. US Patent, No. 7,971,463, 2011.
- [325] T. Iwashita, Method and apparatus for joining. US Patent, No. 6,601,751, 2003.
- [326] R.S. Forrest, D.J. Waldron, Stir forming apparatus and method. US Patent, No. 7,448,528, 2008.
- [327] M.W. Mahoney, W.H. Bingel, Thick-section metal forming via friction stir processing, US Patent, No. 6,866,180. 2005.

- [328] K.N. Balakrishnan, H.T. Kang, P.K. Mallick, SAE Technical Paper No. 2007-01-1701, 2007.
- [329] Y. Ahuja, R. Ibrahim, A. Paradowska, D. Riley, J. Mater. Process. Technol. 217 (2015) 222–231.
- [330] T. Nishihara, Mater. Sci. Forum 426 (2003) 2971–2978.
- [331] T. Nishihara, A. Ito, Weld. World 49 (2005) 22–26.
- [332] S. Lazarevic, Experimental and Metallurgical Analysis of Friction Stir Forming Process, Master Thesis, University of Hawaii, 2012.
- [333] S. Lazarevic, S.F. Miller, J. Li, B.E. Carlson, J. Manuf. Process. 15 (2013) 616–624.
- [334] S. Lazarevic, K.A. Ogata, S.F. Miller, G.H. Kruger, B.E. Carlson, J. Manuf. Sci. Eng. 137 (2015) 051018.
- [335] K.A. Ogata, Material Analysis of Friction Stir Forming and Friction Stir Deposition, Master Thesis, University of Hawaii at Manoa, 2013.
- [336] K. Liu, Feasibility Study on Dissimilar Materials Joint Made by Friction Stir Forming, Master Thesis, University of Hawaii, 2014.
- [337] J. Li, S. Lazarevic, S. Miller, W.M. Wang, W. Cai, L. Xi, K. Wang, M. Banu, 9th International Workshop on Microfactories, October 5–8, 2014, Honolulu, USA, 2017, pp. 195–201.
- [338] S.F. Miller, Manuf. Lett. 1 (2013) 21–24.
- [339] K. Yamamura, K. Torikai, T. Nishinara, Fric. Stir Weld. Proc VI (2011) 281–288.
- [340] H.M. Tabatabaei, T. Nishihara, Weld. World 2016 (2016) 1–9, <http://dx.doi.org/10.1007/s40194-016-0406-9>.
- [341] M. Otsu, M. Yasunaga, M. Matsuda, K. Takashima, Proc. Eng. 81 (2014) 2318–2323.
- [342] M. Otsu, H. Matsuo, M. Matsuda, K. Takashima, J. Japan. Soc. Technol. Plast. 52 (2011) 710–714.
- [343] W.M. Thomas, E.D. Nicholas, S.B. Jones, Friction extrusion, metal working, US Patent, No. 5262123, 1993.
- [344] W.T. Evans, B.T. Gibson, J.T. Reynolds, A.M. Strauss, G.E. Cook, Manuf. Lett. 5 (2015) 25–28.
- [345] W.T. Evans, C. Cox, B.T. Gibson, A.M. Strauss, G.E. Cook, J. Manuf. Process. 23 (2016) 115–121.
- [346] W. Tang, A.P. Reynolds, J. Mater. Process. Technol. 210 (2010) 2231–2237.
- [347] M. Abdollahi, R.A. Behnagh, J. Ghasemi, M.K. Givi, Proceedings of Iran International Aluminum Conference, 25–26, Tehran, Iran, 2014.
- [348] R.A. Behnagh, R. Mahdavinejad, A. Yavari, M. Abdollahi, M. Narvan, Metall. Mater. Trans. B 45 (2014) 1484–1489.
- [349] H. Zhang, X. Zhao, X. Deng, M.A. Sutton, A.P. Reynolds, S.R. McNeill, X. Ke, Int. J. Mech. Sci. 85 (2014) 130–141.
- [350] M. Sharifzadeh, M.A. Ansari, M. Narvan, R.A. Behnagh, A. Araee, M.K. Givi, Trans. Nonferrous Metal. Soc. China 25 (2015) 1847–1855.
- [351] H. Zhang, X. Li, W. Tang, X. Deng, A.P. Reynolds, M.A. Sutton, J. Mater. Process. Technol. 221 (2015) 21–30.
- [352] M.A. Ansari, R.A. Behnagh, M. Narvan, E.S. Naeini, M.K. Givi, H. Ding, Trans. Indian Inst. Metal. 69 (2016) 1351–1357.
- [353] R.A. Behnagh, N. Shen, M.A. Ansari, M. Narvan, M.K. Givi, H. Ding, J. Manuf. Sci. Eng. 138 (2016), 041008.
- [354] F. Abu-Farha, Extruded Tubing via Friction Stir Forming, U.S. Provisional Patent Application, No. 61/547148, 2011.
- [355] F. Abu-Farha, Scr. Mater. 66 (2012) 615–618.
- [356] F. Abu-Farha, Proceedings of the ASME 2012 International Manufacturing Science and Engineering Conference, June 4–8, Notre Dame, Indiana, USA, 2012, pp. 199–207.
- [357] J.L. Milner, F. Abu-Farha, Proceedings of the ASME 2014 International Manufacturing Science and Engineering Conference, June 9–13, Detroit, Michigan, USA, 2014.
- [358] M.S. Khorrami, M. Movahedi, Mater. Des. 65 (2015) 74–79.
- [359] E.D. Nicholas, Weld. World 47 (2003) 2–9.